DECOMPOSITION AND MEASUREMENT OPTIMIZATION IN ELECTRICAL POWER SYSTEMS STATE ESTIMATION

by

Sergio Alain Molina, Ing. Elec.

A Thesis submitted for the degree of
Doctor of Philosophy in Engineering

Department of Electrical Engineering,
Imperial College of Science and Technology,
University of London.

September 1977

ABSTRACT

The monitoring of the electrical power system requires information regarding its state for the analysis, assessment and control of the system. This information is obtained through a state estimation process which comprises the data validation, network configuration and estimation algorithm. The non-linear state estimation in power systems is studied using a linearized model provided by a Taylor series expansion of the measurement equations. A linearity test is incorporated to check the validity of the linearized model. A discussion is made on the weighting factors effect in the state estimation algorithm performance.

The observability of the power system for state estimation is discussed using numerical analysis and graph theory concepts. It shows how the structural properties of the network are associated with its observability. A measurement set is expressed as a directed graph and its observability is related to the reachability matrix concept.

It is the practice to design decentralized areas in a large power system which are almost self-sufficient in operation and which can be decomposed into smaller subproblems. The power system state estimation problem can also be decomposed into smaller subsystems, regions or areas and a computer associated ~~which~~ with each. By this means, it is then possible to reduce the length of data transmission links and to share the dimensionality of the data processing and control.

The state estimation problem is solved here in a decentralized manner by employing local estimators. A qualitative explanation of the forms of decomposing a large scale system is given and its corresponding application to power system state estimation is presented. A semi-automatic procedure to find possible decentralized subsystems is developed which uses an ordering algorithm and heuristics to obtain the near optimal decomposed states of the system.

As it is impractical to measure and telemeter all the possible data of the network, the number of meters and amount of redundancy should be decided giving priority to the financial rather than the technical side of the problem. A suboptimal procedure which uses a shortest spanning tree criterion to allocate the measurement points is presented and discussed. Mathematical modelling of the minimum number of collecting measurement centres problem is presented in a graph theory framework.

ACKNOWLEDGEMENTS

This research was conducted under the supervision of Dr. B.J. Cory, B.Sc.(Eng), D.Sc., A.C.G.I., C.Eng., F.I.E.E., Reader in Electrical Engineering, Imperial College of Science and Technology, whose help and constant encouragement are gratefully acknowledged.

I would like to express my gratitude to the Consejo Nacional de Ciencia y Tecnología and Comisión Federal de Electricidad, Mexico, for the financial support and leave of absence which made this work possible.

I would like to express my appreciation to my former colleagues of the Power Systems Section, Dr. Gustavo E. González and Dr. Eduardo Arriola whose comments and discussions contributed directly or indirectly to this work.

I am particularly grateful to Dr. Roberto D. Galvão for his advice on network optimization and for having provided the computer code for the optimal location of facilities developed by him.

Finally, I wish to thank my wife, Luz Bella, for the long hours spent in typing this thesis.

Con cariño para Tania, nuestra hija, quien ha sabido comprender nuestras limitaciones y con los mejores deseos de que nuestra experiencia londinense sea de lo mas provechoso posible para nuestros pueblos latinoamericanos y para la superación de nosotros mismos.

Con amor para Luz Bella, sin cuya ayuda y estímulo difícilmente hubiera llevado a cabo el presente trabajo y cuya comprensión y paciencia han sido invaluables para seguir adelante con nuestras tareas.

Con fraternal cariño para los Compañeros cuya comprensión y estímulo han ayudado a fortalecer nuestra confianza en el futuro.

CONTENTS

LIST OF FIGURES

LIST OF TABLES

CHAPTER ONE

INTRODUCTION

The present work is concerned with one of the fields, now well established, that are inherent to any on-line control centre in power systems: the state estimation problem. It has been studied extensively in the last eight years and a great number of works related to it have been published, centering the main attention to solving the state estimation problem for the whole network. However, the continuous growth of system size, coupled with the complexity of interconnections, have made it difficult for a single processor to cope with the increasing needs. This has originated the necessity to search for a more efficient solution to the problem.

It is the aim of the present work to contribute towards the developing of a simplified and decentralized method of solution.

1.1 On-line monitoring of power systems

The development of modern control centres in power systems was initiated at the outset of the present decade. The operation of a power system control centre by a relatively small number of system operators per shift, gradually became an intractable task, unless:

a) the volume of data to be observed was displayed in a condensed and easily expanded form;
b) all the information required was reliable and presented in a clear and comprehensible manner; and
c) the personnel was relieved of any type of burdensome operations, such as acquisition, preparation and evaluation of data.

These conditions could only be satisfied with a computerized operations centre, which became an essential necessity.

The monitoring of the power system requires information regarding its instantaneous state for the analysis, assessment and control of the system. This information is obtained through the state estimator which comprises the data validation, network configuration and

estimation algorithm.

Power systems generally have uncertainties due to meter, communication and parameter errors, etc. The state estimation algorithm is a numerical process designed to provide the system operator with a reliable data base from the system measurements and network structure, thus rectifying the present level of error.

On the other hand, it is not economical to measure all quantities that are desired, such as, all line flows and currents, all voltages and all injections. While some of these quantities are expensive to get, such as voltage phase angles with a common reference, others may require the installation of current and/or potential transformers at a prohibitive cost in some system locations. The need for computing some quantities based on other quantities being measured becomes apparent. The possibility of bad data acquisition, a fault in the communication devices, etc., makes it imperative to ensure the validity of the system conditions displayed to the system operator. While it is important to know when a faulty measurement arrives at the control centre, it is equally important to be able to present the system conditions to the operator without the effect of the bad measurements. This is also accomplished by state estimation, which will not only detect and isolate bad measurements but will provide the means to compensate for them, so that in most cases the presence of bad measurements becomes transparent to the operator. The point is then, that for proper monitoring we are required to have a measurement system consisting of high quality on-site devices, high speed communication channels, a real time computer, state estimation calculations and efficient displays.

The state estimation problem (SEP) in power systems has evolved rapidly from its initial formulation to the present on-line implementations. To date, companies in several countries have installed on-line computers to handle the monitoring and -to a varying degree- the

system control, in conjunction with the system operator. The state and parameter estimation techniques in power systems have been applied to:

i) On-line calculation of the complex node voltages (1-7,11-18).

ii) Parameter estimation of the network (8,29,30,33).

iii) Identification of static external equivalents (99,107).

iv) Identification of dynamic equivalents (103,104).

v) Parameter identification for thermal power stations and generators (101,102,108).

In view of the extent of interconnection and interaction of present large power system networks and the great difficulty in implementing a single centralized control structure, the power system engineer has been naturally led along the path of developing a number of multi-level hierarchical systems (110,111). Several authors have proposed hierarchical models for the state estimation of the power system, for the dynamic (109,73) and static cases (50,75). More recently, a demand has been made for the development of decentralized estimators (88).

1.2 Decentralized estimation

In recent years the idea of decentralized areas has been introduced and studied to coordinate multiple control systems, even when control objectives are dissimilar.

The present large power systems can be decomposed into smaller subsystems, regions or areas and a computer is associated to each of these areas. It is then possible to reduce the length of data transmission links and to share the dimensionality of the control and data processing, as illustrated in Chapter 4.

To develop an algorithm for a particular problem, it is essential to have a clear understanding of the physical properties and structure of the system and of its mathematical representation by abstract concepts (models).

Information contained in the set of measurements concerning physical properties and structure of the system has been represented by graph theory concepts to further our understanding of the power systems

state estimation problems.

The structural properties of the electrical power systems or of its algorithms are of utmost importance in developing a decentralized state estimation process and its algorithms, as will become clear throughout this work.

The weighted non-linear least squares estimator fits the equations (Kirchoff laws) to the measured values. Obviously the Ohm and Kirchoff laws are satisfied by the network itself. This information is contained implicitly in the measurements, provided the expected values of the measurement errors are null and there is no faulty metering equipment.

To decentralize the state estimation process, the concept of independence has been used to identify the subsets of measurements that can be grouped to form independent subsystems where the local state vector is estimated by using only local measurements through a local estimation process.

As it is impractical to measure and telemeter all the possible data of the network, the number of meters and amount of redundancy should be decided giving priority to the financial rather than the technical side of the problem. Chapter 6 "looks" at this problem taking into account that it is very important to analyse the communications system because the transmission link costs are very high. Therefore, from the financial point of view, it is advisable to measure all quantities in a selected node.

1.3 Contents of the present work

In Chapter 2, the non-linear state estimation in power systems is studied using a linearized model provided by a Taylor series expansion of the measurement equations. A linearity test is incorporated to check the validity of the linearized model. An analysis of the effect of different weighting factors is made.

In Chapter 3 the set of measurements is expressed as a directed graph. Observability of the network is defined in terms that include

the structural properties of the measurements and the numerical solution process involved. A structural matrix concept (borrowed from graph theory) is introduced: the reachability matrix.

The case of unobserved portions of the network is discussed and a criterion for this case is given.

A discussion on the pseudoinverse technique is made and its limitations and potentialities are dealt with.

In Chapter 4, a decentralized state estimation procedure is presented based on the simple principle of independence, which takes into account the redundancy of the measurements to decompose the system.

A qualitative explanation of the forms of decomposing a large scale system is given by using block diagrams, and the corresponding interpretation of the state estimation process is provided.

In Chapter 5, a description of the main elements (strong components) belonging to the measurements directed graph and its corresponding algorithm is discussed.

A semi-automatic procedure to find the possible decentralized subsystems is developed which uses an ordering algorithm and heuristics to obtain the decomposition of the system.

Two mathematical models describing the measurement system are put forward in Chapter 6. A suboptimal procedure which uses the shortest spanning tree criterion to allocate the measurement points is implemented and its interpretation is discussed. The problem of allocating the minimum number of gathering measurement centres is solved by using an algorithm that solves the equivalent p-median problem.

Main contributions of this thesis:

1. A linearity test to check the validity of the Taylor series linear approximation and monitor the convergence of the Gauss-Newton algorithm in power systems state estimation.

   Discussion of the weighting factors effect in the state estimation

problem.

2. A graph theory framework introduced to represent the measurement system, which contributes to the understanding of its structural features and mathematical modelling.

   A structural observability concept (reachability matrix) introduced for the state estimation in power systems.

   A criterion to deal with a partially observed network.

3. Explanation of the different decomposition criteria for the state estimation problem in power systems.

   A decentralized state estimation for power systems.

   A heuristic procedure to decompose power system networks for the state estimation problem.

4. A suboptimal procedure using one mathematical model proposed to solve the measurement optimization problem.

   Mathematical modelling of the minimum number of collecting measurement centres problem in a graph theory framework.

CHAPTER TWO

POWER SYSTEMS STATE ESTIMATION

2.1 Introduction

The problem of state and parameter estimation in electrical energy systems can be described in the following manner:

Given a set of m measurements containing measurement (and/or modelling) errors, we wish to estimate the n-dimensional state vector describing the system where m is greater than n (redundancy) and observability is maintained (21,22). The estimated state vector is required to have the property of minimizing certain error function criteria. It may be desired to estimate a r-dimensional parameter vector of the model system, with $m \geq n+r$. In general, the solution of the state estimation problem will be required (apart from the parameter estimation) in an on-line mode. When it is required to estimate some parameters of the model of the system, it can be done in an off-line mode (30,29), although it has been suggested to do it together in an on-line mode in power systems (33). In mathematical terms the SEP is equivalent to a non-linear parame ter estimation in multivariable statistical analysis. Appendix 1 describes the properties of a linear least squares estimator. Here the focus of our attention will be on the numerical procedure for the (on-line) problem as an unconstrained non-linear programming. The method of Fletcher and Powell to solve the SEP has already been studied by Handshin (16), who showed its main advantages and disadvantages. Therefore, it will only be described briefly later on.

It is convenient to point out that the problem, in general, is to minimize a sum of squares, for which the methods of Newton are more advantageous (32).

The SEP makes the following demands on an algorithm: i) minimum core requirements; ii) short execution time, and iii) reliability. Several approaches have been suggested, not only for the theoretical analysis but for on-line applications in electrical utilities (11-15). In our case, we assume static state estimation, i.e., the computa-

tion time and the data gathering time together are such that the computer monitoring the system "sees" a static system during this period.

In the past, three methods have been applied to solve the SEP by exploiting certain properties of power systems. A general description of these methods is given in (17). The AEP method (line flows only), (2,3,6) has less requirements of core size and execution time than the other two, but it is less reliable in detecting data errors and identifying them (18). The optimality conditions are shadowed by the approximation assumed to justify the non-linear transformation of the variables, which obscures the statistical properties of the optimal solution (35).

The sequential least squares approach (Extended Kalman Filter, known as the BPA method) makes several assumptions to overcome numerical difficulties arising in its implementation (5,11). In general, the execution time is difficult to assess due to particular conditions of the system, program code, machine, etc., but with these restrictions in mind, its execution time has been found longer than the AEP's algorithm (20).

The third approach can be covered by the general name of Newton type methods (19). The first is the Gauss-Newton, known as the MIT method in power systems (1,32,18). This method requires more core than AEP's and the same order as BPA's and has potential divergence problems. Since these methods will be dealt with in detail in the following sections, at this stage we will only raise some general points relating to the three methods with a discussion on the requirements of a "good estimation algorithm".

Firstly, it is very difficult to obtain a general rule for choosing a particular estimator which is equally acceptable for any system because one estimator which yields good results with one system may not do so with another (18,20). For a certain system, the detection and identification of errors can be done more efficiently with one es-

timator than with another. It is then a question of trading-off reliability versus time. The AEP algorithm (line flows only) is fast, but it is weak in error detection. An improvement has been made by taking into account injection measurements, with the disadvantage that it increases execution time, but improves error detection capability (6,18).

In this chapter results of the following methods are shown: the non-linear least squares; the weighted non-linear least squares; and an extension of the latter using scaled weights. The Gauss-Newton method has been applied to estimate the state vector controlling the steps in the iteration process through a test of the validity of the Taylor series approximation.

2.2 Power system description

2.2.1 Power system model

The state estimation process can be described in the diagram shown in Fig. 2-1.

The structure of the system is obtained from all the elements connected to the nodes of the network. From this information, together with the parameters of the lines, transformers, etc., the admittance matrix of the system is formulated (23,24,25).

2.2.2 Measurement equations

The measurement functions in terms of the state vector and the admittance matrix are:

$$\text{Line flows:} \quad S_k^* = PL_{i,m} - jQL_{i,m} = V_i^* \quad (V_i - V_m)(y_{i,m}) + V_i y_{sh\,k} \tag{2-1}$$

where

k is the number of the line connecting node i to node m.

$y_{sh\,k}$ is the line charging admittance at measured end.

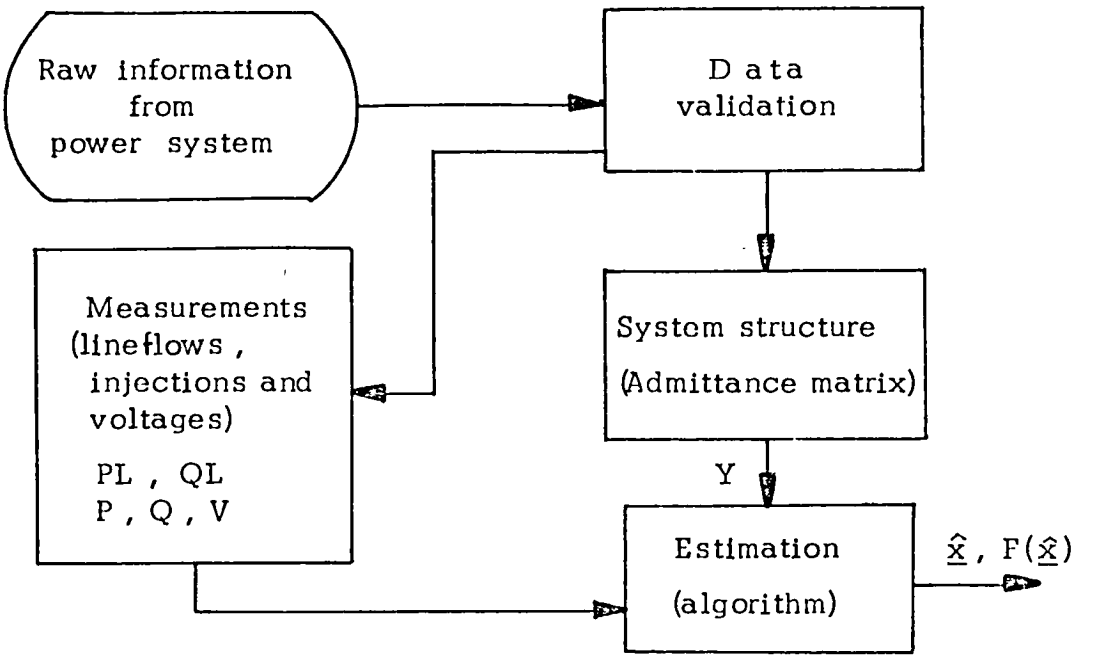

where
P, Q - real and reactive power injections
PL, QL - real and reactive power line flows
V - voltage magnitude
Y - admittance matrix
$\hat{x}$ - estimated state vector
F ($\hat{x}$) residuals sum of squares.

Fig. 2-1 Estimation process in power systems.

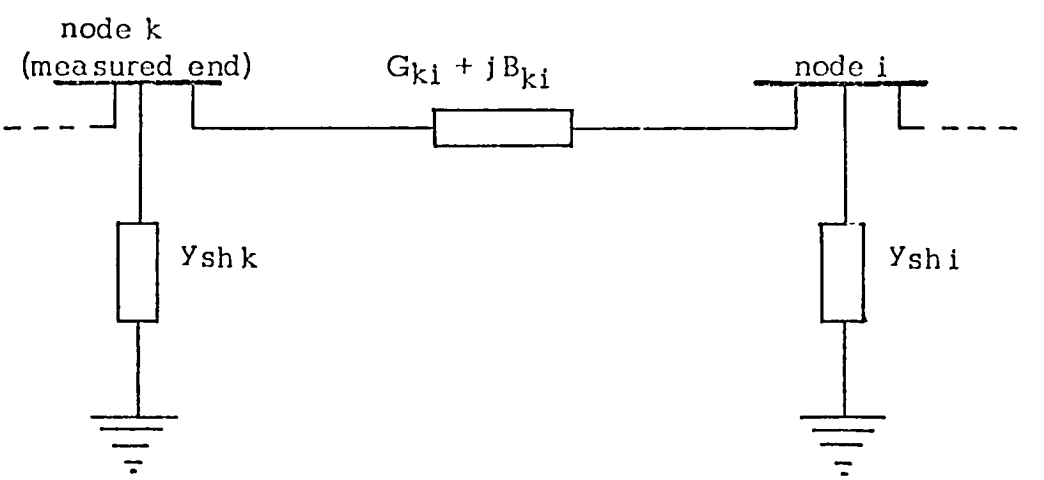

Fig. 2-2 Line parameters used in the formulation of measurement equations.

Node injections :

$$SI_k^* = P_k - jQ_k = V_k^* \sum_i y_{k,i} V_i \qquad (2\text{-}2)$$

$i \in \{\text{nodes connected to } k\}$

Voltage magnitude :

$$|V_k| = \sqrt{e_k^2 + f_k^2} \qquad (2\text{-}3)$$

where

SI_k = complex node injection at node k

V_k = complex voltage at node k

$[y_{k,i}]$ = admittance matrix of the network

e_k = real part of the complex voltage at node k

f_k = imaginary part

$*$ = conjugate of the corresponding complex variable .

As it will be necessary to use the Jacobian elements in the formulation and solution of the SEP, these elements can be computed from the next equations.

Jacobian expressions for line flow measurements are:

$$\frac{\partial P_{ij}}{\partial e_i} = -2 G_{ij} e_i + G_{ij} e_j - B_{ij} f_j \tag{2-4}$$

$$\frac{\partial P_{ij}}{\partial f_i} = -2G_{ij} f_i + G_{ij} f_j + B_{ij} e_j \tag{2-5}$$

$$\frac{\partial P_{ij}}{\partial e_j} = G_{ij} e_i + B_{ij} f_i \tag{2-6}$$

$$\frac{\partial P_{ij}}{\partial f_j} = G_{ij} f_i - B_{ij} e_i \tag{2-7}$$

$$\frac{\partial Q_{ij}}{\partial e_i} = 2e_i (B_{ij} - y_{ij}) - G_{ij} f_j - B_{ij} e_j \tag{2-8}$$

$$\frac{\partial Q_{ij}}{\partial f_i} = 2f_i (B_{ij} - y_{ij}) + G_{ij} e_j - B_{ij} f_j \tag{2-9}$$

$$\frac{\partial Q_{ij}}{\partial e_j} = \frac{P_{ij}}{f_j} \tag{2-10}$$

$$\frac{\partial Q_{ij}}{\partial f_j} = - \frac{P_{ij}}{e_j} \tag{2-11}$$

Jacobian expressions for injection measurements are:

$$\frac{\partial P_k}{\partial e_i} = G_{ki} e_k + B_{ki} f_k \quad ; \qquad k \neq i \tag{2-12}$$

$$\frac{\partial P_k}{\partial e_k} = \sum (-2G_{kj} e_k + G_{kj} e_j - B_{kj} f_j) \quad ; \tag{2-13}$$

$$j \in \{ \text{nodes connected to } k \}$$

$$\frac{\partial Q_k}{\partial e_i} = G_{ki} f_k - B_{ki} e_k \quad ; \quad k = i \tag{2-14}$$

$$\frac{\partial Q_k}{\partial e_k} = \sum (2B_{kj} e_k - 2y_{sh\,m} e_k - G_{kj} f_j - B_{kj} e_j) \quad ; \tag{2-15}$$

$$j \in \{\text{nodes connected to } k\}$$

$$\frac{\partial P_k}{\partial f_i} = \frac{\partial Q_k}{\partial e_i} \quad ; \quad k \neq i \tag{2-16}$$

$$\frac{\partial P_k}{\partial f_k} = \sum (-2G_{kj} f_k + G_{kj} f_j + B_{kj} e_j) \quad ; \tag{2-17}$$

$$j \in \{\text{nodes connected to } k\}$$

$$\frac{\partial Q_k}{\partial f_i} = - \frac{\partial P_k}{\partial e_i} \quad ; \quad k \neq i \tag{2-18}$$

$$\frac{\partial Q_k}{\partial f_k} = \sum (2B_{kj} f_k - 2y_{sh\,m} f_k + G_{kj} e_j - B_{kj} f_j) \quad ; \tag{2-19}$$

$$j \in \{\text{nodes connected to } k\}$$

Jacobian expressions for voltage magnitude measurements are:

$$\frac{\partial |V_k|}{\partial e_j} = 0 \quad ; \quad k \neq j \tag{2-20}$$

$$\frac{\partial |V_k|}{\partial f_j} = 0 \quad ; \quad k \neq j \tag{2-21}$$

$$\frac{\partial |V_k|}{\partial e_k} = \frac{e_k}{(e_k^2 + f_k^2)^{1/2}} \tag{2-22}$$

$$\frac{\partial |V_k|}{\partial f_k} = \frac{f_k}{(e_k^2 + f_k^2)^{1/2}} \tag{2-23}$$

where

$y_{sh\,m}$ is the line charging admittance of line m at the measured end;

$G_{ki} + j B_{ki}$ is the (k,i) element of the admittance matrix of the network.

2.3 Estimation algorithm

2.3.1. Problem statement

The SEP can be stated as follows:

Given $\underline{f}(\underline{x})$, a vector of m function mismatches between the estimated and measured values, where $\underline{x}$ is the n-dimensional state vector describing the system, the performance function

$$F(\underline{x}) = \underline{f}^t \underline{f} \qquad (2\text{-}24)$$

is to be minimized and values of $\hat{\underline{x}}$ found. Without loss of generality, a weighting function W can be included so that $F(\underline{x}) = f^t W f$.

The general problem of minimizing a sum of squares can be solved in various ways but there is no generally accepted algorithm. It can be considered as an unconstrained non-linear optimization problem to be solved by methods which deal with general problems of this type, according to several authors (16,25,26,36). However, the special form of equation (2-24) (sum of squares) and the experience with the Taylor series expansion to linearize the power system equations provides strong support to pursue this method.

2.3.2 Optimization procedure

The general solution is found by using the conditions of optimality

$$\underline{g} = -2 f^t J = \underline{0} \qquad (2\text{-}25)$$

where $\underline{g}$ is the gradient of equation (2-24) and J is the Jacobian matrix with elements i, j equal to $\partial f_i / \partial x_j$; $i = 1,\ldots,m$ and $j = 1,\ldots,n$. These elements are computed with equations (2-4) to (2-23).

In the general case, equation (2-25) represents a set of non-linear equations which can only be solved in an iterative procedure.

Thus, from eq. (2-25), (27,41)

$$x_{k+1} = x_k - \alpha_{k+1} \nabla F_k \tag{2-26}$$

where α is chosen to satisfy $F(x_k, \alpha_{k+1}) < F(x_k, \alpha_k)$, which defines the step length in the iteration process and in general is dependent on the vectors $\underline{x}_k, \underline{x}_{k-1}, \underline{x}_{k-2}, \cdots, \underline{x}_o$ where $\underline{x}_o$ is the starting point. At the limit,

$$\lim_{n \to \infty} \underline{x}_n = \hat{\underline{x}} \tag{2-27}$$

The expression (2-26) defines a sequence of computations to be performed in a minimum seeking procedure to determine the vector $\hat{\underline{x}}$. This is a steepest descent method. In general, it converges to the minimum but its convergence rate is very slow. This rate can be improved by applying a matrix A in the iterative process so that (27,32)

$$\underline{x}_{k+1} = x_k - A_{k+1} \nabla F_k \tag{2-28}$$

If A is chosen to be equal to the inverse of the Hessian matrix of F, then the Newton method results. It provides fast convergence when the starting point is located near the minimum. Hence,

$$x_{k+1} = x_k - (\nabla^2 F_k)^{-1} \nabla F_k \tag{2-29}$$

This method gives non-linear steps and care must be taken to ensure the positive-definiteness of the Hessian matrix. In our particular problem, the Hessian matrix is less sparse than the Jacobian and the matrix inversion is more expensive in terms of time and storage. To overcome the matrix inversion problem, another possibility is to use a positive definite matrix S_k. The expression is

$$\underline{x}_{k+1} = \underline{x}_k - \alpha_{k+1} S_{k+1} \nabla F_k \tag{2-30}$$

where α has the properties defined for the expression (2-26).

S_k is updated at each step by keeping its direction towards the minimum between iterations. In the end, the Hessian matrix is inverted in S. Again, the main problem is storage since S is a full matrix. This procedure is known as the Davidon-Fletcher-Powell algorithm (41). The search for α can be approximated without an exact linear search by maintaining the downhill direction in the updating process (37), but doing it without the matrix S explicitly. With triangular factorization it is possible to obtain an efficient algorithm, as reported by Gill and Murray (38). This general algorithm for unconstrained optimization has not been implemented in power systems problems, although it is likely to make good advantage of the sparsity in the network. But in the SEP the performance function is a sum of squares which can produce a very convenient result as described in the next subsection.

2.3.3 Gauss-Newton method

In general, non-linear models require non-linear procedures for estimation unless a method for the transformation of the variables is available to reduce the model to one that is linear in the parameters. It is possible that there are other specifying assumptions of the model which makes linear least squares applicable. It must be pointed out that the AEP method does not have optimal properties as far as least squares is concerned.

Now, to show the application of the Gauss-Newton method, we take the non-linear model

$$\underline{y} = f(x,Y) + \eta \qquad (2\text{-}31)$$

where $\underline{y}$ is a $m \times 1$ vector; Y is the admittance matrix of $n \times n$ order; $\underline{x}$ is the $n \times 1$ state vector and η the $m \times 1$ measurement error.

In this particular application to the power system equations, it has been found satisfactory to expand in a Taylor series and to

linearize by neglecting terms of order higher than the first.

Writing the sum of squares function as

$$F(\underline{x}) = \underline{\eta}^T \underline{\eta} \tag{2-32}$$

and linearizing eq. (2-31) by guessing a starting point, say, $\underline{x}_o$, around which to write the Taylor series expansion, gives

$$\underline{f}(\underline{x}, Y) = \underline{f}(\underline{x}_o, Y) + \nabla \underline{f}(\underline{x} - \underline{x}_o) + \frac{\nabla^2 \underline{f}}{2} (\underline{x} - \underline{x}_o)^2 \ldots \tag{2-33}$$

Neglecting the second and higher order terms and putting $\underline{f}_o = \underline{f}(x_o, Y)$, we have from eq. (2-33):

$$\underline{y} = \underline{f}_o + \nabla \underline{f}(\underline{x} - \underline{x}_o) + \underline{\eta}_o \tag{2-34}$$

Now let

$$J = \frac{\partial \underline{f}}{\partial \underline{x}} = \begin{bmatrix} \left.\frac{\partial f_{(1)}}{\partial x_1}\right|_o & \cdots & \left.\frac{\partial f_{(1)}}{\partial x_n}\right|_o \\ \vdots & & \vdots \\ \left.\frac{\partial f_{(m)}}{\partial x_1}\right|_o & \cdots & \left.\frac{\partial f_{(m)}}{\partial x_n}\right|_o \end{bmatrix} \tag{2-35}$$

where $\frac{\partial f_{(i)}}{\partial x_j}$ is the partial derivative of the corresponding function of the measurement i with respect to x_j.

The matrix J in (2-35) is of dimension $m \times n$. Now, let

$$\underline{r}_o = \underline{y} - \underline{f}_o \tag{2-36}$$

and

$$J_o = \left.\frac{\partial \underline{f}}{\partial \underline{x}}\right|_{x=x_o} \tag{2-37}$$

by combining (2-34), (2-36) and (2-37) we have

$$\underline{r}_o = J_o(\underline{x} - \underline{x}_o) + \underline{\eta}_o \tag{2-38}$$

Eq. (2-38) is a linear model on the state vector and as such can be solved with the well known linear least squares equations. These are described in Appendix 1.

Thus,

$$\Delta\underline{x}_o = (\underline{x} - \underline{x}_o) = (J^T J)^{-1} J^T \underline{r}_o \tag{2-39}$$

and we can evaluate

$$\underline{x}_1 = \underline{x}_o + \Delta\underline{x}_o \,. \tag{2-40}$$

We now start the next iteration and obtain

$$\underline{f}_1 = \underline{f}(\underline{x}_1, Y) \tag{2-41}$$

$$\underline{r}_1 = \underline{y} - \underline{f}_1 \tag{2-42}$$

$$J_1 = \left.\frac{\partial \underline{f}}{\partial \underline{x}}\right|_{\underline{x}=\underline{x}_1} \tag{2-43}$$

and the linear relation

$$\underline{r}_1 = J_1(\underline{x} - \underline{x}_1) + \underline{\eta}_1 \tag{2-44}$$

so we have

$$\Delta\underline{x}_1 = (J_1^T J_1)^{-1} J_1^T \underline{r}_1 \tag{2-45}$$

$$\underline{x}_2 = \underline{x}_1 + \Delta\underline{x}_1 \tag{2-46}$$

etc.

The process is continued, reaching the end when one or several of the following conditions are satisfied, depending on the chosen criterion:

a) the sum of squares equals a required value (zero when n=m. For practical purposes, a reasonably small number applies, rather than zero);

b) the deviation between iterations in the sum of squares reaches a pre-specified tolerance;

c) the difference between $\underline{x}_i$ and $\underline{x}_{i-1}$ is smaller or equal to a required minimum;

d) the maximum number of function evaluations is reached.

The sequence of equations (2-34), (2-41- 2-46) can be summarized as follows:

$$\underline{x}_{i+1} = \underline{x}_i - B_i^{-1} J_i^T \underline{r}_i \tag{2-47}$$

where

$$B_i = J_i^T J_i \tag{2-48}$$

The computed sequence of values obtained from each linear least squares step leads us, in principle, to the point $\hat{\underline{x}}$ and gives consistent estimates. The method gives a maximum likelihood estimators for each iteration if the errors are normally distributed. Details of the asymptotic variance-covariance matrix of non-linear least squares estimates are given in (39).

Let us now examine eq. (2-47) and compare it with (2-29). This enables us to substitute the Hessian matrix F by its approximate, B. Thus,

$$B_i^{-1} \doteq (\nabla^2 F_k)^{-1} \tag{2-49}$$

which is equivalent to substituting the Hessian matrix in eq. (2-29) by its approximate $J^T J$ (41).

The Gauss-Newton algorithm is therefore as follows:

1.- Set initial values for $\underline{x}_o$;

2.- compute F ;

3.- compute J ;

4.- form $A = J^T J$ and $J^T \underline{r}$;

5.- compute $\Delta \underline{x}$ using $A \Delta \underline{x} = J^T \underline{r}$;

6.- compare $\Delta \underline{x}$ against tolerance (another criterion can be used or augmented), if it is reached, go to 8 ;

7.- update $\underline{x}_{k+1} = \underline{x}_k + \Delta \underline{x}$ and return to 2;

8.- stop.

2.3.4 Marquardt method

It is to be noted that there may be some cases in power systems in which non-linear effects predominate, for which the surface of the objective function forms "ridges" as in Fig. 2-3. In these cases the directions generated by the Gauss-Newton method form angles nearly 90 degrees away from the steepest descent direction and can produce convergence problems. Computer experiments have shown that when there is an error in the parameters of the model or in the data points, the Newton method can exhibit erratic behaviour.

Regarding the convergence problems, Marquardt and Levenverg have suggested that a bias to the "downhill" direction be applied to the Newton step (9,10,40), which can be done in the following way:

Rewriting the Newton step and, since in the remaining equations we shall only be concerned with a single iteration, dropping the subscripts, gives

$$J^T J \, \Delta \underline{x} = J^T \underline{r} \qquad (2\text{-}50)$$

Let us now try a better approximation to the Hessian matrix by introducing a parameter λ and the matrix D and writing the system of equations as

$$(J^T J + \lambda D) \, \Delta x = J^T r \qquad (2\text{-}51)$$

Matrix D is a diagonal matrix that can be obtained from i) $D = I$, or ii) $D = \text{diag}\,(J^T J)$. λ has the properties of α in the expression (2-26). λ in (2-51) has the following properties: i) when $\lambda = 0$, the solution of (2-51) reduces to the solution of (2-50), the Newton step; ii) when λ is large ($\rightarrow \infty$), the expression (2-51) gives a step proportional to the steepest descent method in the same direction. A geometrical interpretation of the idea can be illustrated

in Fig. 2-4, which is drawn on the plane defined by the Taylor series point and the line of steepest descent at the starting point 0; TS is the Taylor series point and OSD is the direction of the steepest descent.

Since the sum of squares must decrease initially along OSD and since the Taylor series approximation predicts a reduced sum of squares at the point TS then it is reasonable to suppose that reduced values of the sum of squares can be found over a part of the area OTSSD. Overall strategy demands that the base point for the next iteration be as far away as possible from 0 but that the number of evaluations of the least squares surface be kept to a minimum.

With these considerations the next base point will be taken at the first point found with a reduction in the sum of squares. Clearly the first point to be investigated must be the Taylor series point, TS. If this is not successful then the validity of the linear approximation to the model at 0 does not range as far as TS.

Fig. 2-5 shows the flow chart for the Marquardt method. We are not going into details, since a modified method is being described. It can be seen that now we are creating an additional problem, the selection of λ such that it satisfies the condition of decreasing the value of the objective function F, i.e., $F(x,\lambda) > F(x+\Delta x,\lambda)$. Levenberg showed that this is possible but if λ is too large, there will be problems of slow convergence rate associated with the steepest descent method. On the other hand, if λ is too small (including zero) and the function F has narrow valleys, there will be numerical problems. Then a compromise has to be made. It has been recognized that on many occasions the Taylor series expansion linearizing the system equations has given satisfactory results (28). This means that since we do not have strong non-linear effects, it is wise not to throw away the advantages of the Newton step. To ensure this, it is possible to test the linear approximation adequacy

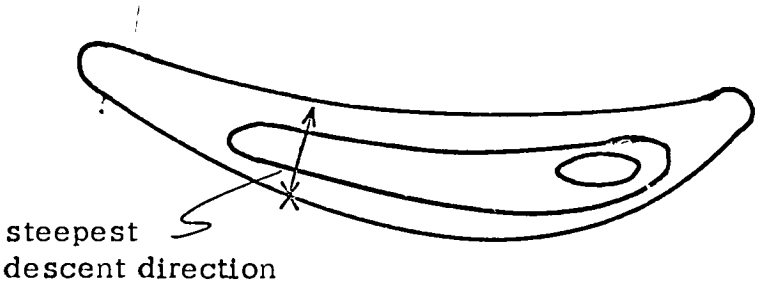

Fig. 2-3 Objective function surface with "ridges".

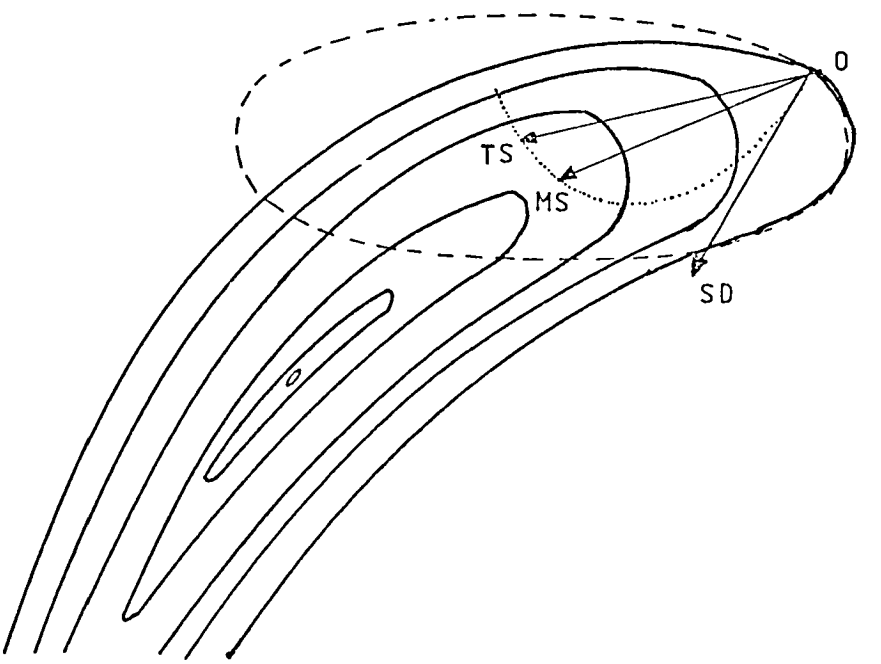

Fig. 2-4 Geometrical interpretation of Marquardt method.

and take advantage of the feature of the Newton method to provide a minimum in the local vicinity.

2.3.5 Linearity test

Given a linear model

$$\underline{y} = A\underline{x} + \underline{r} \tag{2-52}$$

where

$\underline{y}$ is a m-dimensional vector

$\underline{x}$ is a n- " "

$\underline{r}$ is a m- " "

A is a m×n matrix

and the function

$$F(\underline{x}) = \underline{r}^T \underline{r} \tag{2-53}$$

we can write for $\underline{x}$ and $\underline{x}+\Delta\underline{x}$, the following expressions

$$F(\underline{x}) = r_1^T r_1 \tag{2-54}$$

$$F(\underline{x}+\Delta\underline{x}) = r_2^T r_2 \tag{2-55}$$

or

$$F(\underline{x}) = (\underline{y} - A\underline{x})^T (y - A\underline{x}) \tag{2-56}$$

$$F(\underline{x}+\Delta\underline{x}) = (\underline{y} - A(\underline{x}+\Delta\underline{x}))^T (y - A(\underline{x}+\Delta\underline{x})) \tag{2-57}$$

Expanding the products and subtracting (2-57) from (2-56) we have

$$\begin{aligned} F(\underline{x}) - F(\underline{x}+\Delta\underline{x}) &= (\Delta\underline{x})^T A^T \underline{y} + \underline{y}^T A(\Delta\underline{x}) - (\Delta\underline{x})^T A^T A\underline{x} - \\ &\quad \underline{x}^T A^T A(\Delta\underline{x}) - (\Delta\underline{x})^T A^T A(\Delta\underline{x}) \\ &= (\Delta\underline{x})^T A^T (\underline{y} - A\underline{x}) + (\underline{y}^T - \underline{x}^T A^T) A(\Delta\underline{x}) - \\ &\quad (\Delta\underline{x})^T A^T A(\Delta\underline{x}) \end{aligned} \tag{2-58}$$

Using (2-52) and the commutativity of scalar product between

vectors, we obtain

$$F(\underline{x}) - F(\underline{x}+\Delta\underline{x}) = 2(\Delta\underline{x})^T A^T \underline{r}_1 - (\Delta\underline{x})^T A^T A(\Delta\underline{x}) \qquad (2\text{-}59)$$

Returning to the non-linear model we can now define a ratio which expresses the validity of the linear Taylor series approximation. Substituting

$$\underline{r} = \underline{r}_1$$

$$J = A$$

$$B = A^T A$$

into eq. (2-59), then the ratio φ can be expressed as

$$\varphi = \frac{F(x) - F(x+\Delta x)}{2\,\Delta\underline{x}^T J^T \underline{r} - \Delta\underline{x}^T B\,\Delta\underline{x}} \qquad (2\text{-}60)$$

It is convenient to note that when $\lambda = 0$,

$$B\,\Delta\underline{x} = A^T \underline{r}$$

Then, from eq. (2-60) we have

$$F(\underline{x}) - F(\underline{x}+\Delta x) = \Delta\underline{x}^T A^T \underline{r}\,\varphi \qquad (2\text{-}61)$$

The term $A^T \underline{r}$ is always computed, so the test in the case of $\lambda = 0$ requires only one vector multiplication.

The ratio φ in (2-60) takes values near to unity when a linear model is fitted. This implies that λ ought to be small or reduced. If the ratio φ is near to or less than zero, then λ ought to be increased. However, for some intermediate values of φ, it has been suggested (10) that constant bounds a and b be incorporated such that $0<a<b<1$, in the test of φ. It is considered that with $a = 0.25$ and $b = 0.75$, the number of modifications to λ will be reduced with guaranteed convergence.

As shown in the flow chart in Fig. 2-5, when necessary λ is increased by multiplying by v. In the algorithm used, a range be-

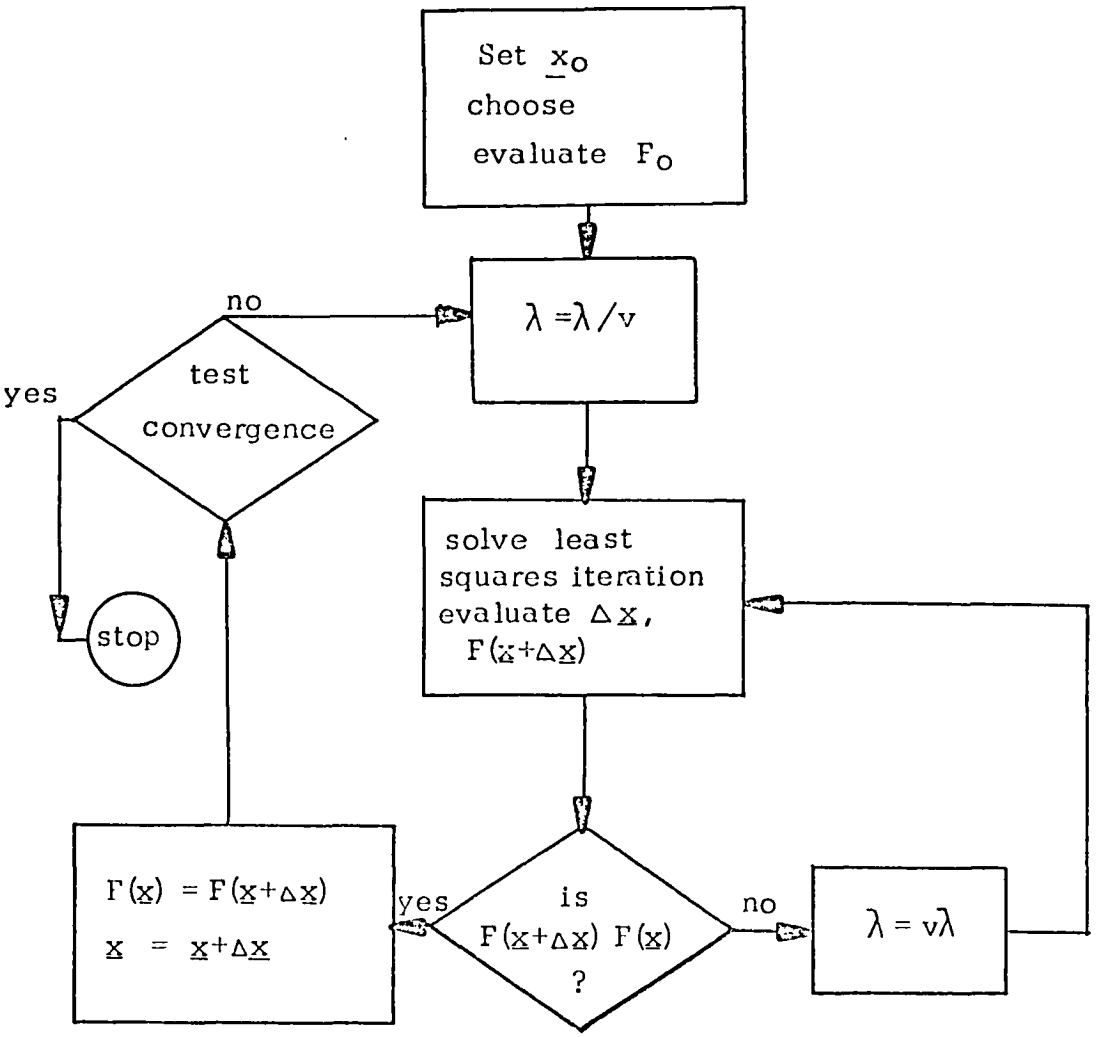

Fig. 2-5 Flow chart for the Marquardt method.

tween 2 and 10 is assigned to v. Detailed theoretical considerations and other features are given in (10,42). The rightness of the linearity test and its bounds was verified by the values obtained with the different systems tested. Tables 2-1 and 2-2 show the values obtained for 4 examples.

2.3.6 Algorithm description

The flow chart for the modified Marquardt method is shown in Fig. 2-6. The estimation procedure is as follows:

1.- Setting up of initial conditions.

a) Read system parameters and structure;

b) obtain system conditions from a load flow analysis;

c) set flat voltage profile, i.e., voltage angle equal to zero and magnitude equal to 1 for all unknown node voltages of the system;

d) set up measurement system simulation.

2.- Problem solution.

a) Set $\lambda = 0$, compute F_o, J_o and $J_o \underline{r}_o$;

b) evaluate residuals and sum of squares;

c) compute Jacobian elements;

d) set up i) $J^T W J$; ii) $J^T W \underline{r}$;

e) evaluate $\Delta \underline{x}$;

f) test for linearity conditions and reduction of F. If φ is near unity, set $\underline{x}_{k+1} = \underline{x}_k + \Delta \underline{x}$; otherwise evaluate λ and return to (b), this time skipping steps (c) and (d) i));

g) check with specified stopping rule, in our case comparing changes in state vector ≤ 0.0001. If stopping rule is satisfied, stop. Otherwise return to (c).

Some useful simplifications can be applied. For example, the Jacobian evaluation can be skipped provided its elements have only small changes after the first correction. This applies especially if

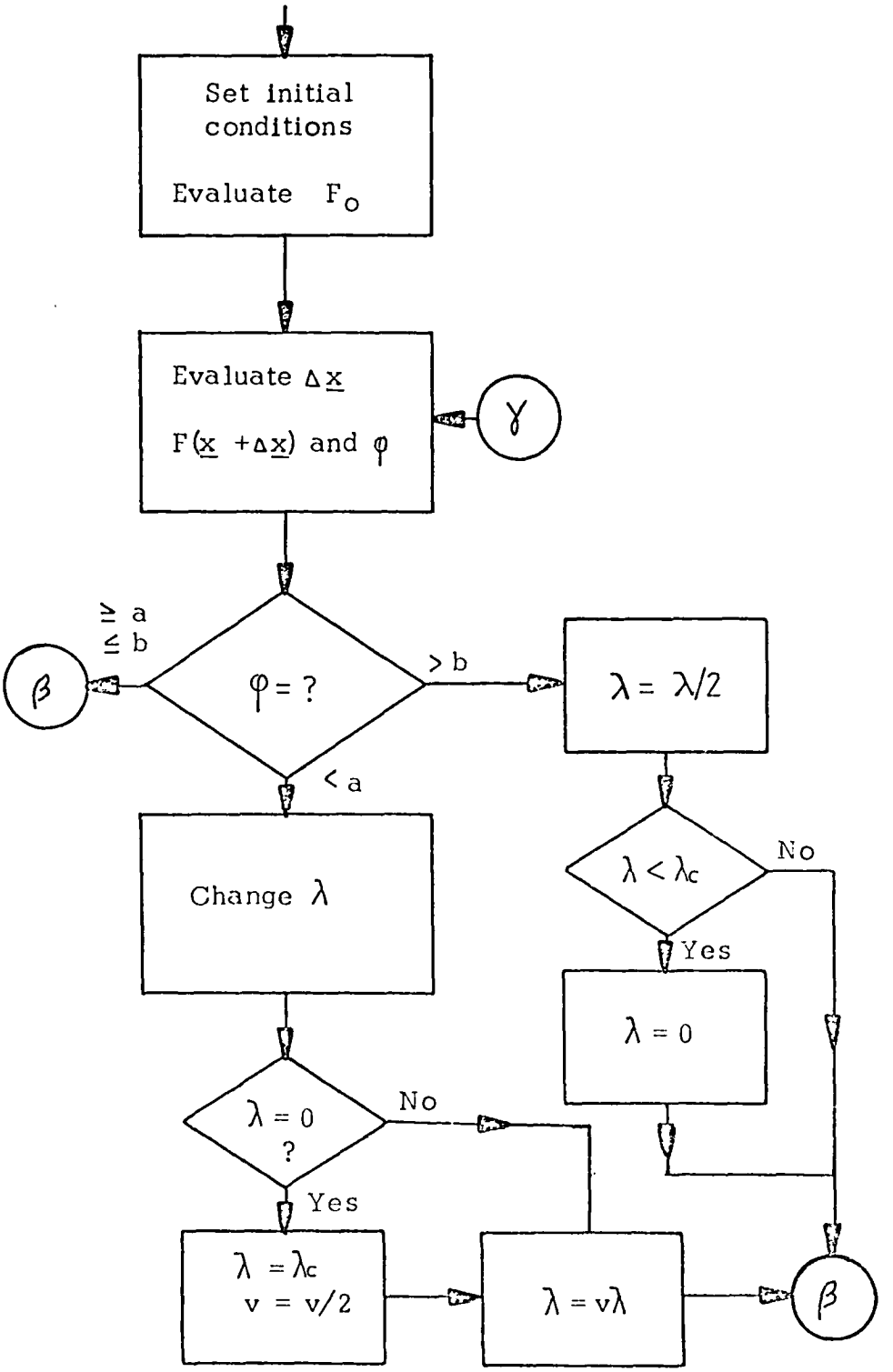

Fig. 2-6 Flow chart for the modified Marquardt method.

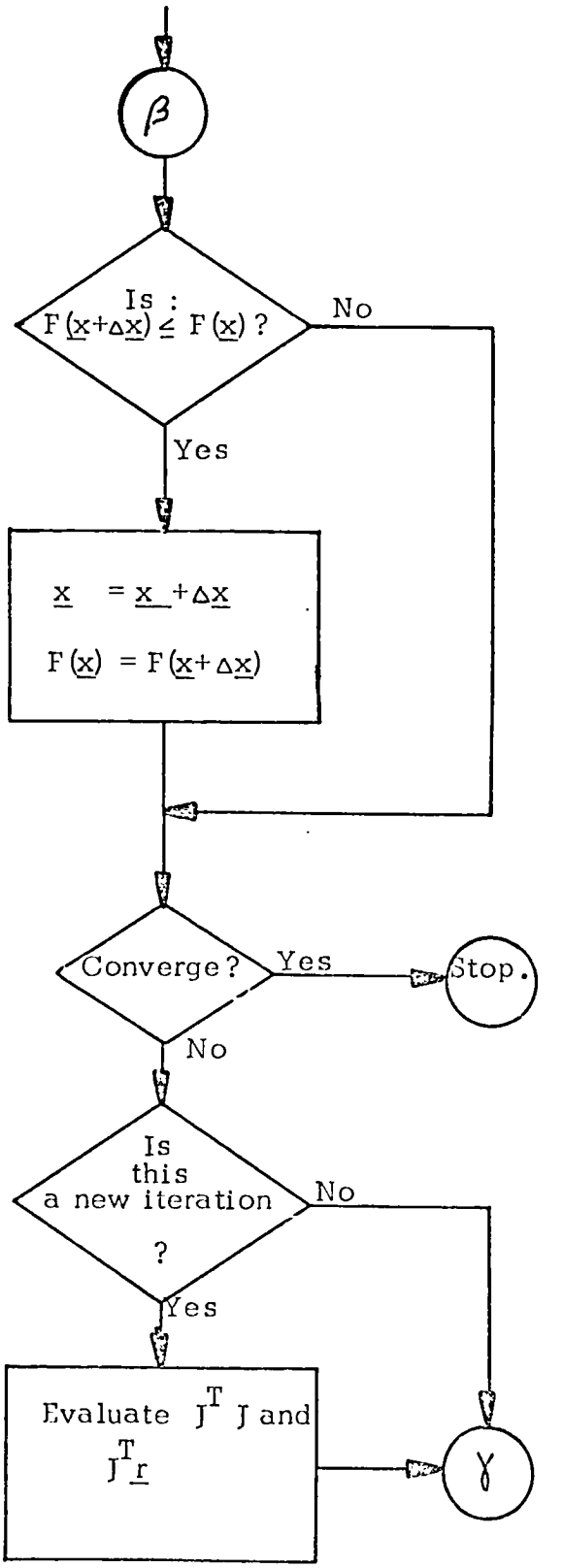
β
Is : F(x+Δx) ≤ F(x) ?
No
Yes
x = x + Δx
F(x) = F(x+Δx)
Converge?
Yes
Stop.
No
Is this a new iteration ?
No
Yes
Evaluate J^T J and J^T r
γ

Fig. 2-6 (cont'd)

Table 2-1 Values of φ for the 14 node system.

Iteration number	Measurements	
	24 LM and 6 Inj.*	26 LM
1	0.7795	0.8511
2	0.9916	1.0000
3	0.9966	1.0010
4	0.8114	1.0047

Table 2-2 Values of φ for the 23 node system .

Iteration number	Measurements	
	24 LM and 6 Inj.	32 LM
1	0.8984	0.8964
2	0.9995	0.9998
3	0.9877	0.9999
4	0.7622	0.9976

* LM = complex line flow measurement.

Inj. = complex node injection measurement.

we start with a precomputed solution and the system conditions have only changed by, say, 10 - 20%.

The setting up of $J^T W J$ can be done as in (44), where an automatic procedure is used to obtain the matrix structure and the optimal order of the system of equations. The computer programs developed to test the algorithm used Cholevsky's method to solve the linear system of symmetric equations. For practical applications, sparsity techniques should be used. Another successful technique is the Zollenkopf bi-factorization method which exploits the sparsity feature of the power system network (45).

2.4 Simulation

2.4.1 Measurement error modelling

In the numerical tests the measurement errors were modelled as follows:

$$\text{Standard deviation} = 0.0035 \times (\text{full scale}) + 0.02 \times (\text{load flow magnitude}) \quad (2\text{-}62)$$

An automatic procedure was developed which took into account several ranges of values to include a general error simulation for several systems. For example, a line with a power flow from 0 to 40 MW will have a full scale meter of 50 MW. Fig. 2-7 shows the corresponding program flow chart. The system data are on a basis of 100 MVA, and the full scale is set to unity at the beginning.

The simulated error is computed as follows:

$$\text{Error} = \text{range} \times (\text{random number}) \quad (2\text{-}63)$$

where the value of the random number is produced by a uniform distribution pseudo-random generator and is bounded between -1 and 1. The range is the corresponding value of the standard deviation as given by eq. (2-62) multiplied by $\sqrt{3}$ (43). This is shown in Fig. 2-8 i) which depicts the density function of a uni-

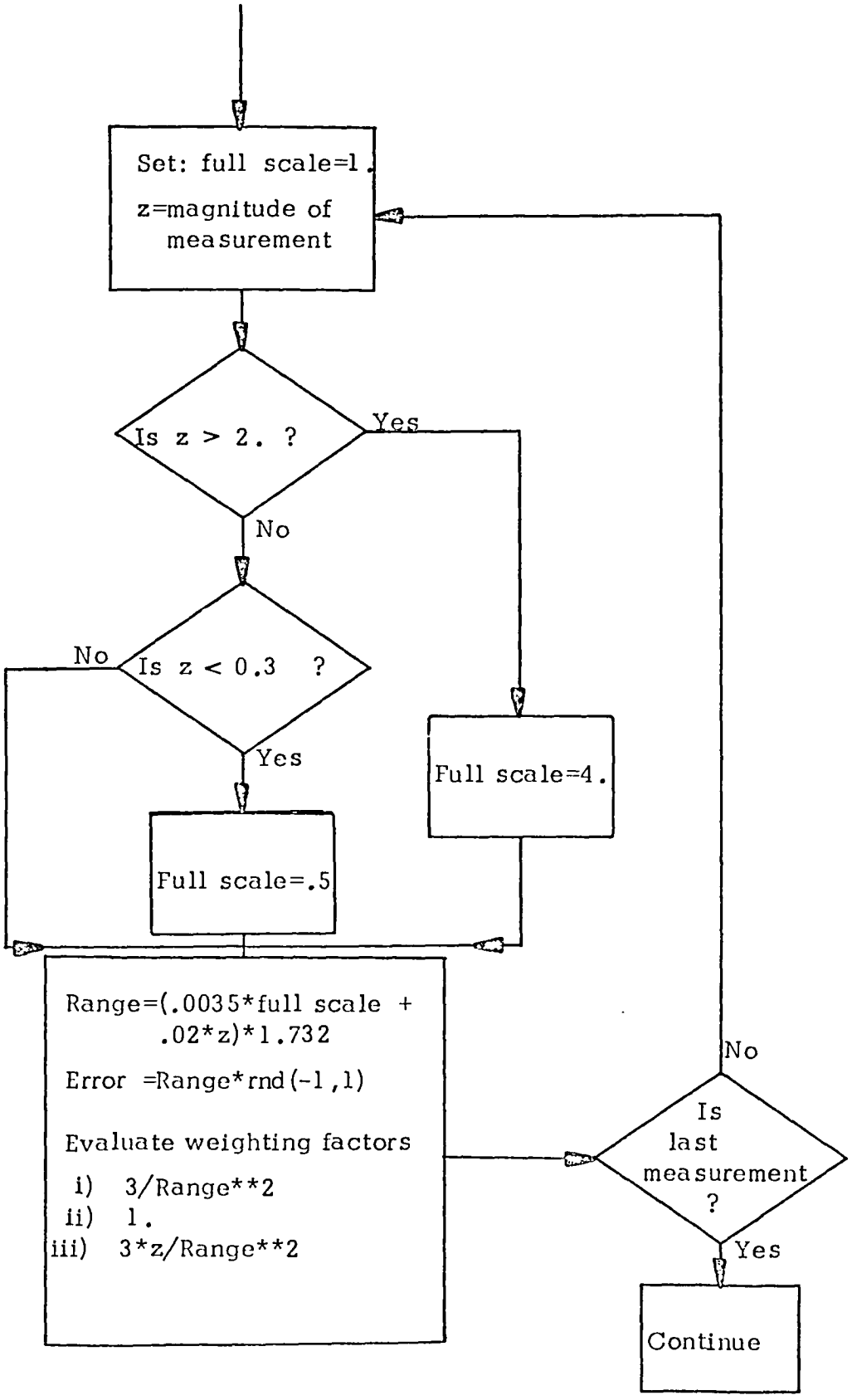

Fig. 2-7 Flow chart of measurement simulation.

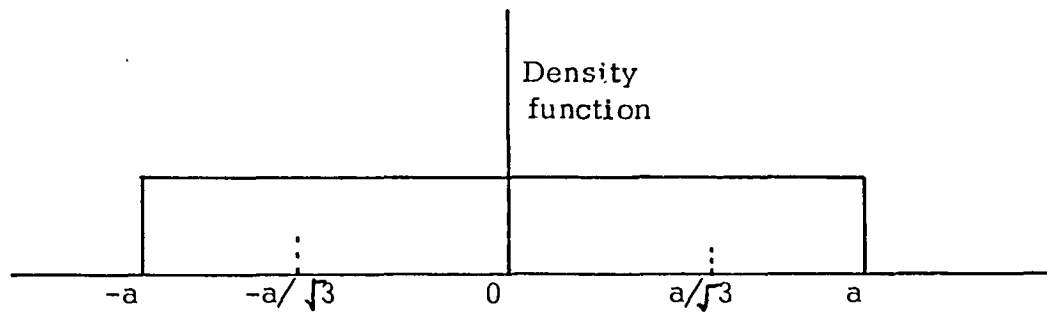

(i)

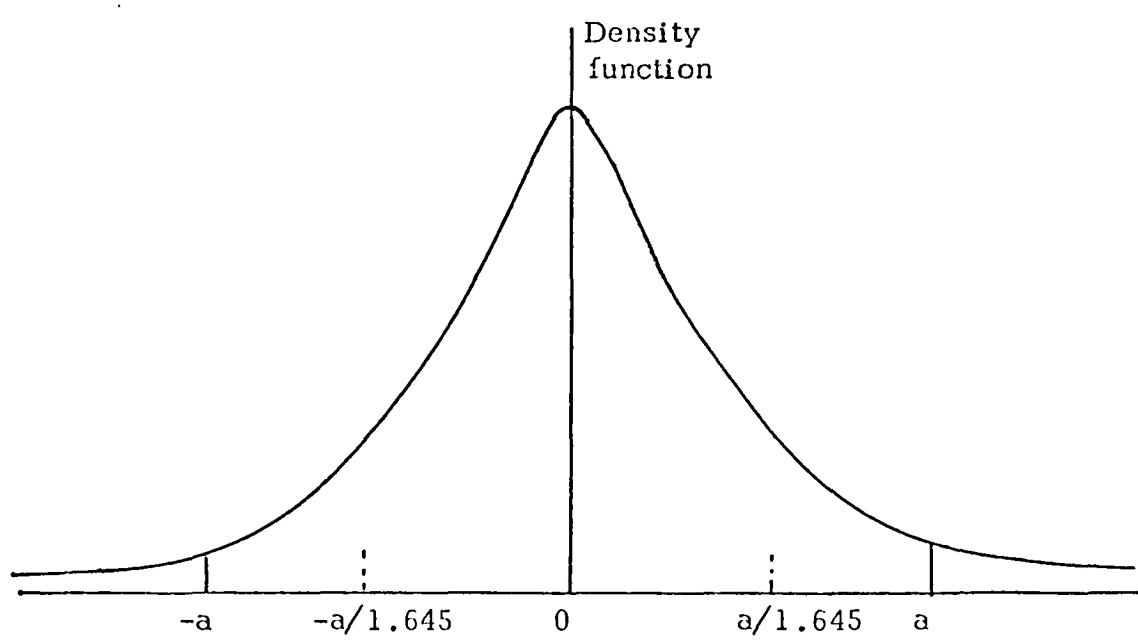

(ii)

Fig. 2-8 (i) Uniform random variable

(ii) Normal random variable

form random variable. This function has been chosen because it provides the worst case, the greatest dispersion for a given standard deviation. Comparing with the normal distribution, this gives a greater closeness to the true values in the chosen range, as shown in Fig. 2-8 ii).

2.4.2 Considerations on weights

The aim in applying weights in the performance function (2-24), as described in Appendix 1, is to associate the residuals of each measurement with the accuracy that one can expect from that particular measurement. These weights are evaluated from the variance values corresponding to a uniform distribution in our case. Then we have

$$\text{Weight} = 3/(\text{value of range})^2 \qquad (2\text{-}64)$$

However, if we use the expression (2-62) there are certain conditions which will arise in a practical situation that we need to consider. An example will clarify this point.

Let us have the variance for a uniform distribution given by

$$\text{Variance} = 10^{-4} \times (2y + 0.35)^2/3 \qquad (2\text{-}65)$$

Computing the weights for different values of y, we obtain the second column of Table 2-3.

Table 2-3 Weights and scaled weights.

y	w = 1/variance	w = Abs(y)/variance
1.00	5200	5200
0.75	6800	5100
0.50	14500	7250
0.25	31000	7750
0.10	71200	7120
0.00	81700	0000

Table 2-3 shows a modified weight, scaled by the division of the variance with the absolute value of y. It is easy to see that the effect of making the weights equal to the reciprocal of the variance given by eq. (2-65) is opposite to the desired one, since it gives more weight to those measurements which in relative terms are more inaccurate as is apparent from the second column of the table. The third column provides a more regular behaviour. Extending this idea, the next step is to consider equal weights for all the measurements.

When the scaled weights are used, the RHS of eq. (2-64) is multiplied by the corresponding absolute value of the measurement.

2.5 Numerical results

The systems analysed are: a 5 node and 7 line system (23), a 14 node and 20 line system (55) and a portion of the CEGB network, which consists of 23 nodes and 30 lines (58). The corresponding data for these systems are given in Appendix 4.

Figures 2-12 to 2-19 show the measured points for the different systems tested. The criterion emplyed in the choice of measurement points was to select those nodes with the largest number of lines, since it is usual that the cost is heavily dependent on the amount of gathering and measuring equipment at each node.

Table 2-6 shows the number of iterations required to find a solution with a stopping criterion of change in node voltages ≤ 0.0001. It can be seen that the number of iterations is fairly independent of the size of the system. The last iteration is generally unnecessary but is computed to detect the changes in the state vector.

Table 2-7 shows the change of the objective function versus iteration numbers for some of the different systems tested.

Tables 2-8 to 2-21 show the voltages obtained with the different systems for the weighting factors used, together with the "true" values from load flow. It can be noticed that there is little difference

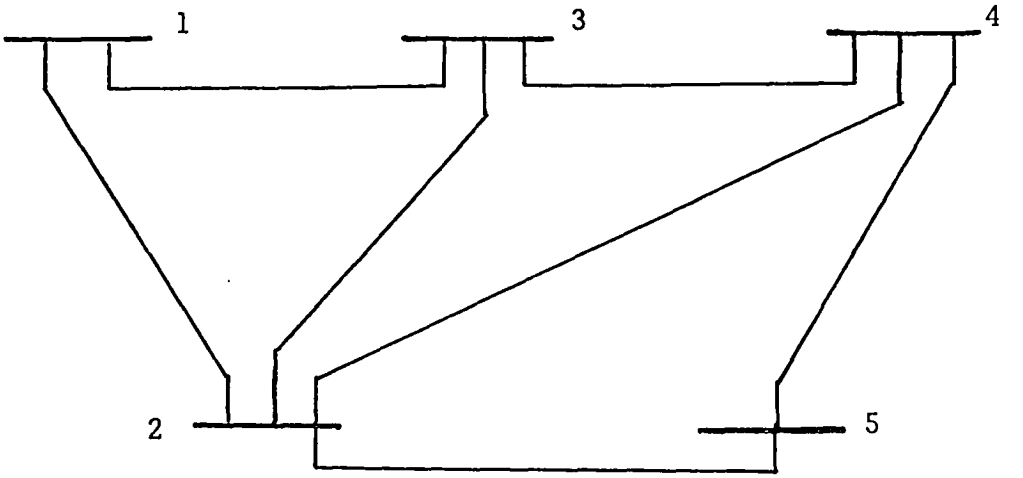

(a)

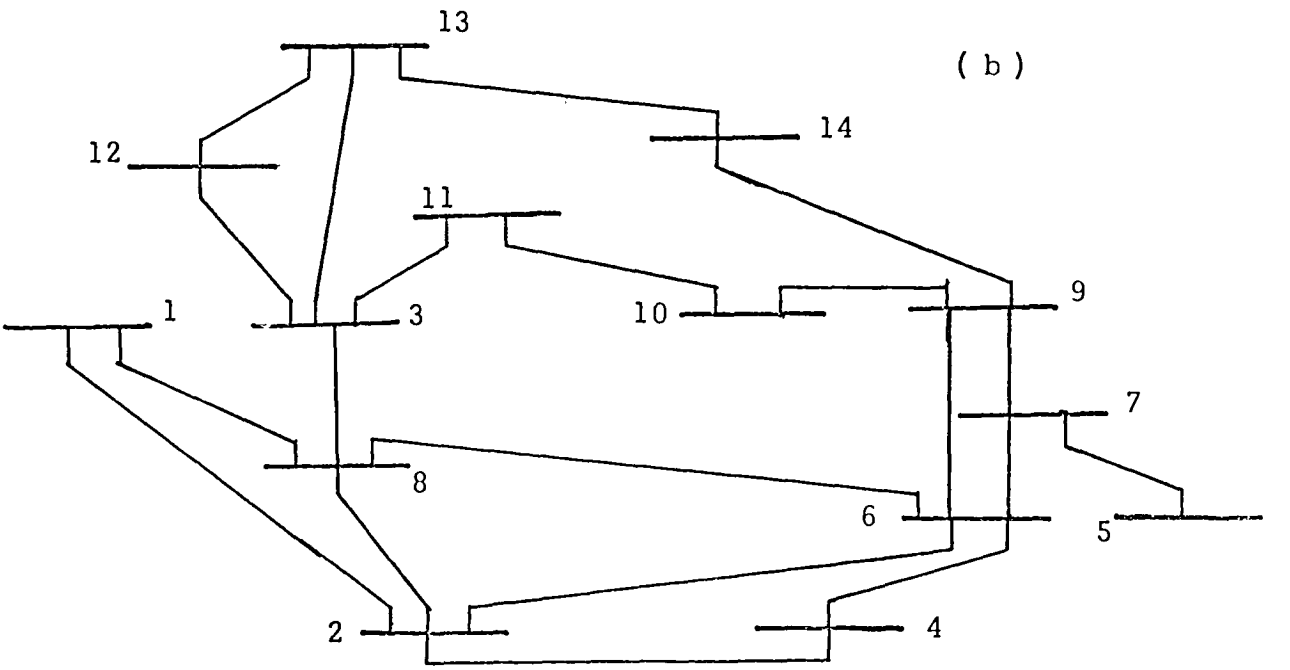

Fig. 2-9 (a) Five node, seven line system.
(b) Fourteen node, twenty line system.

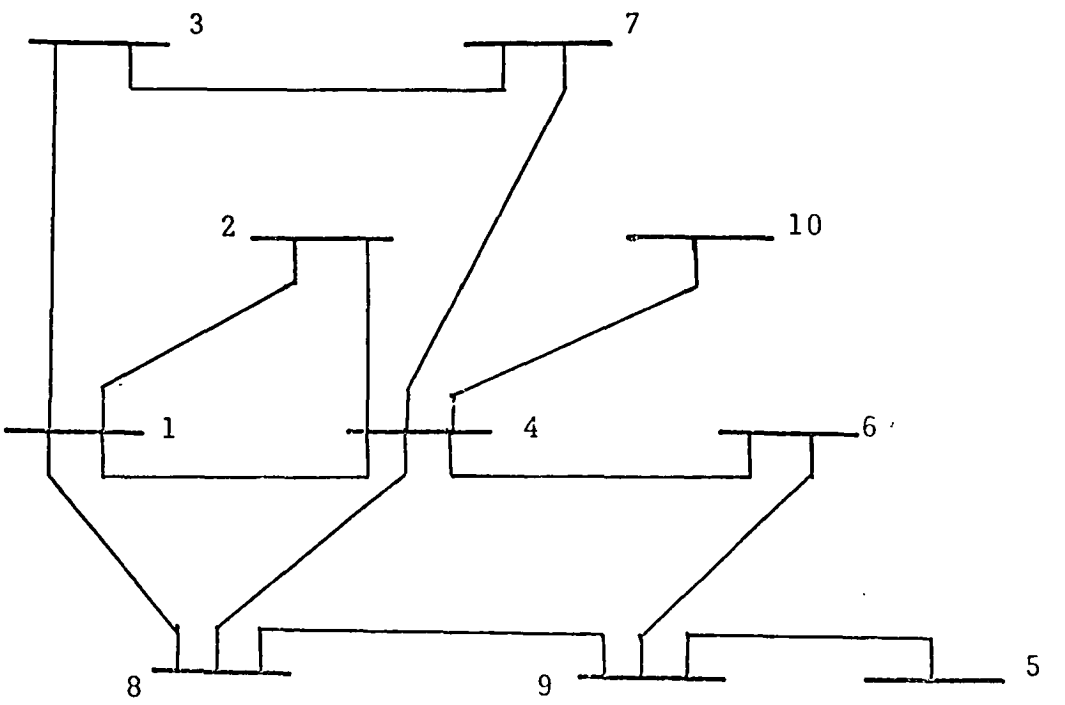

Fig. 2-10 Ten node, thirteen line system.

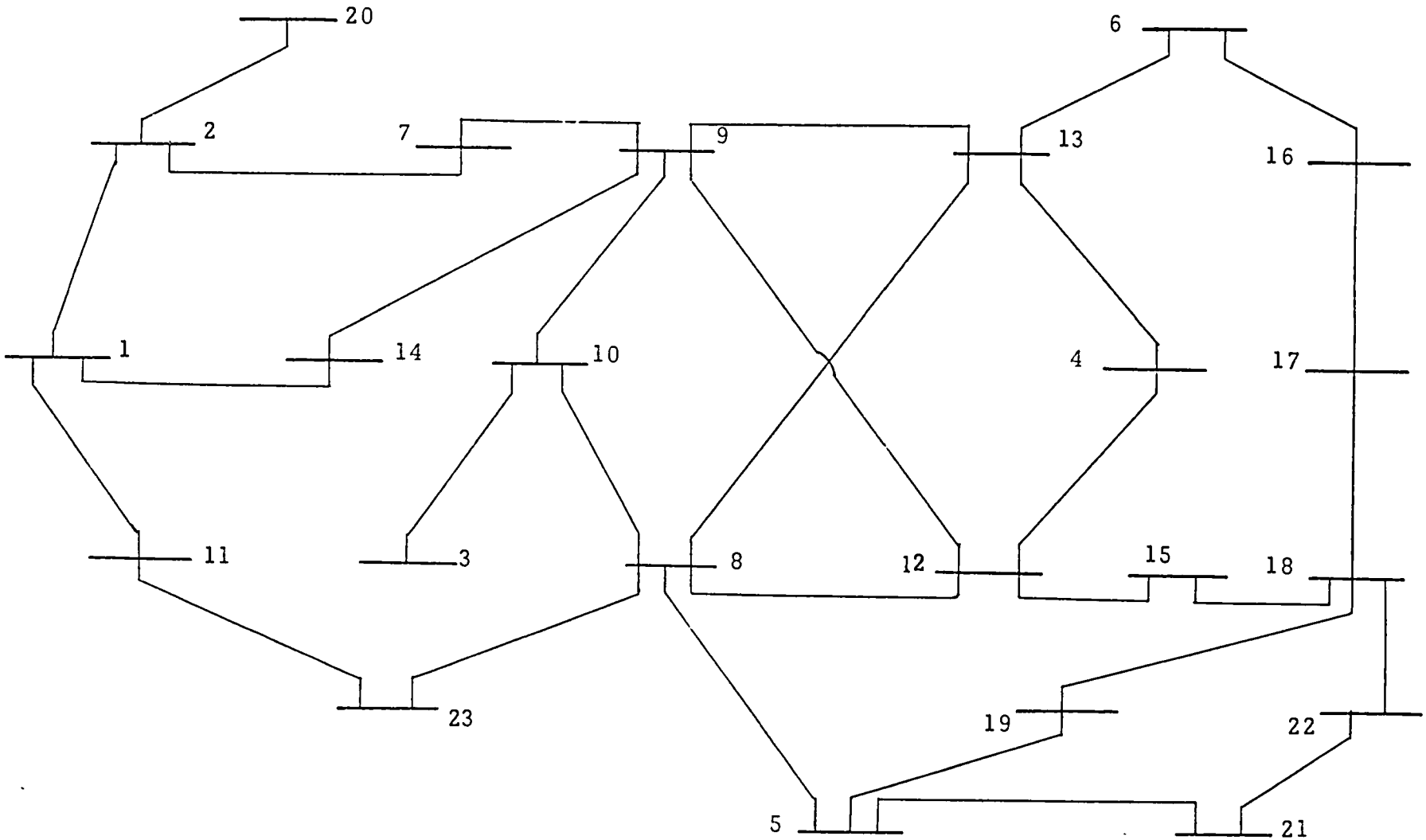

Fig. 2-11 Twenty three node, thirty line system.

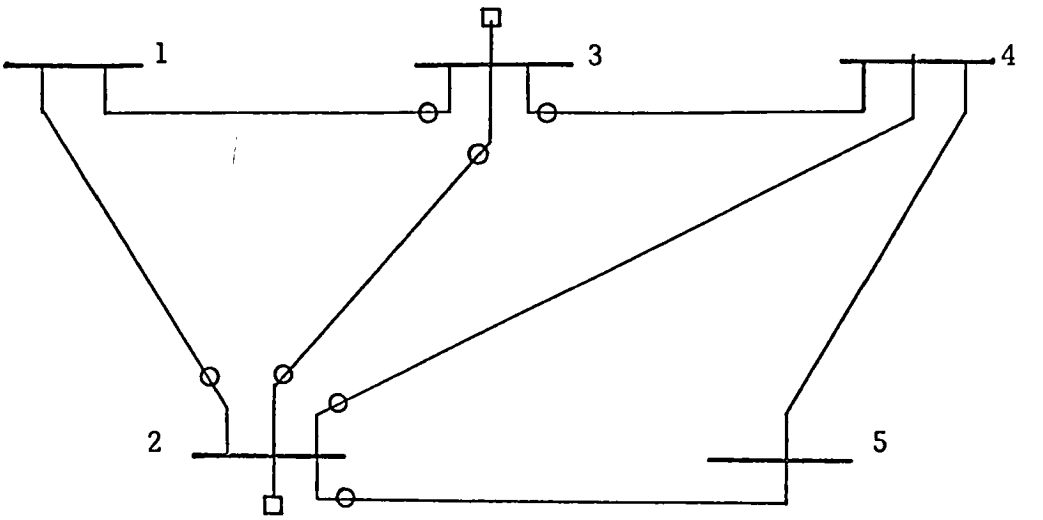

○ Complex line flow measurement

□ Complex injection measurement

Fig. 2-12 2 complex injections and 7 complex line flows measurement sample.

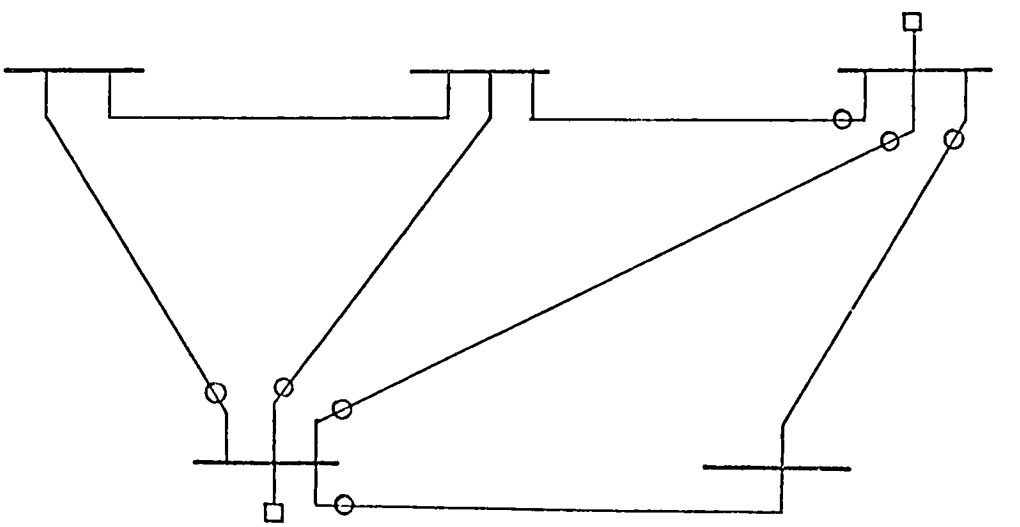

Fig.2-13 2 complex injections and 7complex line flows measurement sample.

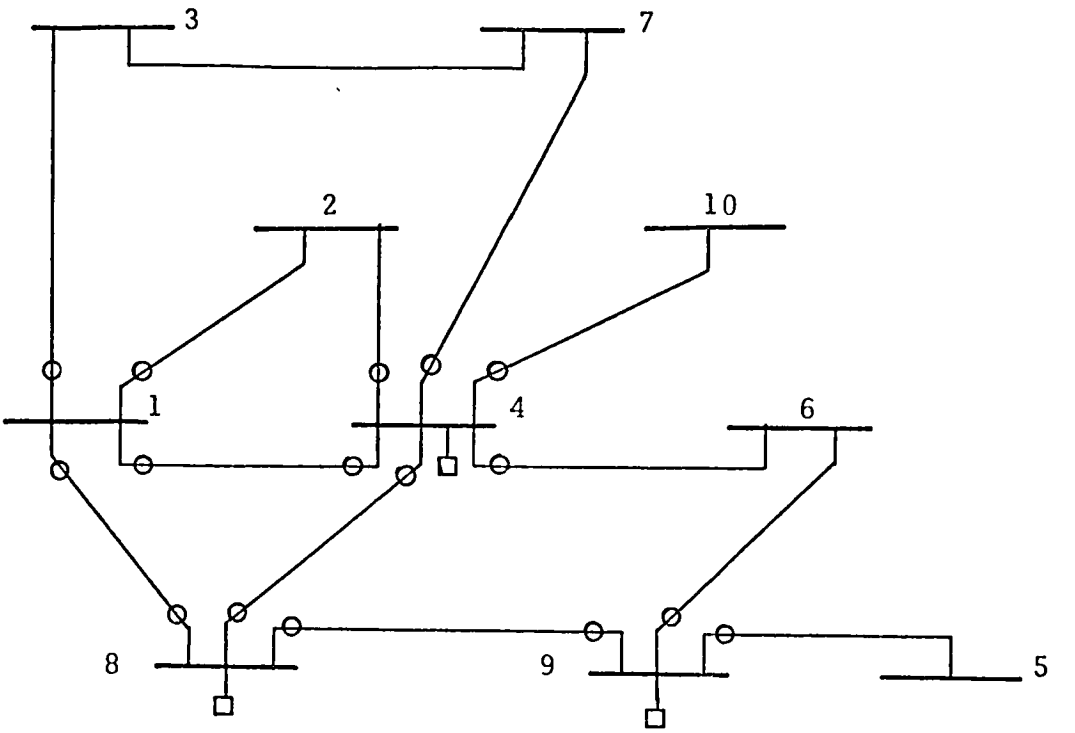

Fig. 2-14 3 complex injections and 16 complex line flows measurement sample.

□ Complex injection measurement

○ Complex line flow measurement

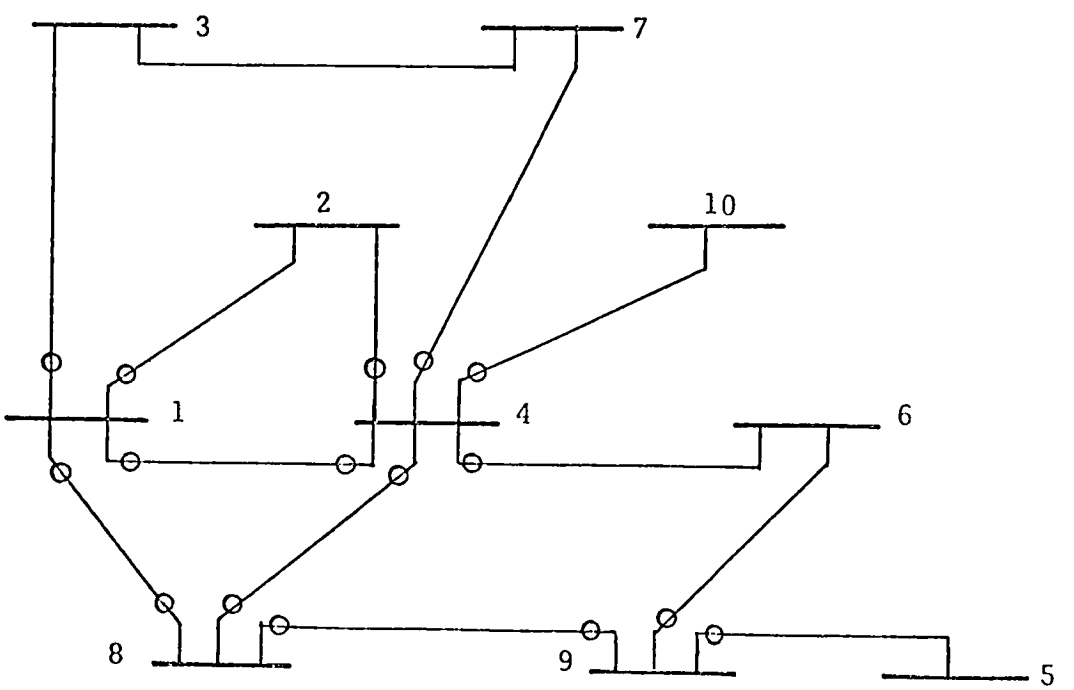

Fig. 2-15 16 complex line flows measurement sample.

□ Complex injection measurement

○ Complex line flow measurement

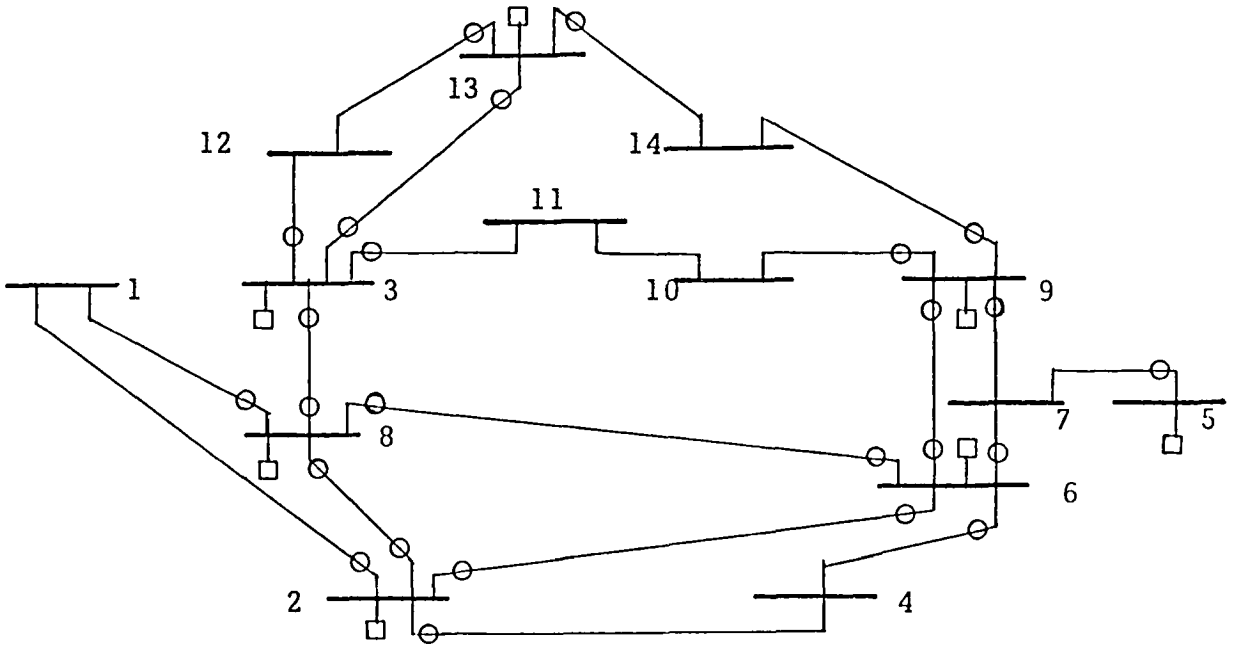

Fig. 2-16 7 complex injections and 25 complex line flows measurement sample.

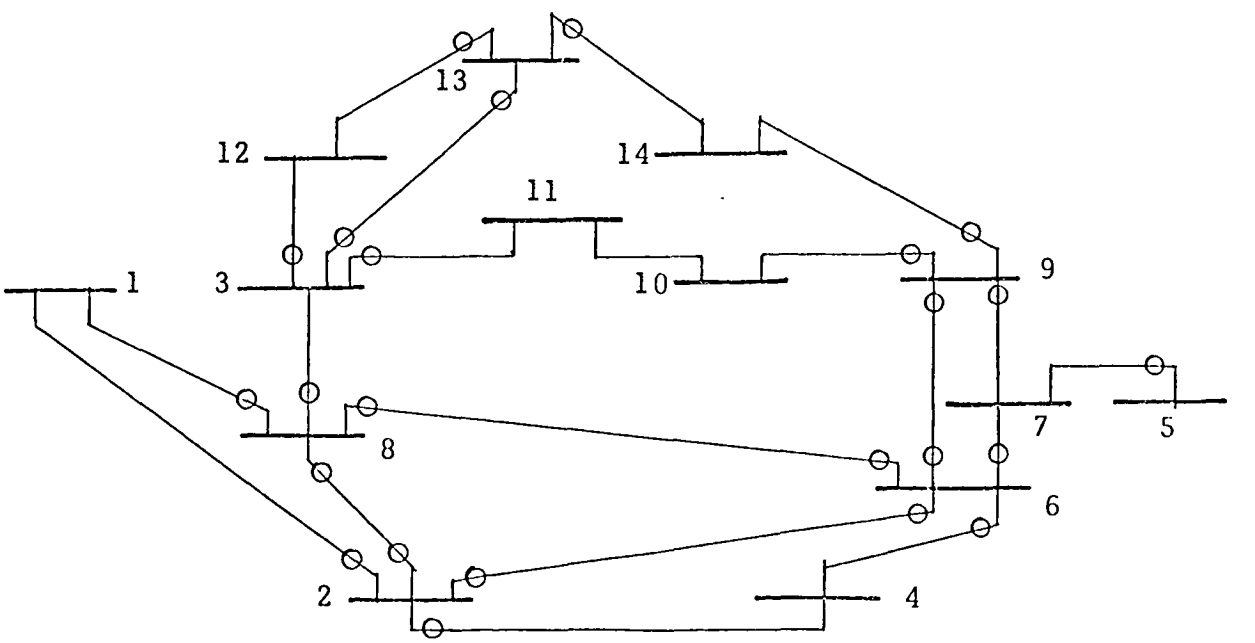

Fig. 2-17 25 complex line flows measurement sample.

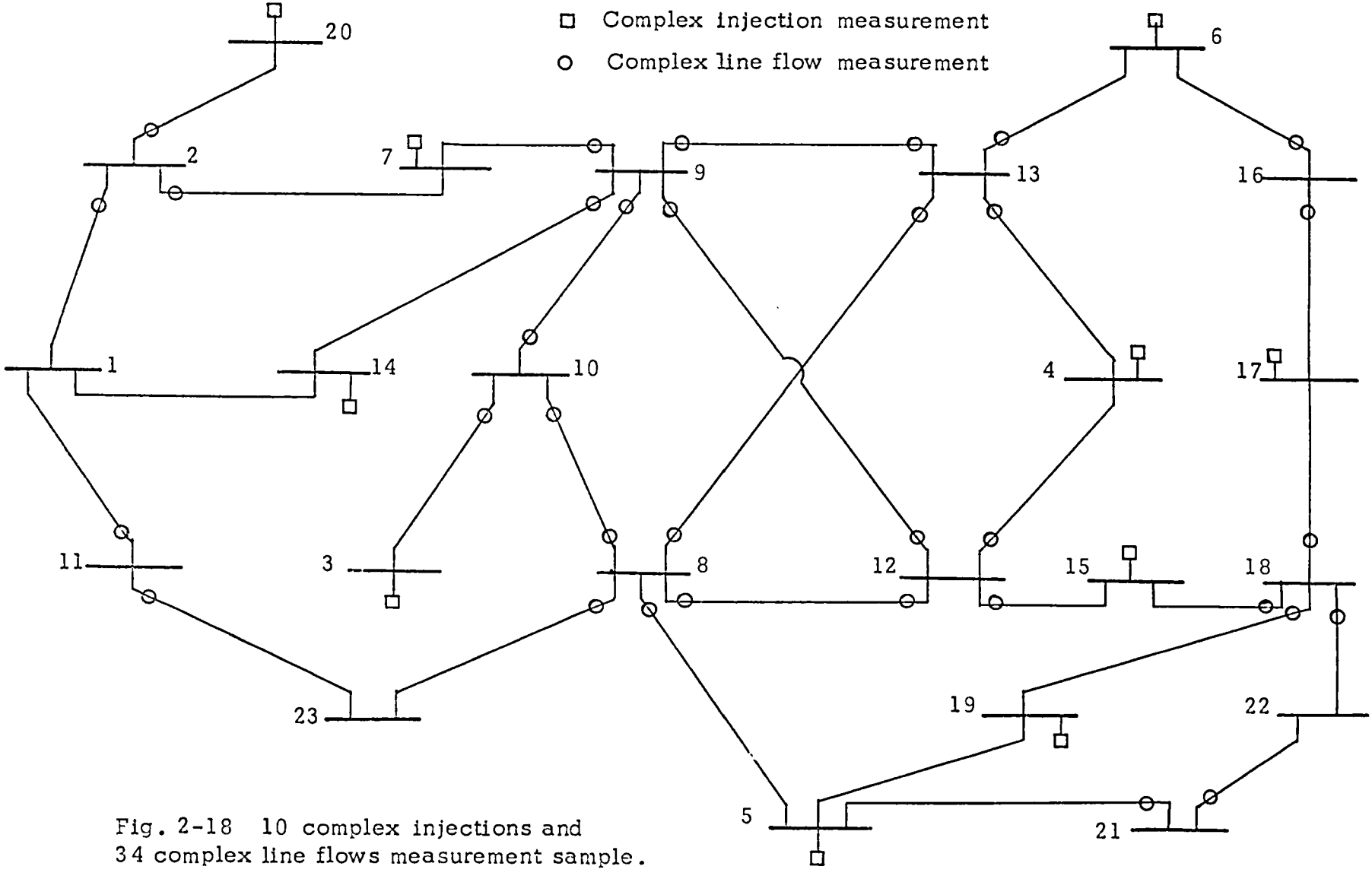

Fig. 2-18 10 complex injections and
34 complex line flows measurement sample.

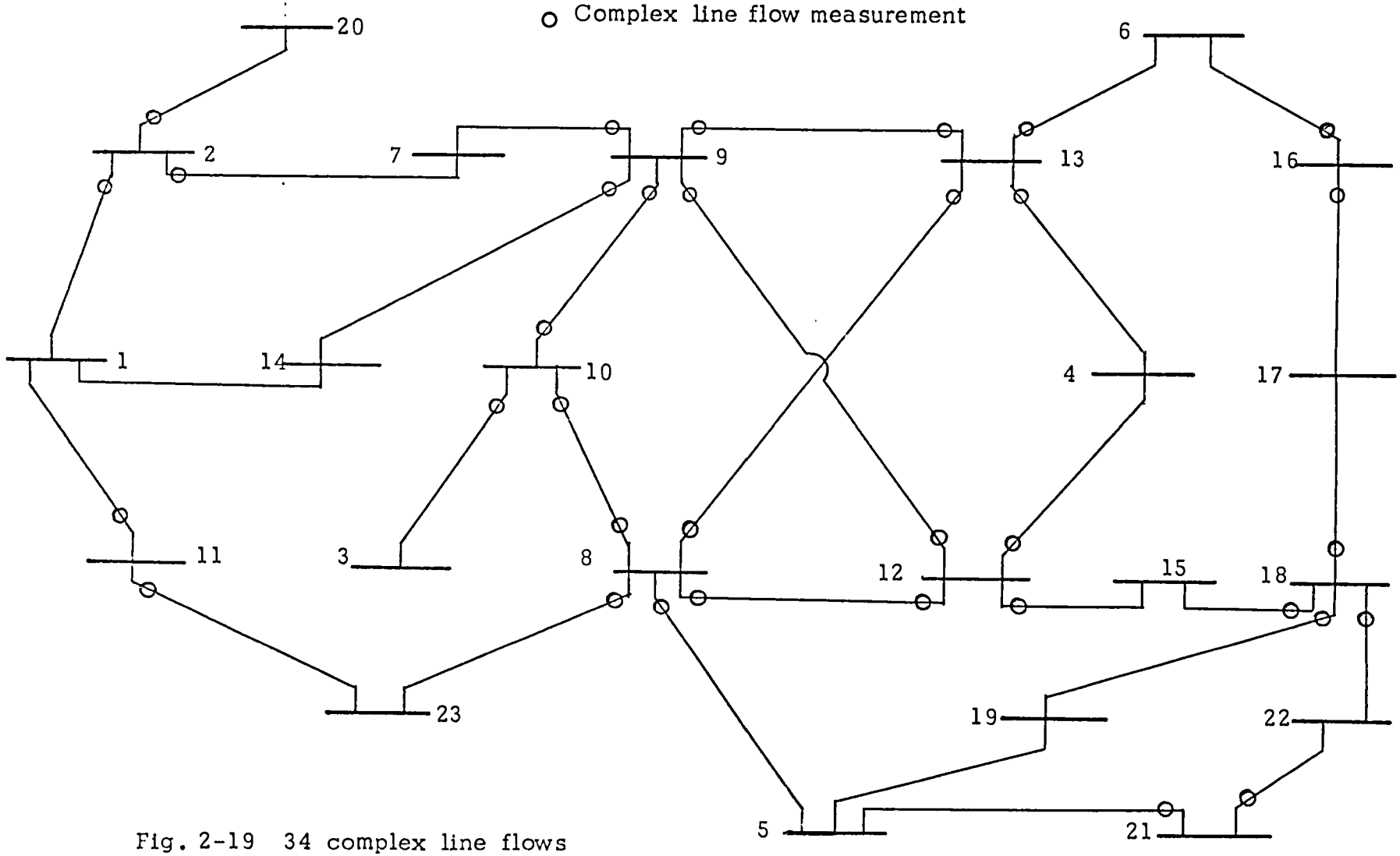

Fig. 2-19 34 complex line flows measurement sample.

in the voltage values.

The residual sum of squares and the root mean square error (tables 2-4, 2-5, 2-22 and 2-23) are given by the expressions:

$$F_k(\hat{\underline{x}}) = \underline{r}_{(k)}^T \underline{r}_{(k)} \qquad (2\text{-}66)$$

$$k = \begin{cases} 1) \text{ residual of true - measured} \\ 2) \text{ residual of measured - estimated} \\ 3) \text{ residual of true - estimated} \end{cases}$$

$$\text{Residual RMS} = \frac{F_k(\hat{\underline{x}})}{\text{No. of measurements}} \qquad (2\text{-}67)$$

It can be noticed that the results obtained with the three weighting factors are reasonably similar when no bad data are present.

In order to save computer time it was decided to test intensively and extensively the 5 node and 7 line system with the three different methods to determine the behaviour in the presence of bad data and to assess the error detecting capability of the algorithms. We have chosen four main cases to test the algorithms with gross measurement errors, adding these to each case, modifying injections at nodes 2, 3 and 4 and the line flow from node 2 to node 4. The amount of gross measurement error is + 50% and + 100% of the true value for each case. The results are displayed in tables 2-25 to 2-28.

The residuals shown in tables 2-25 and 2-26, correspond to the elements of vector $\underline{r}_{(k)}$ in expression (2-66). Four values of gross measurement errors were considered: + 100 and + 50% of the true values. They were simulated by adding these quantities to the true values. Table 2-25 shows the residuals obtained with a gross measurement error in the 5 node system from reference (23), having two measured injections and 7 line flows as shown in Fig. 2-12. The gross measurement is added to the real power of the line connecting nodes 2 and 4 at node 2. Table 2-27 contains the estimated voltages

Table 2-4 Residual sum of squares of a system of 5 nodes and 7 lines, measuring seven complex line flows and two complex injections. Measurement errors simulated with a uniform distribution. (See Fig. 2-12)

Gross meas. error	Measurement	true - estimated			measured - estimated		
		1	2	3	1	2	3
none	.00120	.00046	.00080	.00050	.00076	.00054	.00050
-50%	.02090	.02325	.00498	.00858	.02593	.01623	.01722
+50%	.02106	.01400	.00419	.00220	.01829	.01650	.01735
-100%	.07933	.35100	.01665	.00056	.30024	.06375	.07775
+100%	.07955	.00214	.01500	.00614	.07173	.06410	.06671

Table 2-5 Residual root mean square of a system of 5 nodes and 7 lines, measuring seven complex line flows and two complex injections. Measurement errors simulated with a uniform distribution*.

Gross meas. error	Measurement	true - estimated		
		1	2	3
none	.0082	.0051	.0067	.0053
-50%	.0341	.0359	.0166	.0218
+50%	.0342	.0088	.0153	.0111
-100%	.0664	.1396	.0304	.0056
+100%	.0665	.0109	.0289	.0185

* Average taken from five runs.

Numbers in column headings correspond to:

1 weights equal to the reciprocal of the variance;
2 all weights equal to one; and
3 weights equal to the absolute valueof the measurement divided by the variance.

Table 2-6 Number of iterations starting from flat voltage level (1.0 +.j0.0).

System	Number of injection meas.	Number of line meas.	1	2	3
5 nodes	2	5	4	4	4
	2	6	4	4	4
7 lines	0	8	3	3	3
	(a) 2	7	4	4	4
10 nodes	3	10	4	4	4
13 lines	9	9	4	4	4
	9	21	4	4	4
14 nodes	7	25	5	4	4
20 lines	0	25	4	4	4
	13	17	4	4	4
23 nodes	10	34	5	8	5
30 lines	0	34	4	4	4
	0	46	4	4	4

(a) This row groups different combinations of 2 injection measurements with 7 line measurements and with same number of iterations.

Table 2-7 Values of the objective function.

System	Case	Method	Iteration number 1	2	3	4
23 nodes	34 LM	1	490000	19700.	81.400	24.4300
		2	101.40	4.8960	0.0052	0.00239
		3	253000	40000.	35.890	14.8000
14 nodes	7 Inj. 25 LM	1	392000	46700.	896.23	45.3800
		2	9.1600	0.1806	0.0036	0.00120
		3	84700.	2948.0	71.080	10.5400
10 nodes	3 Inj. 16 LM	1	377000	8296.0	32.780	31.6400
		2	72.740	0.8040	0.0091	0.00860
		3	189000	3708.0	33.460	32.5400

LM = line flow measurements

Inj. = injection measurements.

Table 2-8 Voltage values for a system of 5 nodes and 7 lines, with 2 injections and 7 line flow complex measurements (see Fig. 2 - 12).

Node No.	"true" values		estimated values @	
	E	F	E	F
1	1.0600	0.0000	1.0600	0.0000
2	1.0462	-.0513	1.0460	-.0515
3	1.0203	-.0892	1.0210	-.0881
4	1.0192	-.0951	1.0198	-.0938
5	1.0121	-.1090	1.0108	-.1109

Table 2-9 Voltage values for a system of 5 nodes and 7 lines, with 2 injections and 7 line flow complex measurements (see Fig. 2-12).

Node No.	estimated values *		estimated values +	
	E	F	E	F
1	1.0600	0.0000	1.0600	0.0000
2	1.0464	-.0508	1.0462	-0.512
3	1.0214	-.0874	1.0212	-.0878
4	1.0204	-.0928	1.0201	-.0934
5	1.0113	-.1010	1.0111	-.1103

Note.- Column headings E and F correspond to the real and imaginary parts of the complex node voltage respectively. Node 1 is the reference bus.

@ weights equal to the inverse of the variance;
* all weights equal to one;
+ weights equal to the absolute value of the measurement divided by the variance.

Table 2-10 Voltage values for a system of 5 nodes and 7 lines, with 2 injections and 7 line flow complex measurements (see Fig. 2-13).

Node No.	"true" values		estimated values @	
	E	F	E	F
1	1.0600	0.0000	1.0600	0.0000
2	1.0462	-.0513	1.0458	-.0521
3	1.0203	-.0892	1.0193	-.0912
4	1.0192	-.0951	1.0182	-.0969
5	1.0121	-.1090	1.0113	-.1104

Table 2-10 (Cont'd)

Node No.	estimated values *		estimated values +	
	E	F	E	F
1	1.0600	0.0000	1.0600	0.0000
2	1.0457	-.0521	1.0458	-.0521
3	1.0194	-.0912	1.0194	-.0911
4	1.0183	-.0969	1.0183	-.0968
5	1.0112	-.1106	1.0112	-.1105

Note.- For column headings and symbols, see page 59 .

Table 2-11 Voltage values for a system of 10 nodes and 13 lines, with 3 injections and 16 line flow complex measurements (see Fig. 2-14).

Node No.	"true" values		estimated values @	
	E	F	E	F
1	1.0400	0.0000	1.0400	0.0000
2	1.0484	0.0345	1.0482	0.0340
3	1.0425	-.1163	1.0417	-.1162
4	1.0341	-.1105	1.0341	-.1112
5	0.9927	-.1858	0.9928	-.1869
6	1.0282	-.1562	1.0280	-.1574
7	1.0204	-.1375	1.0206	-.1379
8	0.9457	-.1277	0.9454	-.1281
9	0.9795	-.1862	0.9793	-.1873
10	1.0299	-.0705	1.0303	-.0705

Table 2-12 Voltage values for a system of 10 nodes and 13 lines, with 3 injections and 16 line flow complex measurements (see Fig. 2-14).

Node No.	estimated values *		estimated values +	
	E	F	E	F
1	1.0400	0.0000	1.0400	0.0000
2	1.0485	0.0354	1.0482	0.0345
3	1.0417	-.1162	1.0417	-.1162
4	1.0345	-.1111	1.0344	-.1110
5	0.9921	-.1879	0.9927	-.1869
6	1.0281	-.1573	1.0282	-.1571
7	1.0204	-.1378	1.0207	-.1376
8	0.9447	-.1290	0.9451	-.1285
9	0.9792	-.1874	0.9794	-.1870
10	1.0306	-.0705	1.0306	-.0703

Note.- For column headings and symbols, see page 59.

Table 2-13 Voltage values for a system of 10 nodes and 13 lines, with 16 line flow complex measurements (see Fig. 2-15).

Node No.	"true" values		estimated values @	
	E	F	E	F
1	1.0400	0.0000	1.0400	0.0000
2	1.0484	0.0345	1.0486	0.0351
3	1.0425	-.1163	1.0428	-.1150
4	1.0341	-.1105	1.0341	-.1107
5	0.9927	-.1858	0.9920	-.1866
6	1.0282	-.1562	1.0283	-.1558
7	1.0204	-.1375	1.0201	-.1379
8	0.9457	-.1277	0.9452	-.1279
9	0.9795	-.1862	0.9786	-.1867
10	1.0299	-.0705	1.0294	-.0713

Table 2-14 Voltage values for a system of 10 nodes and 13 lines, with 16 line flow complex measurements (see Fig. 2-15).

Node no.	estimated values *		estimated values +	
	E	F	E	F
1	1.0400	0.0000	1.0400	0.0000
2	1.0486	0.0356	1.0486	0.0353
3	1.0428	-.1150	1.0428	-.1150
4	1.0340	-.1107	1.0341	-.1106
5	0.9920	-.1862	0.9921	-.1863
6	1.0283	-.1557	1.0284	-.1556
7	1.0201	-.1379	1.0202	-.1378
8	0.9448	-.1277	0.9449	-.1277
9	0.9786	-.1864	0.9786	-.1864
10	1.0294	-.0713	1.0295	-.0712

Note.- For column headings and symbols, see page 59.

Table 2-15 Voltage values for a system of 14 nodes and 20 lines, with 7 injections and 25 line flow complex measurements (see Fig. 2-16).

Node No.	"true" values		estimated values @	
	E	F	E	F
1	1.0600	0.0000	1.0600	0.0000
2	1.0410	-.0907	1.0414	-.0907
3	1.0369	-.2628	1.0369	-.2637
4	0.9851	-.2223	0.9858	-.2215
5	1.0602	-.2519	1.0610	-.2526
6	1.0020	-.1825	1.0025	-.1824
7	1.0329	-.2455	1.0334	-.2463
8	1.0082	-.1557	1.0085	-.1557
9	1.0204	-.2724	1.0209	-.2727
10	1.0147	-.2739	1.0152	-.2742
11	1.0218	-.2698	1.0213	-.2711
12	1.0186	-.2744	1.0183	-.2753
13	1.0136	-.2746	1.0135	-.2757
14	0.9952	-.2861	0.9951	-.2868

Table 2-16 Voltage values for a system of 14 nodes and 20 lines, with 7 injections and 25 line flow complex measurements (see Fig. 2-16).

Node No.	estimated values *		estimated values +	
	E	F	E	F
1	1.0600	0,0000	1.0600	0.0000
2	1.0413	-.0907	1.0414	-.0906
3	1.0370	-.2430	1.0372	-.2630
4	0.9855	-.2210	0.9858	-.2210
5	1.0608	-.2534	1.0611	-.2528
6	1.0023	-.1824	1.0025	-.1822
7	1.0331	-.2470	1.0335	-.2465
8	1.0084	-.1557	1.0085	-.1555
9	1.0207	-.2734	1.0211	-.2729
10	1.0150	-.2749	1.0154	-.2744
11	1.0216	-.2702	1.0218	-.2703
12	1.0188	-.2743	1.0190	-.2743
13	1.0136	-.2750	1.0139	-.2750
14	0.9950	-.2869	0.9954	-.2866

Note.--For column headings and symbols, see page 59.

Table 2-17 Voltage values for a system of 14 nodes and 20 lines, with 25 line flow complex measurements (see Fig. 2-17).

Node No.	"true" values		estimated values @	
	E	F	E	F
1	1.0600	0.0000	1.0600	0.0000
2	1.0410	-.0907	1.0409	-.0912
3	1.0369	-.2628	1.0378	-.2629
4	0.9851	-.2223	0.9857	-.2211
5	1.0602	-.2519	1.0617	-.2516
6	1.0020	-.1825	1.0029	-.1813
7	1.0329	-.2455	1.0338	-.2450
8	1.0082	-.1557	1.0090	-.1545
9	1.0204	-.2724	1.0211	-.2725
10	1.0147	-.2739	1.0156	-.2741
11	1.0218	-.2698	1.0222	-.2697
12	1.0186	-.2744	1.0196	-.2747
13	1.0136	-.2746	1.0143	-.2750
14	0.9952	-.2861	0.9965	-.2863

Table 2-18 Voltage values for a system of 14 nodes and 20 lines, with 25 line flow complex measurements (see Fig. 2-17).

Node No.	estimated values *		estimated values +	
	E	F	E	F
1	1.0600	0.0000	1.0600	0.0000
2	1.0412	-.0913	1.0412	-.0913
3	1.0380	-.2629	1.0379	-.2629
4	0.9859	-.2211	0.9858	-.2214
5	1.0619	-.2525	1.0621	-.2524
6	1.0029	-.1818	1.0029	-.1818
7	1.0340	-.2459	1.0342	-.2458
8	1.0091	-.1549	1.0091	-.1549
9	1.0214	-.2734	1.0216	-.2734
10	1.0159	-.2749	1.0161	-.2749
11	1.0224	-.2698	1.0224	-.2698
12	1.0198	-.2748	1.0197	-.2748
13	1.0145	-.2750	1.0145	-.2750
14	0.9967	-.2869	0.9969	-.2869

Note.- For column headings and symbols, see page 59.

Table 2-19 Voltage values for the system Of 23 nodes and 30 lines, with 10 injections and 34 line flow complex measurements (see Fig. 2-18).

Node No.	"true" values		estimated values	
	E	F	E	F
1	1.0186	0.0000	1.0186	0.0000
2	1.0214	-.0290	1.0215	-.0287
3	1.0313	0.0902	1.0321	0.0905
4	1.0360	0.1707	1.0365	0.1697
5	1.0053	0.3032	1.0570	0.3033
6	0.9895	0.3513	0.9899	0.3510
7	0.9954	0.0060	0.9959	0.0060
8	0.9863	0.1679	0.9868	0.1670
9	1.0037	0.0399	1.0041	0.0400
10	0.9824	0.0480	0.9827	0.0480
11	1.0100	0.0228	1.0100	0.0223
12	1.0256	0.1474	1.0260	0.1464
13	1.0183	0.1860	1.0185	0.1850
14	1.0010	0.0055	1.0014	0.0057
15	1.0071	0.1428	1.0074	0.1419
16	0.9888	0.2531	0.9892	0.2524
17	0.9890	0.2157	0.9893	0.2152
18	0.9970	0.1959	0.9973	0.1975
19	0.9941	0.1882	0.9945	0.1876
20	0.9870	-.0676	0.9871	-.0674
21	1.0009	0.2420	1.0014	0.2410
22	1.0022	0.2399	1.0027	0.2389
23	0.9809	0.0846	0.9813	0.0852

Note.- For column headings, see page 59.

Table 2-20 Voltage values for the system of 23 nodes and 30 lines, with 10 injections and 34 line flow complex measurements (see Fig. 2-18).

Node No.	estimated values *		estimated values +	
	E	F	E	F
1	1.0186	0.0000	1.0186	0.0000
2	1.0263	-.0305	1.0222	-.0292
3	1.0407	0.0867	1.0332	0.0895
4	1.0464	0.1650	1.0379	0.1685
5	1.0170	0.2963	1.0073	0.3016
6	1.0017	0.3457	0.9913	0.3504
7	1.0037	0.0036	0.9968	0.0054
8	0.9966	0.1625	0.9882	0.1659
9	1.0126	0.0371	1.0052	0.0393
10	0.9916	0.0447	0.9839	0.0470
11	1.0109	0.0219	1.0102	0.0222
12	1.0359	0.1419	1.0273	0.1453
13	1.0285	0.1805	1.0200	0.1838
14	1.0065	0.0040	1.0020	0.0053
15	1.0175	0.1373	1.0087	0.1409
16	1.0004	0.2477	0.9906	0.2515
17	1.0002	0.2104	0.9907	0.2142
18	1.0080	0.1800	0.9987	0.1943
19	1.0051	0.1819	0.9958	0.1863
20	0.9920	-.0690	0.9878	-.0679
21	1.0122	0.2350	1.0028	0.2397
22	1.0135	0.2329	1.0041	0.2376
23	0.9882	0.0826	0.9825	0.0846

Note.- For column headings and symbols, see page 59.

Table 2-21 Voltage values for the system of 23 nodes and 30 lines, with 34 line flow complex measurements (see Fig.2-19).

Node No.	estimated values @		estimated values *		estimated values +	
	E	F	E	F	E	F
1	1.0186	0.0000	1.0186	0.0000	1.0186	0.0000
2	1.0218	-.0293	1.0220	-.0291	1.0220	-.0291
3	1.0319	0.0891	1.0317	0.0894	1.0318	0.0891
4	1.0363	0.1692	1.0360	0.1698	1.0362	0.1697
5	1.0056	0.3019	1.0050	0.3027	1.0054	0.3024
6	0.9900	0.3483	0.9895	0.3487	0.9898	0.3487
7	0.9957	0.0052	0.9958	0.0055	0.9958	0.0055
8	0.9868	0.1666	0.9867	0.1676	0.9868	0.1671
9	1.0039	0.0384	1.0040	0.0386	1.0040	0.0386
10	0.9823	0.0465	0.9821	0.0467	0.9822	0.0464
11	1.0095	0.0226	1.0095	0.0226	1.0095	0.0226
12	1.0260	0.1457	1.0257	0.1461	1.0260	0.1461
13	1.0187	0.1848	1.0185	0.1854	1.0187	0.1853
14	1.0008	0.0033	1.0009	0.0035	1.0009	0.0035
15	1.0074	0.1412	1.0071	0.1416	1.0073	0.1415
16	0.9893	0.2519	0.9888	0.2525	0.9891	0.2523
17	0.9895	0.2140	0.9890	0.2146	0.9893	0.2144
18	0.9974	0.1945	0.9969	0.1950	0.9973	0.1949
19	0.9945	0.1867	0.9941	0.1872	0.9944	0.1871
20	0.9878	-.0677	0.9880	-.0675	0.9880	-.0675
21	1.0012	0.2404	1.0007	0.2409	1.0010	0.2407
22	1.0025	0.2383	1.0020	0.2389	1.0024	0.2387
23	0.9807	0.0825	0.9806	0.0827	0.9806	0.0825

Note.; For column headings and symbols, see page 59.

Table 2-22 Residual sum of squares with different weighting factors .

System	Case	Measurement error	true - estimated			measured - estimated		
			1	2	3	1	2	3
10 nodes	16 LM	0.00998	0.00271	0.00436	0.00274	0.00794	0.00562	0.00651
	3 Inj., 16 LM	0.01958	0.00296	0.01031	0.00560	0.01449	0.00929	0.01087
14 nodes	25 LM	0.00130	0.00077	0.00069	0.00069	0.00068	0.00059	0.00060
	7 Inj. 25 LM	0.00170	0.00036	0.00052	0.00041	0.00134	0.00111	0.00117
23 nodes	34 LM	0.02052	0.01570	0.01810	0.01650	0.00342	0.00242	0.00282
	10 Inj. 34 LM	0.06765	0.02178	0.04881	0.03438	0.04257	0.02372	0.02645

Table 2-23 Root mean square error of residuals with different weighting factors.

System	Case	Measurement error	true - estimated			measured - estimated		
			1	2	3	1	2	3
10 nodes	16 LM	0.0177	0.0092	0.0117	0.0093	0.0158	0.0133	0.0143
	3 Inj. 16 LM	0.0227	0.0088	0.0165	0.0121	0.0195	0.0156	0.0169
14 nodes	25 LM	0.0051	0.0039	0.0037	0.0037	0.0037	0.0034	0.0035
	7 Inj. 25 LM	0.0052	0.0024	0.0029	0.0025	0.0046	0.0042	0.0043
23 nodes	34 LM	0.0174	0.0152	0.0163	0.0156	0.0081	0.0060	0.0064
	10 Inj. 34 LM	0.0277	0.0157	0.0236	0.0198	0.0220	0.0164	0.0173

Table 2-24 Standard deviation of the real and imaginary part of the node voltage in the 5 node and 7 line system(see Fig. 2-9). All values multiplied by 10^4.

Case	Node Number 2		3		4		5	
	E	F	E	F	E	F	E	F
7 LM 2 Inj.	1.88	3.78	3.44	6.50	3.42	6.39	3.97	7.54
14 LM 5 Inj.	1.17	2.47	2.07	4.01	2.11	4.05	2.51	4.57

Table 2-25 Residuals for a system of 5 nodes and 7 lines with 2 injections and 7 line flow measurements with gross measurement error in the real power of line from node 2 to node 4 corresponding to measurement number 7. (See Fig. 2-13)

Meas.	-100% GME			-50% GME		
No.	1	2	3	1	2	3
1	0.03835	0.04223	0.00199	0.01137	0.02886	0.01916
2	-.00040	-.00125	-.00352	0.01236	0.00415	0.00712
3	-.25549	-.01521	0.01165	-.05764	-.00343	-.01856
4	0.01095	0.00199	0.00080	0.00843	0.00441	0.00462
5	0.21539	0.05117	0.00732	0.05006	0.01776	0.02814
6	0.00722	0.00377	0.00156	-.00270	-.00472	-.00379
7	-.04842	-.22626	-.27911	-.07895	-.11325	-.10173
8	0.00917	0.00550	0.00329	0.00409	0.00159	0.00258
9	-.23320	-.04096	-.00474	-.06663	-.02772	-.04224
10	-.00079	-.00136	0.00161	-.00242	-.00572	-.00444
11	0.12516	0.04660	-.00552	0.02927	0.01792	0.02447
12	-.00600	-.00387	-.00098	-.00431	-.00605	-.00613
13	-.18557	-.03187	-.01163	-.06735	-.02218	-.03925
14	-.00426	0.00259	0.00176	-.00324	-.00364	-.00386
15	-.18826	-.03142	0.00481	-.06191	-.02778	-.03935
16	0.00976	0.00261	-.00023	0.00167	-.00019	0.00018
17	-.20672	-.04472	-.00198	-.04529	-.01375	-.02386
18	0.00496	0.00103	-.00121	-.00187	-.00227	-.00237

	+50% GME			+100% GME		
	1	2	3	1	2	3
1	-.00282	-.02336	-.00911	-.00353	-.04246	-.01464
2	-.00696	-.00302	-.00442	-.00716	-.00382	-.00512
3	0.02694	0.01818	0.02319	0.03194	0.03032	0.03450
4	-.00294	-.00220	-.00197	-.00321	-.00284	-.00234
5	-.01159	-.02198	-.01559	-.01552	-.04442	-.02815
6	-.00269	-.00273	-.00260	-.00289	-.00398	-.00336
7	0.14170	0.12687	0.13593	0.27911	0.24123	0.26302
8	0.00217	0.00230	0.00245	0.00196	0.00102	0.00167
9	0.01588	0.02253	0.02011	0.02023	0.04108	0.03248
10	0.0129	0.00419	0.00257	0.00134	0.00593	0.00316
11	-.01015	-.03593	-.02046	-.01255	-.06442	-.03253
12	0.00070	0.00311	0.00237	0.00086	0.00500	0.00320
13	0.01906	0.01709	0.01831	0.02228	0.02929	0.02764
14	0.00150	0.00243	0.00238	0.00164	0.00244	0.00263
15	0.00428	0.01121	0.00696	0.00786	0.03009	0.01815
16	-.00040	-.00119	-.00066	-.00067	-.00281	-.00145
17	0.01116	0.02125	0.01504	0.01498	0.04300	0.02723
18	-.00001	-.00089	-.00045	-.00017	-.00180	-.00086

GME = Gross Measurement Error.

For column headings, see page 56.

for this example.

The first case, -100%, is equivalent to having the measurement almost equal to zero (this corresponds to y=0 in eq. (2-65)).

Using the different types of weighting, different residuals were obtained. Spotting the error was particularly difficult in the normal weighting case, due to the fact that it gives more weight to those measurements which are relatively more inaccurate. In the other two cases, the greatest residual is the one that corresponds to the faulty measurement. It is important to observe that in the case of the scaled weights the residual in the faulty measurement is practically the value of the added error.

With the -50% gross error, the greatest residual is located in the faulty measurement for three different weightings. The residual in the faulty measurement is of the same order as the error.

On the other hand, in the case of +50% error, the three methods behave properly but the scaled and normal weighting methods are better.

In the last example, with +100 % error, the normal weighting is best since it gives less weight to the faulty measurement and the greatest residual is practically the error value. The other two methods give the greatest residual in the faulty measurement too.

As is apparent from the tests, the scaled and the unitary weights behaved consistently in every example in the presence of gross measurement errors. Their closeness to the true voltage values follows the same pattern. The better the correspondence to the error value in the residual the better the closeness to the true values of the voltage.

The residuals in Table 2-26 correspond to the gross measurement error in an injection and the error is simulated for the real power at node 4. With -100% error, the best solution is obtained with the scaled weights as expected, since it gives less weight to this type or error. The next case shows that the largest residual is not at the

Table 2-26 Residuals for a system of 5 nodes and 7 lines with 2 injections and 7 line flow measurements with gross measurement error in the real power of injection at node 4 corresponding to measurement number 1 (see Fig. 2-13).

Meas.	-100% GME			-50% GME		
No.	1	2	3	1	2	3
1	0.02083	0.13779	0.40233	0.07215	0.06348	0.06153
2	0.00634	0.00428	0.00369	-.00152	-.00145	-.00116
3	0.01543	0.03160	0.00694	0.00577	0.01295	0.00710
4	0.00804	0.00182	0.00267	0.00444	0.00123	0.00222
5	0.06383	0.02615	-.00447	0.01689	0.01077	0.01404
6	-.00252	-.00320	-.00450	0.00050	0.00026	0.00043
7	0.10294	0.05354	-.00185	0.02650	0.02006	0.02265
8	0.00534	0.00412	0.00171	-.00108	-.00144	-.00126
9	0.01208	-.06272	-.01194	0.02095	-.02298	-.02620
10	-.00270	-.00679	-.00253	-.00073	-.00271	-.00199
11	-.07011	-.07017	-.00430	-.02464	-.04140	-.04487
12	-.00389	-.00429	-.00230	0.00071	0.00065	0.00098
13	-.21014	-.03211	-.02153	-.07676	-.01309	-.02157
14	-.00119	-.00142	-.00112	-.00092	-.00154	-.00102
15	-.21608	-.14737	-.00256	-.06929	-.06746	-.06344
16	-.00450	-.00364	-.00385	0.00104	0.00150	0.00139
17	-.09288	-.04458	0.00927	-.02891	-.02266	-.02517
18	0.00067	-.00185	-.00422	0.00233	0.00201	0.00207

	+50% GME			+100% GME		
	1	2	3	1	2	3
1	-.19225	-.08489	-.13221	-.38571	-.13751	-.26179
2	-.00187	-.00111	-.00122	-.00195	-.00052	-.00138
3	-.00212	-.01880	-.00674	-.00254	-.01392	-.00926
4	0.00507	0.00173	0.00255	0.00498	-.00411	0.00201
5	-.01033	-.01924	-.01717	-.01229	-.02804	-.02776
6	-.00119	-.00320	-.00261	-.00125	-.00135	-.00359
7	-.01377	-.03391	-.02596	-.01689	-.05267	-.04306
8	-.00026	-.00276	-.00192	-.00040	0.00040	-.00334
9	0.03040	0.04587	0.04693	0.03018	0.04487	0.06553
10	-.00037	0.00047	-.00010	-.00032	0.00511	0.00046
11	0.00572	0.02815	0.02280	0.00791	0.07257	0.04444
12	0.00079	0.00209	0.00143	0.00083	0.00292	0.00172
13	0.02151	0.01841	0.01938	0.02638	0.01286	0.02595
14	-.00072	-.00038	-.00043	-.00066	0.00829	0.00087
15	0.02601	0.09145	0.05717	0.03284	0.14489	0.09493
16	0.00147	0.00047	0.00105	0.00153	-.00025	0.00097
17	0.01452	0.03400	0.02632	0.01754	0.07309	0.04283
18	0.00228	0.00275	0.00273	0.00211	-.00080	0.00235

For column headings, see page 56.

Table 2-27 State vector values obtained with the case of Table 2-25.

State vector	-100% GME			-50% GME		
	1	2	3	1	2	3
e_2	1.05057	1.04643	1.04597	1.04727	1.04617	1.04661
f_2	-.04187	-.05044	-.05160	-.04897	-.05154	-.05058
e_3	1.03938	1.02387	1.02011	1.02521	1.02155	1.02287
f_3	-.04547	-.08147	-.08988	-.07779	-.08565	-.08301
e_4	1.03982	1.02336	1.01901	1.02458	1.02070	1.02211
f_4	-.04753	-.08583	-.09575	-.08255	-.09072	-.08788
e_5	1.00661	1.00995	1.01133	1.01106	1.01110	1.01112
f_5	-.12596	-.11280	-.11000	-.11294	-.11095	-.11169

	+50% GME			+100% GME		
	1	2	3	1	2	3
e_2	1.04570	1.04570	1.04565	1.04561	1.04539	1.04542
f_2	-.05193	-.05180	-.05187	-.05211	-.05249	-.05239
e_3	1.01904	1.01835	1.01876	1.01865	1.01632	1.01753
f_3	-.09154	-.09317	-.09217	-.09237	-.09756	-.09476
e_4	1.01779	1.01684	1.01743	1.01737	1.01448	1.01606
f_4	-.09773	-.10012	-.09867	-.09863	-.10535	-.10162
e_5	1.01203	1.01265	1.01233	1.01212	1.01331	1.01265
f_5	-.10792	-.10717	-.10744	-.10761	-.10584	-.10659

Table 2-28 State vector values obtained with the case of Table 2-26.

State vector	-100% GME			-50% GME		
	1	2	3	1	2	3
e_2	1.05062	1.04629	1.04601	1.04785	1.04630	1.04652
f_2	-.04086	-.05093	-.05153	-.04724	-.05085	-.05037
e_3	1.02973	1.02250	1.01997	1.02325	1.02113	1.02161
f_3	-.06744	-.08374	-.08941	-.08121	-.08580	-.08479
e_4	1.03124	1.02317	1.01882	1.02316	1.02098	1.02142
f_4	-.06735	-.08561	-.09539	-.08490	-.08954	-.08864
e_5	1.01831	1.00961	1.01199	1.01391	1.00999	1.01018
f_5	-.09605	-.11426	-.10932	-.10340	-.11183	-.11175

	+50% GME			+100% GME		
	1	2	3	1	2	3
e_2	1.04617	1.04622	1.04620	1.04604	1.04467	1.04596
f_2	-.05127	-.05109	-.05114	-.05155	-.05396	-.05149
e_3	1.02061	1.01975	1.01997	1.02034	1.01578	1.01885
f_3	-.08917	-.09036	-.09010	-.08976	-.09833	-.09217
e_4	1.01916	1.01749	1.01812	1.01879	1.01269	1.01650
f_4	-.09561	-.09866	-.09743	-.09640	-.10837	-.10057
e_5	1.01194	1.01278	1.01274	1.01179	1.01247	1.01335
f_5	-.10814	-.10625	-.10616	-.10843	-.10698	-.10444

Note.- e_i = real part of ith node voltage
f_i = imaginary part of ith node voltage.

faulty measurement. These two cases produce smearing of the error but the voltage values obtained for the unitary and scaled weights methods show fairly good results and the estimated voltages are practically close to the true values. In the third test, +50% error, the greatest residual in the three methods is located in the faulty measurement. This time the best is the normal weighting followed by the scaled weighting method. The test with +100% error shows the same pattern as the last one. It is worthwhile noting that the voltage values follow the true values as the residual gets closer to the gross measurement error. Moreover, for practical purposes any of the voltages obtained with the scaled or normal weights give a good solution to the problem. These estimated values are shown in Table 2-28.

2.6 Comments

In the present work we are mainly interested in the algorithms since statistical properties of least square methods in general can be found elsewhere (56) and the asymptotical properties of non-linear least squares estimation can be seen in (39).

Having in mind the difficulties in choosing an algorithm and since the Gauss-Newton method is fairly general, it is possible to find one algorithm best suited for a particular system.

Any method has to be chosen with regard to the connectedness of the network, the presence of short lines, transformer types and other particular components of the system. It is not easy to give a precise rule unless a lengthy computer simulation is carried out, but in general we found greater reliability in the presence of gross measurement errors with the proposed modification of the weighting factor, as the results in tables 2-25 to 2-28 show, especially in relation to the smearing problem since the measurement with the greatest residual was the problematic one. With the modified weights algorithm the smearing is reduced or at least equal to values found by other algo-

rithms and, more importantly, the level of degradation of the estimation is low and comparable to the residual sum of squares of the measurement in normal conditions. This property enhances the error detecting capability of the proposed modified algorithm.

The Marquardt method (9) is provided when the Gauss-Newton fails. As shown by the results, the tested systems have a well behaved surface for the objective function and there was no need to use the Marquardt iteration steps. A similar approach was suggested by Jazwinsky (47) by adding a positive-definite matrix to the matrix $J^T J$ so as to ensure positive-definiteness when needed.

We have proposed a reliable way to solve the SEP, having a robust and reliable algorithm that at least takes us to the local minimum. We should point out that in the load flow problem, the idea of incorporating some kind of control during the iterations was suggested in (46,48,54) following the "downhill" direction. In our test a simplification has bee n made to find the parameter (λ in our case) that ensures the reduction of the objective function. λ need only be calculated when required and only one additional vector multiplication is needed.

Our testing procedure for the validity of the Taylor series approximation on the systems tested showed no need to switch to the Marquardt iteration, as shown by tables 2-1 and 2-2. One important feature is that the test can be applied to the estimation process in general, using it in a tracking mode (18,20,31) and computing the Jacobian matrix only when it is needed.

The present algorithms may have several other applications, the immediate ones being: a) the model coordination method in hierarchical state estimation (50); b) optimization problems in power systems (51); c) reformulation of the optimal load flow as in (52), and d) the stochastic load flow, as a particular case of our problem, following (53) and (59).

CHAPTER THREE

GENERALIZED INVERSE METHOD, OBSERVABILITY AND RANK DEFICIENCY IN POWER SYSTEMS STATE ESTIMATION.

3.1 Introduction

Power systems state estimation has proved to be a reliable tool for monitoring systems and it is capable of producing a consistent data base useful for the control and the security assessment needs of the power system controller. However, no system can be 100% reliable and it is necessary to have some way of detecting any abnormality that may occur in the event of a fault in the measurement system, associated with the state estimation process. A fault may produce a situation where a portion of the system cannot be "seen" with a given set of measurements. This is the case when one or more voltages can not be estimated. This condition can be described in terms of a "reachability" matrix. On the other hand, when all the nodes of the network can be reached (observed), an observability criterion can be defined (22).

In an emergency condition, when a fault occurs in the measurement system producing a corresponding loss of information, one or more nodes may be left unobserved. The first step is to determine which nodes are missing. Once these are known the problem can be solved on the estimable portion, as explained in the next paragraphs. If the unobserved nodes are not identified, the linear system of equations is inconsistent and we may require the use of the generalized inverse approach (60,61).

The solution of the SEP in electrical power systems requires pre-processing (data validation) the set of measurements and network configuration in order to have the least possible amount of spurious data fed into the numerical process of solution. This pre-processing of the measurements can be done by comparing full scale meter values against measured values, logical checking of circuit breaker positions against power-flow, local summation of flows, etc. (16).

The next step is to ensure the connectedness of the network and its correspondence with the measurements. In this step of the process it is usually possible to detect unobservable nodes leaving a singularity condition in the linear system of equations to be solved. Allam and Borkowska (60,61) have made some suggestions as to how to deal with this singularity condition but the usefulness of this approach is limited to the observed portion of the network, as explained in Section 3.3.3 of this thesis.

The matrix structure of the measurements for a given condition of the system can be represented by a directed graph, which will be dealt with in the next section. Before that, some matrices of graphs will be explained. The basic concepts are contained in Appendix 2 and the terminology used corresponds to reference (62).

3.2 Graph theory and measurements

3.2.1 Algebraic representation of a graph

A convenient way of representing a graph algebraically is by using matrices, as follows:

Given a graph G, its adjacency matrix is denoted by $A = [a_{ij}]$ and is formed by

$a_{ij} = 1$ if arc (x_i, x_j) exists in G;

$a_{ij} = 0$ if arc (x_i, x_j) does not exist in G.

Thus, the adjacency matrix of the graph shown in Fig. 3-1 (b) is:

$$A = \begin{array}{c} \\ x_1 \\ x_2 \\ x_3 \\ x_4 \\ x_5 \end{array} \begin{array}{c} \begin{array}{ccccc} x_1 & x_2 & x_3 & x_4 & x_5 \end{array} \\ \begin{bmatrix} 1 & 1 & 1 & 0 & 0 \\ 0 & 0 & 0 & 0 & 0 \\ 0 & 0 & 0 & 0 & 0 \\ 0 & 1 & 1 & 0 & 1 \\ 0 & 1 & 0 & 1 & 1 \end{bmatrix} \end{array} \qquad (3\text{-}1)$$

The adjacency matrix defines completely the structure of the graph.

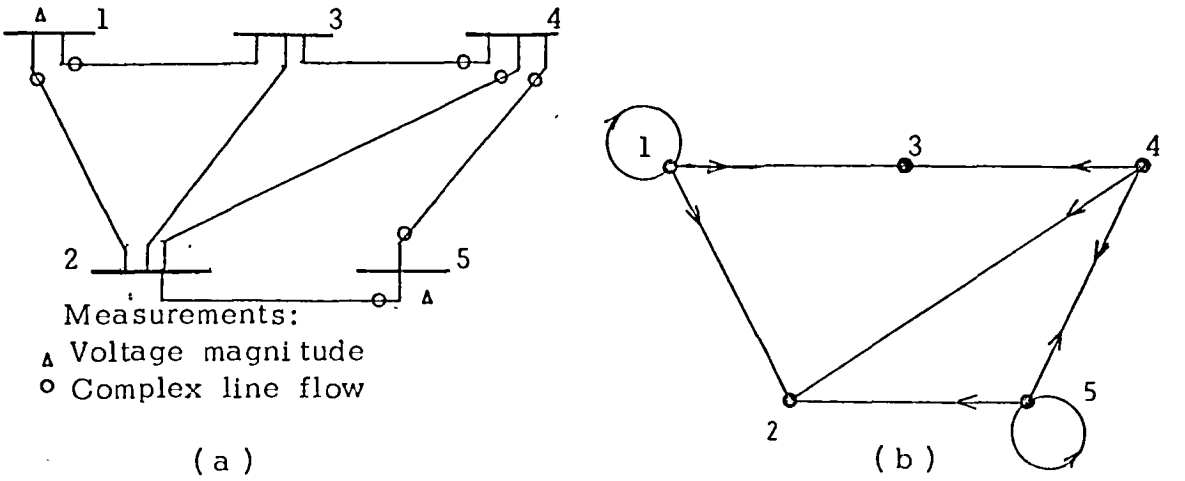

Fig. 3-1 Sample power system. (a) one line diagram with measured points. (b) Its equivalent directed graph.

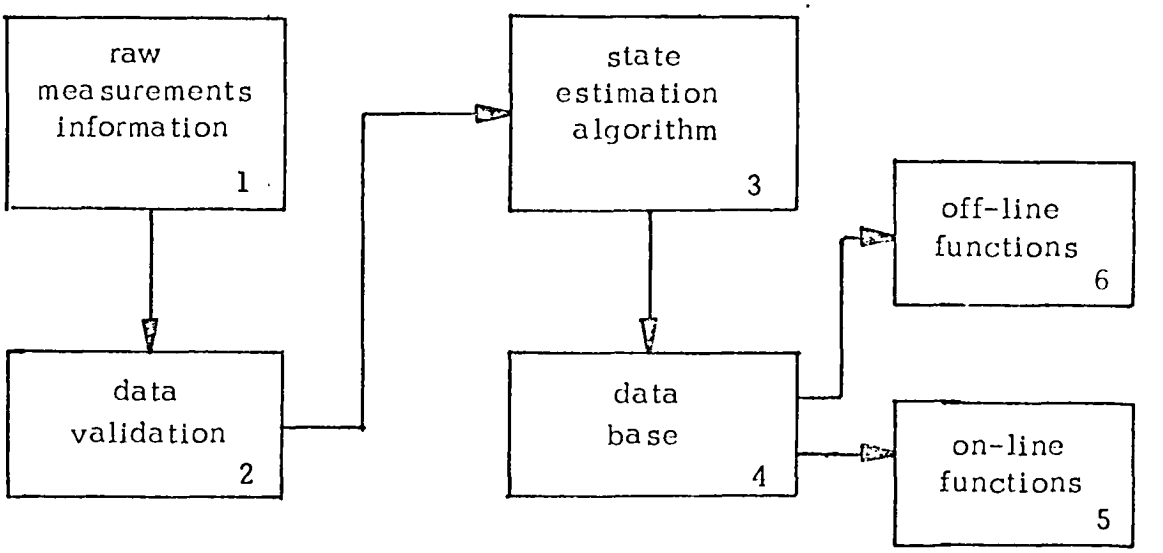

Fig. 3-2 Block diagram of state estimation process and functions.

For example, the sum of all the elements in row x_i of the matrix gives the outdegree of vertex i and the sum of the elements in column x_i gives the indegree of vertex i.

Given a graph G of n vertices and m arcs, the incidence matrix of G is denoted by $B = [b_{ij}]$ and is an $n \times m$ matrix defined as follows:

$b_{ij} = 1$ if x_i is the initial vertex of arc a_j ;

$b_{ij} = -1$ if x_i is the final vertex of arc a_j and

$b_{ij} = 0$ if x_i is not a terminal vertex of arc a_j or if a_j is a loop.

This is analogous to the transpose of the element-node incidence matrix in reference (23). In our example the incidence matrix is:

$$B = \begin{array}{c} \\ x_1 \\ x_2 \\ x_3 \\ x_4 \\ x_5 \end{array} \begin{array}{c} \begin{array}{ccccccccc} a_1 & a_2 & a_3 & a_4 & a_5 & a_6 & a_7 & a_8 & a_9 \end{array} \\ \begin{bmatrix} 1 & 1 & & & & & & & \\ & -1 & & -1 & & -1 & & & \\ -1 & & -1 & & & & & & \\ & & & 1 & 1 & 1 & & -1 & \\ & & & & & -1 & 1 & 1 & \end{bmatrix} \end{array} \qquad (3\text{-}2)$$

Since each arc is adjacent to two vertices, each column of the incidence matrix contains one 1 and one -1 entry, except when the arc forms a loop in which case it contains only zero entries.

If G is a nondirected graph the incidence matrix is defined as above except that all entries of -1 are now changed into +1.

3.2.2 Graph representation of measurements

A set of measurements can be represented by a directed graph whose elements are defined as follows: the complex state vector elements form the vertex set of the graph, X and the complex measurements

form the arcs of the graph G. This directed graph is represented by A(G,X). The arc direction is given by the point measured and the nodes related by the measurement. Hence, the complex line flow measurement made at, for example, node i for the line joining nodes i and j will produce an arc from vertex i to vertex j in the corresponding directed graph.

As an example let us assume a system of 5 nodes and 7 lines as shown in Fig. 3-1 (a). Its corresponding directed graph is shown in Fig. 3-1 (b). To obtain this directed graph we proceed as follows:

i) A voltage measurement is represented by a loop (a loop is defined as an arc whose initial and final vertices are the same). This corresponds to 1 in the respective diagonal element in the adjacency matrix, since this measurement only relates to the node.

ii) A line flow measurement between nodes i and j measured at node i is represented by an arc from vertex i to vertex j. This is expressed in the adjacency matrix by putting a 1 in the cell (i,j).

iii) An injection measurement requires special consideration since it relates all the nodes directly connected to the node where it is measured. It is represented as a group of arcs which must be labelled so as to identify their origin, i.e., as deriving from an injection measurement. Thus, an injection is best described by putting 1's in all the elements (i,j) of the adjacency matrix, where j takes the values of all the vertices directly connected to vertex i.

The adjacency matrix A corresponding to the example of Fig. 3-1 is then

$$A = \begin{bmatrix} 1 & 1 & 1 & 0 & 0 \\ 0 & 0 & 0 & 0 & 0 \\ 0 & 0 & 0 & 0 & 0 \\ 0 & 1 & 1 & 0 & 1 \\ 0 & 1 & 0 & 1 & 1 \end{bmatrix} \qquad (3\text{-}3)$$

In this example, we have excluded injections in order to simplify it. If an injection was measured, for example in node No. 3, the third row in matrix A will appear as 1 1 1 1 0.

The adjacency matrix provides a systematic representation of the measurements taken from the system. It is important to note the difference that exists between the directed graph of the measurements represented by the adjacency matrix and the power system network which can be represented by a nondirected graph whose adjacency matrix corresponds to the matrix structure of the bus admittance matrix.

3.2.3 Reachability matrix

The representation of the measurement system as a graph permits us to pose the next problem: does the graph cover all the nodes of the system and is it possible to reach any node, starting from a node with an outdegree greater than zero ?

If we can go from a vertex x_i to a vertex x_j, we say that x_j is reachable from x_i. If this reachability is restricted to paths of limited cardinality (defined in Appendix 2), we say that set $H(x_i)$ is that set of vertices reachable from vertex i along a path of cardinality 1; $H(H(x_j)) = H^2(x_j)$ is the set of vertices formed by those vertices reachable from x_j along a path of cardinality 2, and so on.

If the nodes of the network associated through the measurement system are reachable from any arbitrary node with outdegree greater

than zero, it is possible to estimate all those state variables that are reachable from the given set of measurements.

The reachability matrix is then formed as follows:

Set

$$r_{ij} = 1 \quad \text{if } x_j \text{ can be reached from } x_i \text{ ; } r_{ij} = 0 \text{ , otherwise}$$

The reachability matrix of Fig. 3-1 (b) is formed by starting from node 1 from which it is possible to go to nodes 2 and 3; this row then appears as the first row in matrix (3-4). From nodes 2 and 3 it is not possible to go to nodes 4 and 5 , so zeroes are put into theserows. But it is always possible to go from any node i to itself along a path of cardinality zero, so a one is placed on the diagonal element.

The reachability matrix of the graph shown in Fig. 3-1 (b) is given by

$$R = \begin{array}{c} \\ x_1 \\ x_2 \\ x_3 \\ x_4 \\ x_5 \end{array} \begin{array}{c} \begin{array}{ccccc} x_1 & x_2 & x_3 & x_4 & x_5 \end{array} \\ \begin{bmatrix} 1 & 1 & 1 & 0 & 0 \\ 0 & 1 & 0 & 0 & 0 \\ 0 & 0 & 1 & 0 & 0 \\ 0 & 1 & 1 & 1 & 1 \\ 0 & 1 & 1 & 1 & 1 \end{bmatrix} \end{array} \qquad (3-4)$$

We now define the "reaching" matrix $Q = [q_{ij}]$ which is obtained by

$$q_{ij} = 1 \quad \text{if } x_j \text{ can reach } x_i \text{ ; } q_{ij} = 0 \quad \text{otherwise.}$$

It is clear that the columns of the matrix Q are the same as the rows of matrix R; i.e., $Q = R^T$.

It is apparent from (3-4) that all the nodes of the graph are covered since it is possible to go from 1 to 3 , from 5 to 4 and from 4 to 3 and 2.

By inspecting the reachability matrix R it is possible to check the state variables that can be estimated with a given set of measurements.

In the case of a connected symmetric graph it is clear that all the nodes can be reached from any node and the reachability matrix R is full of 1's.

Matrices Q and R will be used again in the evaluation of the "strong" components of a graph in Chapter 5.

3.2.4 Reachability matrix algorithm

To find the reachability matrix R it is necessary to search all possible paths that are generated starting from any node. It is obvious that those nodes with outdegree of zero are exempted. The algorithm is as follows:

1) Initialize $R(i,j) = 0$ for all $i,j = 1,2,\ldots,n$, where n is the number of vertices in the graph.
2) Form the elements of matrix R from the arcs information,
   $R(i,j) = 1$ if there is an arc between vertices i, j.
   $R(i,j) = 0$ otherwise.
3) Find the paths from node k, $(k=1,\ldots,n)$, modifying matrix R at element $R(i,j)$, $(i,j=1,\ldots,n)$, if there exists a path between nodes i, j through node k.
4) Is $k=n$? If yes, stop. If not, return to (3).

It is important to note that this procedure is very compact and requires very little storage since all the information can be expressed in binary variables and all the operations are logical.

3.3 Observability in power systems SEP

3.3.1 Singularity condition.

Two methods of solution that have been applied to the SEP in power systems (1,3) require the solution of a sequence of linear systems with equations of the type

$$A\underline{x} = \underline{b} \qquad (3-5)$$

where A is a $m \times n$ matrix; $\underline{x}$ is a n-dimensional vector of unknowns in the linear system of equations for the current iteration; $\underline{b}$ is the

corresponding m-dimensional vector of residuals for the current iteration.

The least squares solution of (3-5) is given by

$$\hat{x} = (A^T A)^{-1} A^T \underline{b} \qquad (3-6)$$

provided $A^T A$ is not singular (for simplicity we assume the weights all equal to one without loosing generality).

But it may happen that in some cases, the matrix $A^T A$ is singular or nearly singular and the inverse required cannot be calculated. Here two types of singularity can be described. The first, which will be analysed later, is related with the observability problem, i.e., when at least one column of matrix A is composed of zero valued elements. The second case arises when the matrix $A^T A$ has the following features: i) very small eigenvalues and ii) instability of the numerical process due to the finite arithmetic of the representation of numbers in the computer; this ill-condition can occur relatively easily because the condition number of $A^T A$ is the square of the condition number of A .

The condition number of a matrix is given by tne ratio of the largest eigenvalue to thc smallest. Its interpretation in terms of random errors is that the condition number for a symmetric matrix gives the ratio of the largest semi-axis to the smallest for an ellipsoid of dispersion of a vector whose components are the errors of the unknowns (41,63). The next example will illustrate this point .

Let us have the quadratic function given by

$$Q(\underline{x}) = \tfrac{1}{2} \underline{x}^T H \underline{x} \qquad (3-7)$$

where H is a positive definite matrix which can be decomposed into

$$H = V^T D V \qquad (3-8)$$

where V is an orthogonal matrix, i.e., $V^T V = V V^T = I$ and D is the diagonal matrix whose elements are the positive eigenvalues of

H. If we consider a new variable $\underline{z}=V\underline{x}$, which transforms the function $Q(\underline{x})$ to the form

$$Q(\underline{z}) = \tfrac{1}{2}\underline{z}^T D\underline{z} \qquad (3-9)$$

the isocontours $Q(\underline{z})$ = constant, are n-dimensional ellipsoids centred at the origin $\underline{x}=\underline{0}$, which cut the ith coordinate axis at the points $\underline{z}_i = \text{constant} \times (d_i)^{-\frac{1}{2}}$, where d_i are the components of D. We see that the value z_i (principal axis) associated with the eigenvalue d_i is inversely proportional to $d_i^{\frac{1}{2}}$, so that small d_i corresponds to ellongation of the ellipsoid in the direction z_i. Such elongation implies that the variable z_i is poorly determined in the numerical solution.

3.3.2 Observability criteria

In an operational situation all the information from the power system is fed into a computer. A data validation process then takes place and once the data has been checked, the adjacency matrix or an analogous matrix is built up.

However, in the planning stage the one line diagram may be used to check the data, network connectedness and whether or not a given set of measurements spans all the nodes (complex node voltages). In a real time situation most of the information about the structure is made up in the form of logical variables and an automatic procedure is necessary, i.e., an algorithm is required so that the computer can "see" the network and find if the nodes are all interconnected and if the whole network is observable with the available set of data.

It is said that a system is observable if the whole state vector can be uniquely obtained from the given set of observations. Reference (22) uses modern control theory to explain observability and provides a geometrical interpretation of the small eigenvalues in the linear system of equations. However, it is felt that a simpler explanation to the problem may be possible by using only the condition number

and rank deficiency of the matrix A^TA in (3-6) shown by columns without non-zero elements. In the equivalent directed graph, this corresponds to node(s) that cannot be reached from any other node of the network. Its corresponding row in the reaching matrix Q is full of zeroes with the exception of the diagonal element. A solution to the rank deficient problem can be obtained by using the partial observability criterion as will be explained later. In the ill-conditioned case, more stable methods such as the Householder transformations and singular value decomposition can be employed if the need arises.

Nevertheless, the results contained in Chapter 2 of this work, have shown in most cases the linear Taylor series approximation is convenient and the function to be optimized is fairly well behaved, making the sequence of the linear system of equations well conditioned.

Given a network of n nodes and m complex measurements ($m \geq n-1$), the corresponding Jacobian matrix J is of the order $2m \times (2n-2)$, then the observability condition can be defined as follows:

Definition 1. The system is observable if the rank of J is $k = 2n-2$ and the matrix $H = J^T J$ is nonsingular.

Definition 2. The system is partially observable if the rank of J is $k < 2n-2$ and a matrix $J_1^T J_1$ is nonsingular, where J_1 is of order $2m \times (2k)$.

Let us explain the first condition. The state vector of the system can be estimated through the sequence of the linear system of equations given in expression (3-6). The solution to the system of equations requires that the matrix $H = J^T J$ be nonsingular. However, it may occur that even when matrix J is of full rank, matrix H may turn out to be singular since its condition number is the square of that of J.

Before advancing on this point, it is convenient to recall that the

system of equations involved in the estimation process is non-linear, but that it is solved as a sequence of linear systems of equations. A necessary and sufficient condition for observability is that the rank of matrix A in the linear system of equations (3-5) be equal to n. In order to satisfy this condition and be able to estimate the state vector of the system, it is necessary to have at least the same number of measurements as that of elements in the state vector and that the group of measurements cover all the state variables of the network.

Therefore, observability of the state estimation can be expressed as the possibility of going from the measurement block one to the data base block 4 in the block diagram shown in Fig. 3-2 through the mathematical process involved, state estimation algorithm block 3.

Two types of unobservability condition may arise during the solution process of the SEP. Firstly, the set of measurements does not cover all the elements of the state vecotr, i.e., the redundant system of equations becomes rank deficient and matrix A^TA singular. Secondly, the rank of A is the maximum rank but the condition number of A^TA is large.

In practice it may occur that a system is nearly singular when there exists rounding-off errors in the computations so it may be difficult to decide whether a particular value, at any stage of reduction, is a real deviation from zero or a rounding-off error in the place of a zero. In our case, the detection of zero columns does not present any problems. When information for all nodes is not available it is convenient to have a method to detect singular values, like the Golub and Reinsch algorithm (65), which will be explained in Section 3.3.4.

When ill-conditioning occurs and the rank of the matrix is known to be n, one needs to apply more stable algorithms, like the QR orthogonal factorization given by the Businger-Golub algorithm,(detailed in Appendix 5) where the matrix A is expressed as

$$A = P\begin{bmatrix} U \\ 0 \end{bmatrix} \tag{3-10}$$

in which P is a m×m orthogonal matrix and U is a n×n upper triangular matrix.

The vector $\underline{x}$ from (3-5) is thendetermined by back substitution in the equation

$$U\underline{x} = \underline{y} \tag{3-11}$$

where $\underline{y}$ is the n×1 vector consisting of the first elements of $P\underline{b}$.

If A is rank deficient, the solution to (3-5) is not unique and a particular solution could be arbitrarily large. When this condition arises, it is better to find the unique solution that provides the vector $\underline{x}$ with minimum norm (66). This is the pseudoinverse solution and its effect will be shown later, in Section 3.3.4 . It is now convenient to summarize the relationship between pseudoinverses and least squares solutions, following references (65,66).

3.3.3 Pseudoinverses

The concept of a generalized inverse matrix has its roots in the theory of simultaneous linear equations. The solution of a set of linear equations

$$A\underline{x} = \underline{b} \tag{3-5}$$

where A is a m×n matrix of rank $r \leq n$, may have two forms:

i) If $m = n = r$, a unique solution $\underline{x} = A^{-1}\underline{b}$ exists.

ii) When A is rectangular or square singular a simple representation of a solution in terms of A is more difficult and the use of generalized inverse matrices has been suggested by Penrose (67). A unique matrix A^- is defined satisfying the conditions

$$AA^-A = A \tag{3-12}$$

$$A^-AA^- = A^- \tag{3-13}$$

$$(AA^-)^T = AA^- \tag{3-14}$$

$$(A^-A)^T = A^-A \tag{3-15}.$$

A solution to (3-5), as shown in (67) requires a generalized inverse which satisfies only (3-12). Pringle and Rayner (68) pointed out that this type of generalized matrix applied in statistics to the analysis of the linear model and in particular, that the estimates of estimable linear functions and the variances of these estimates where invariant under the choice of a generalized inverse. This statement will be clarified later in the computational methods description. This invariant property will be of great help in the particular conditions applying to the SEP in power systems.

The pseudoinverse can be stated explicitly in terms of least squares as follows:

Given a m×n matrix A and a vector $\underline{b}$ of order m, how shall we determine a vector $\underline{x}$ of order n such that the residual vector $(\underline{b}-A\underline{x})$ has the minimum norm ?* In general, the vector $\underline{x}$ is not unique and it is pertinent to ask a further question: which of the $\underline{x}$ vectors giving the minimum residual has the minimum norm ? This unique vector is referred to as the minimal least squares solution and is given by $X\underline{b}$, where X is the pseudoinverse. Clearly when A is square and non-singular the solution is $A^{-1}\underline{b}$.

If m>n and the rank (A) =n, then the least squares solution is

$$\underline{x} = (A^T A)^{-1} A^T \underline{b} \qquad (3\text{-}16)$$

and for this case the pseudoinverse A^{-} will be

$$A^{-} = (A^T A)^{-1} A^T \qquad (3\text{-}17)$$

which can be verified by substitution in expressions (3-12 - 3-15).

At this point it is convenient to comment on the work of Allam (60), who uses an oblique pseudoinverse proposed by Milne (69) which is a constrained generalized inverse. In general the vector $\underline{x}$ in (3-5) is not unique and one can find arbitrary solutions for its

* The Euclidean norm, defined by $\|\underline{x}\| = \left(\sum_{i=1}^{n} |x_i|\right)^{\frac{1}{2}}$ is used. This is, of course, the ordinary Euclidean length (66).

singular elements, including the trivial solution. The oblique pseudoinverse is a constrained generalized inverse which provides one of the many possible solutions to the non-estimable variables. Allam's generalized inverse is the matrix given by the solution of the normal equations (41)

$$(J^T J)\Delta \underline{x} = J^T \underline{r} \tag{3-18}$$

which is the same as eq. (2-50). Provided $J^T J$ is nonsingular, Allam's generalized inverse is the matrix $(J^T J)^{-1} J^T$. A particular case is when J is nonsingular and the matrix J^{-1} satisfies relations (3-12 - 3-15).

To solve the singularity condition problem, the pseudoinverse approach may be useful, but it is important to note that the main point in the solution is the rank of the covered portion of the network.

Let us have a matrix A of dimensions m×n, where m>n, with rank k<n, where k is known and let it be possible to partition A in the form

$$A = (B_1 : B_2) \tag{3-19}$$

by a permutation of columns if necessary, such that B_1 is a matrix m×k and B_2 is a matrix m×(n-k). Then one possible choice of pseudoinverse of A is

$$A^{-1} = \begin{bmatrix} C \\ 0 \end{bmatrix} \tag{3-20}$$

where

$$C = (B_1^T B_1)^{-1} B_1^T \tag{3-21}$$

This will be illustrated in the next example.

Let us have the system shown in Fig. 3-3. The matrix structure of the measurements Jacobian is given by expression (3-22), where J_{ij}, (i=1,4; j=1,8) is a 2×2 submatrix. The elements in the submatrices J_{k2}, (k=1,8) are all zero since there is no

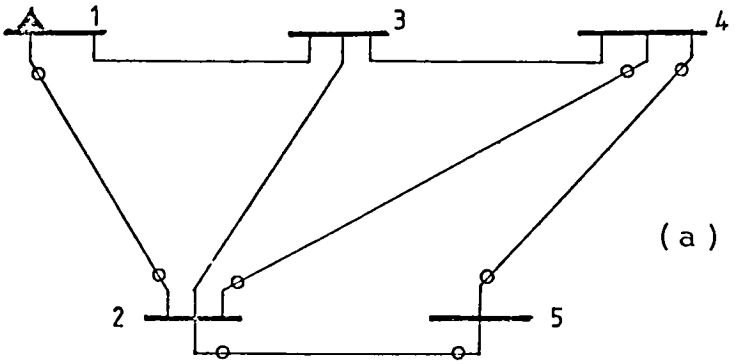

Measurements:
Voltage magnitude
Complex line flow

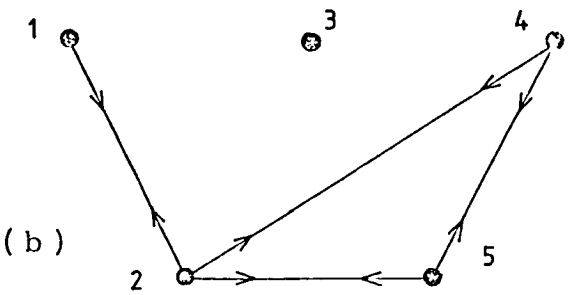

Fig. 3-3 Sample power system. (a) one line diagram with measured points. (b) its equivalent directed graph.

measurement relating the voltage at node 3. This is apparent in the corresponding directed graph, Fig. 3-3 (b), where the node 3 is isolated from the rest of the graph.

$$J = \begin{bmatrix} J_{11} & \cdot & \cdot & \cdot & J_{14} \\ \cdot & & & & \cdot \\ \cdot & \cdot & \cdot & \cdot & \cdot \\ \cdot & & & & \cdot \\ J_{81} & \cdot & \cdot & \cdot & J_{84} \end{bmatrix} \tag{3-22}$$

By a permutation of columns, we have:

$$J = \begin{bmatrix} J_{11} & J_{14} & J_{13} & J_{12} \\ \cdot & & & \cdot \\ \cdot & \cdot & \cdot & \cdot \\ \cdot & & & \cdot \\ J_{81} & J_{84} & J_{83} & J_{82} \end{bmatrix} \tag{3-23}$$

Expression (3-23) can be written as

$$J = \begin{bmatrix} B_1 & B_2 \end{bmatrix} \tag{3-24}$$

where

$$B_1 = \begin{bmatrix} J_{11} & J_{14} & J_{13} \\ \cdot & \cdot & \cdot \\ \cdot & \cdot & \cdot \\ J_{81} & J_{84} & J_{83} \end{bmatrix} \tag{3-25}$$

$$B_2 = \begin{bmatrix} J_{12} \\ \cdot \\ \cdot \\ J_{82} \end{bmatrix} = \begin{bmatrix} 0 & 0 \\ 0 & 0 \\ & \cdot \\ 0 & 0 \\ 0 & 0 \end{bmatrix} \tag{3-26}$$

Substituting (3-25) and (3-26) into the normal equations (2-50), we obtain

$$(B_1 \;\; B_2)^T (B_1 \;\; B_2)\, \underline{x} = \begin{bmatrix} B_1^T \\ \\ B_2^T \end{bmatrix} \underline{r} \qquad (3\text{-}27)$$

$$\begin{bmatrix} B_1^T B_1 & 0 \\ 0 & 0 \end{bmatrix} \underline{x} = \begin{bmatrix} B_1^T \underline{r} \\ 0 \end{bmatrix} \qquad (3\text{-}28)$$

This proves the validity of eq. (3-20) and illustrates Definition 2 in Section 3.2.2 .

The pseudoinverse approach in general requires longer time and larger computer storage than the Cholesky method and for the case when the problem can not be solved due to near-singularity condition of matrix A^TA, neither can the rank be determined, the singular value decomposition as shown in (65) will provide the elements where the eigenvalues are very small. The rank of the system can then be determined and the singular valued points set to zero as will be described in the next section.

3.3.4 Singular value decomposition

In practice, matrices are rarely exactly rank deficient when they are ill-conditioned and, if they were, errors in the computation would obscure this fact. For these cases it is necessary to determine the rank, and one way of obtaining it is by using the singular value decomposition (SVD) contained in the algorithm developed by Golub and Reinsch (65), (Appendix 6).

Let A be a real $m \times n$ matrix with $m \geq n$. It has been shown (70) that it can be decomposed into

$$A = U D V^T \qquad (3\text{-}29)$$

where

$$U^T U = I_n \qquad (3\text{-}30)$$

$$V^T V = I_n \qquad (3\text{-}31)$$

$$VV^T = I_n \tag{3-32}$$

and

$$D = \text{diag}\,(d_1, d_2, \ldots, d_n) \tag{3-33}$$

The matrix U consists of n orthonormalized eigenvectors associated with the n largest eigenvalues of AA^T, and the matrix V consists of the orthonormalized eigenvectors of A^TA. The diagonal elements of D are the non-negative square roots of the eigenvalues of A^TA. They are called singular values.

Let us consider that

$$d_1 \geq d_2 \geq \ldots \geq d_n \geq 0 \tag{3-34}$$

Thus if rank (A) = k, then $d_{k+1} = d_{k+2} = \ldots = d_n = 0$. The decomposition (3-29) is called the singular value decomposition.

The solution of the system of linear equations (3-5) can be obtained using the pseudoinverse X. As has already been stated, this matrix has a unique solution when satisfying the four conditions (3-12 - 3-15).

It is easy to verify that if $A = UDV^T$, then $X = VD^+U^T$, with

$$D^+ = \text{diag}\,(d_i^+) \qquad \text{and}$$

$$d_i^+ = \begin{cases} 1/d_i & \text{for } d_i > 0 \\ 0 & \text{for } d_i \quad 0 \end{cases} \tag{3-35}$$

Thus the pseudoinverse may easily be computed from the solution provided by the singular value decomposition algorithm.

3.4 Discussion on the state estimation algorithms

3.4.1 AEP algorithm

For a given structure of measurements, i.e., a given graph, the condition number of the coefficients matrix of the linear system of equations depends on the associated network structure. This can be seen by analysing the expression from the solution of the

sequence of systems of linear equations.

Using the AEP method (3,98), we obtain (Appendix 3):

$$B^T D B \hat{E} = B^T D (\underline{V}_m) \qquad (3\text{-}36)$$

where B is the m×n incidence measurements matrix to nodes. B contains in each row the nonzero elements, +1 and -1. D is a diagonal matrix formed by $d_{jj} = w_j E_p^2 / Z_j^2$ where w_j is the weight associated with measurement j, Z_j the line impedance of the corresponding measured line and E_p the magnitude of the voltage at node p where the measurement is done.

The observability of the system with a given measurement set is clearly dependent upon the condition number of the matrix $B^T D B$ which is fairly constant provided the structure of the measurement system and the fairly constant values of the elements in D have not changed. Thus, it is clear that the dominant factor is the structure incidence matrix of the measurements.

3.4.2 Gauss-Newton algorithm

With the Gauss-Newton method (explained in Chapter 2), the situation differs slightly, but again the main factor affecting the value of the condition number is the structure of the measurement parameters associated with each measurement equation, i.e., the admittance matrix elements associated with the measurements. This can be seen by considering that the values of the node volages are bounded between close limits, for example, $0.95 \leq |V| \leq 1.05$, where $|V|$ is the magnitude of the node voltage per unit value.

Thus, the main factors influencing the matrix $J^T J$ are the admittance matrix values for a given measurement configuration. This can be seen in the expression (3-37) which is an element i,j in the Jacobian matrix corresponding to an injection measurement at node k with $k \neq j$, with respect to the real part of the complex voltage at node j:

$$\frac{\partial P_k}{\partial e_j} = G_{kj}\, e_k + B_{kj}\, f_k \qquad (3\text{-}37)$$

Clearly for an approximately constant voltage profile, large changes in the Jacobian will correspond to changes in the parameters of the measurements structure. This can be extended to any Jacobian element where e_k and f_k are the real and imaginary parts of the node k voltage, G_{kj} and B_{kj} are the real and imaginary parts of the line admittance between nodes k and j.

3.5 Numerical results

Table 3-1 shows the condition number for several tests with different sets of measurements applied to the 5 node and 7 line system of reference (23). Observing this table we should note the following points:

Increasing the number of measurements does not necessarily mean a reduction in the condition number.

For the same number of measurements but at different points the condition number differs notably. This can be seen with test numbers 6 and 7 which have the same line measurements at the same points but different node injection measurement. State vector elements are the same for all the nodes with exception of node 5 where there is a difference of 0.00127 in the real part and 0.0003 in the imaginary part between them. However, with respect to the true values the estimation with the smallest condition number provides the closest value.

For a given set of measurements the normal level of measurement error produces approximately the same condition number as shown in tests 4 and 3, which have the same set of measurements, but in test 4 the level of error is reduced to zero. The condition number value is almost the same for both cases.

Eigenvalues associated with non-observed state vector elements are very small and practically made up by the rounding-off errors

Table 3-1 Condition number evaluated at the solution point for different cases with the 5 node system.

Test	Case	Eigenvalues largest	Eigenvalues smallest	Condition number	Remarks
1	14 LM 4 Inj.	9858.50	81.000	121.71	All line ends and all injections are measured.
2	7 LM 4 Inj.	8992.73	181.440	49.56	Lines at nodes 2 and 4 and all injections are measured.
3	14 LM	5058.05	68.228	74.14	All line ends are measured.
4	14 LM	5011.22	64.642	77.52	As above, with noise level reduced to zero.
5	4 Inj.	5590.55	11.089	504.16	Equivalent to the normal load flow solution.
6	8 LM 1 Inj.	4977.30	4.928	1009.90	Node 5 is related only to injection at node 4.
7	8 LM 1 Inj.	2173.42	18.063	120.33	Node 5 is related only to injection at node 2.
8	8 LM 1 Inj.	7084.59	10E-29	708E+29	Node 5 is not observed.
9	8 LM	796.37	33E-29	240E+28	Node 4 is not observed
10	5 LM 3 Inj.	7724.65	19.010	406.36	Node 5 is related only to injections at nodes 2 and 4.

Note.- LM = complex line flow measurement; Inj. = complex injection measurement.

in the computation. They would be zero with exact arithmetic. Hence the condition number can be very large.

The results obtained have shown that reducing the dimension of the Jacobian matrix of the measurements, by the number of columns corresponding to the unobserved nodes, it is possible to obtain the state vector corresponding to the observed portion of the network.

Table 3-2 shows the state vector elements estimated using the singular value decomposition of Section 3.3.4. The same cases were run with the Gauss-Newton method taking into consideration the columns made up of zero valued elements corresponding to the unobserved nodes and reducing the dimension of the linear system of equations to that of the observed portion. The results were the same as for the Table 3-2. The values obtained for the estimable portion of the system were practically the same as those obtained for the whole system with the added measurements that permit the observation of the whole network. This is clearly shown for the nodes 2, 3 and 4 in tests 6, 7, 8 and 10 and especially in case 8 in which node 5 is not observed. The same can be said for case 9, for nodes 2, 3 and 5 in which node 4 is not observed.

These tests were conducted with a small system but they can be extended to larger ones. Table 3-3 shows the results obtained with the 14 node and 20 line system (55) in which node 14 is not observed and the results are comparable to the solution obtained with the network fully observed as shown in tables 2-15 to 2-18.

3.6 Comments

The reachability matrix of the measurements directed graph shows which variables can be observed by a given set of measurements. The relationship between observability and reachability shows which elements of the state vector can be estimated and the elements that can not be observed correspond to those vertices that can not be reached.

Table 3-2 State vector estimated values using the singular value decomposition method.

Element	test number 6	7	8	9	10
1	1.0461	1.0461	1.0464	1.0463	1.0467
2	-.0518	-.0518	-.0511	-.0509	-.0505
3	1.0200	1.0200	1.0206	1.0205	1.0208
4	-.0900	-.0900	-.0894	-.0892	-.0882
5	1.0187	1.0187	1.0194	1.0000	1.0197
6	-.0960	-.0960	-.0953	0.0000	-.0939
7	1.0102	1.0115	1.0000	1.0117	1.0128
8	-.1099	-.1096	0.0000	-.1095	-.1071

Table 3-3 State vector obtained by using the Gauss-Newton method with 22 complex line flow measurements and 5 complex injection measurements. Node 14 is unobserved.

State vector element No.	estimated value	true value	State vector element No.	estimated value	true value
1	1.0420	1.0410	14	-.1554	-.1557
2	-.0902	-.0907	15	1.0222	1.0204
3	1.0384	1.0369	16	-.2719	-.2724
4	-.2638	-.2628	17	1.0166	1.0147
5	0.9867	0.9851	18	-.2735	-.2739
6	-.2209	-.2223	19	1.0229	1.0218
7	1.0624	1.0602	20	-.2712	-.2698
8	-.2517	-.2519	21	1.0201	1.0186
9	1.0034	1.0020	22	-.2756	-.2744
10	-.1819	-.1825	23	1.0155	1.0136
11	1.0347	1.0329	24	-.2755	-.2746
12	-.2453	-.2455	25	1.0000	0.9952
13	1.0093	1.0082	26	0.0000	-.2861

The effect of the condition number on the state estimation process has also been investigated and it has been shown that the values that may be computed for the unobserved elements (singular case) are such (arbitrary in general) that their usefulness is in doubt. Moreover, the case of unobserved elements can be described as a trivial solution of the system of equations.

It was shown that for the case when the system of linear equations is not of full rank due to unobserved portions of the network, it is possible to solve the estimable elements provided there is a voltage measurement which will give the level of voltage and angle reference inside the observable (reachable) portion. This can be done, without applying more complicated and more costly methods, by using the already well known and tested methods like the AEP or Gauss-Newton techniques by reducing the dimension of the state vector, leaving out the elements that can not be reached even if they are electrically connected.

CHAPTER FOUR

DECOMPOSITION IN POWER SYSTEMS STATE ESTIMATION

4.1 Introduction

Real-time power system problems have become increasingly large and complex, interconnecting different utilities to form pools and superpools, while on the other hand the time available for their solution appears to be decreasing and becoming more critical. These factors place an increasing burden on the system operation engineer, requiring enlargement of computer aids for problem solving. In recent years the more and more powerful computer systems have been incorporated into the control centres in electric utilities. In particular the state estimation process becomes more complicated and with the increase of system size and of number and length of communications channels, all these factors make less cost effective the centralized approach to static state estimation. To solve this problem a new decentralized state estimation scheme which overcomes the difficulties mentioned above is proposed in this chapter. Some other methods are also assessed and advantages and disadvantages of their application are discussed.

4.2 Hierarchical systems

With recent developments in relative increase in computing power by mini-computers and micro-processors it is possible to share the computing loads between different areas or subsystems. Hierarchical systems theory (71) has been used to solve the problems of optimization, state estimation and identification in power systems (50,72,73,74). In our case,the SEP, two suggested methods are explored based on hierarchical systems theory (HST) (50,73) and a third one using the theory of teams (75) is discussed.

Using HST, the principle is used of a central controller which sends out input instructions and receives output data of the sub-

systems appropriate to their needs. Fig. 4-1 depicts a hierarchical structure with two levels formed by 2 subsystems A and B. In other words, a complex system can be represented by a multitude of smaller and simpler but interacting subsystems. Each of these subsystems has its own control and/or optimization problem which it seeks to solve. Consequently, the overall system may be decomposed as follows: at the top level of the hierarchy there is only one subsystem,the controller. Each level below the top level has one or more subsystems. Each subsystem receives information fed back from the controller and sends coordinating information to the other subsystems including the controller. The action taken at one level in the hierarchy has the effect of providing constraints on the possible actions in the lower levels. The problem then is one of achieving the desired coordination among the various subsystems in such a manner that the overall system objectives are attained in an optimal manner.

Thus, it is possible to work with several smaller, more easily handled subproblems. Two types of subsystems are candidates for decomposition. The first corresponds to those systems which may possess a natural hierarchical structure which easily lend themselves to decomposition. In power systems there are clearly defined structures, namely, levels of voltage, areas, different utilities, etc. In the second case,the complexity of the problem may force the search for a hierarchical structure in order that the problem may be reduced in size to the point where a solution is possible and practical. Once a decomposition is obtained of whatever type, the solution to the overall problem proceeds in the following iterative manner:

First, the controller sets the initial conditions and supplies initial values to the constraints in the subsystem. Each subsystem then solves its own optimization problem subject to the constraints.

When the subsystems have interaction the connecting variables may be treated as additional constraints on the subsystem. Once all the subsystems problems have been solved, the results are fed back to the controller. With this information the controller adjusts the constraint variables and supplies updated values to the subsystems which in turn solve their individual problem. The process is continued until the subsystems solve their problems in such a way that all the constrained variables are satisfied and the overall cost function is optimized. This approach has been applied to power systems by Kobayashi and Narita (50). Similarly, the methods of system identification and hierarchical systems theory have been integrated to produce a sequential algorithm for state and parameter estimation in large scale systems (73).

In power systems state estimation two main ways of forming subsystems can be suggested with respect to the exchange of information between subsystems. In the first one each subsystem transmits the state estimates $\hat{\underline{x}}$ and error covariance information from the local estimator to the controller (central control). Then the controller makes the corresponding analysis and sends back information and the process iterates until a stopping criterion is reached. Once the solution is obtained the controller makes the residual analysis to check against presence of bad data and accepts the estimation or, if rejected, triggers off the bad data detection procedure.

For the second method each subsystem will have enough information to do the local validation of the estimation and -what is more important- it should be capable of obtaining the local solution without the need of exchanging information with other systems. For power systems the second approach is clearly the most attractive since it is highly desirable to have each subsystem estimating its own state and validating it independently. This last point also leads to the possibility of reducing the work load on the central controller.

The first approach using the model coordination method (71) was

applied to a typical power system (50). The idea consists in decomposing the system into areas having a hierarchy consisting of a central control computer and several area computers for regional on-line monitoring and supervision. The system shown in Fig. 4-2 consists of two areas and one tie line between the areas. It can be seen that the interconnecting nodes 1 and m have common variables to both areas and,if predicted a priori, the objective function in the state estimation process can be minimized for the whole system. Local policies can be taken into account to constrain either the magnitude and/or the angle between the common nodes. But in practice this approach requires an iterative procedure to reach the minimum of the cost function with an intermediate step for handling the constraints imposed by the interconnection variables associated with the common node. This increases the computational burden and requires the sending of iteration information between areas and the control centre, independently of the type of algorithm used to minimize the sum of square residuals for each area. So changes in the iterative process in one area generate changes in the other area, which in turn implies that some knowledge of the other area is required in the first area. This approach increases the amount of data to be transmitted and slows down the process. This kind of decomposition greatly saves on core memory requirements if the solution algorithm for the whole system involves full matrix operation. But the need for feedback information between iterations requires more time to solve the problem compared to an integrated method, which uses the whole system information.

A recent paper (75), which uses iterative information to solve this problem calls the process "decentralized state estimation". This proposition uses the theory of teams to coordinate the solution process between areas. With this method the entire system

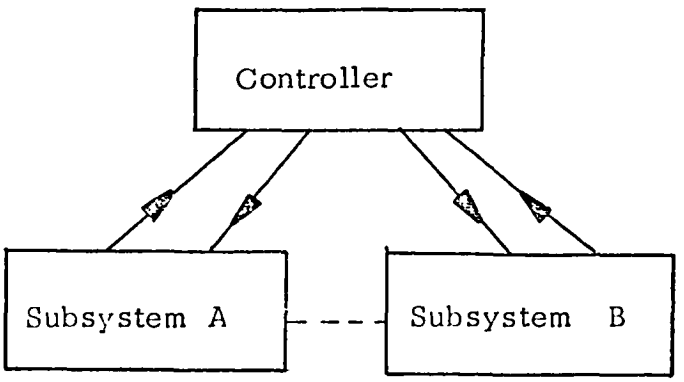

Fig. 4-1 Two level Hierarchical System.

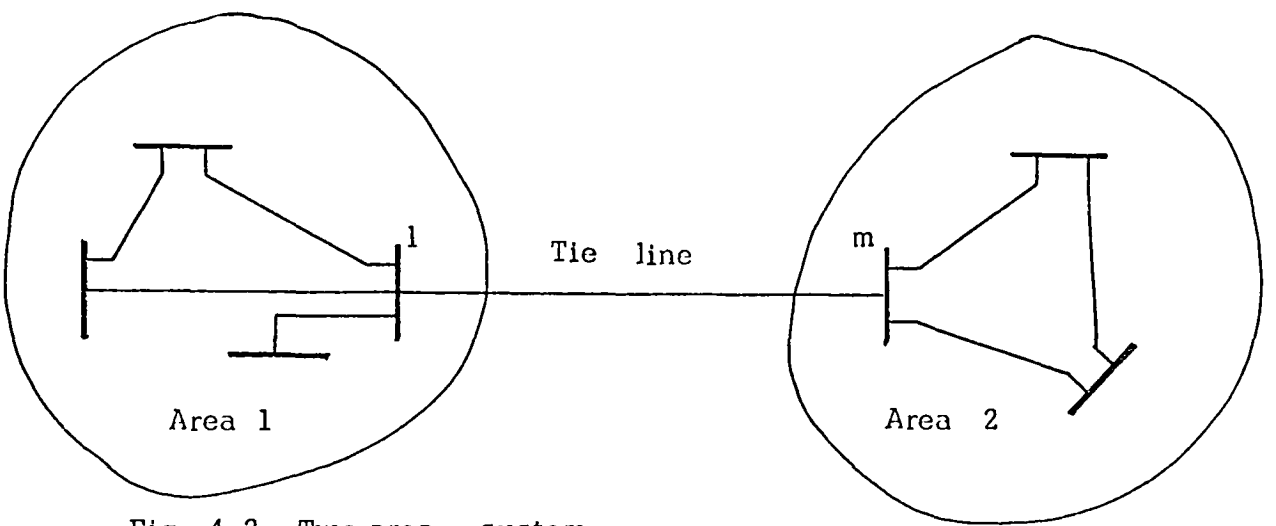

Fig. 4-2 Two area system

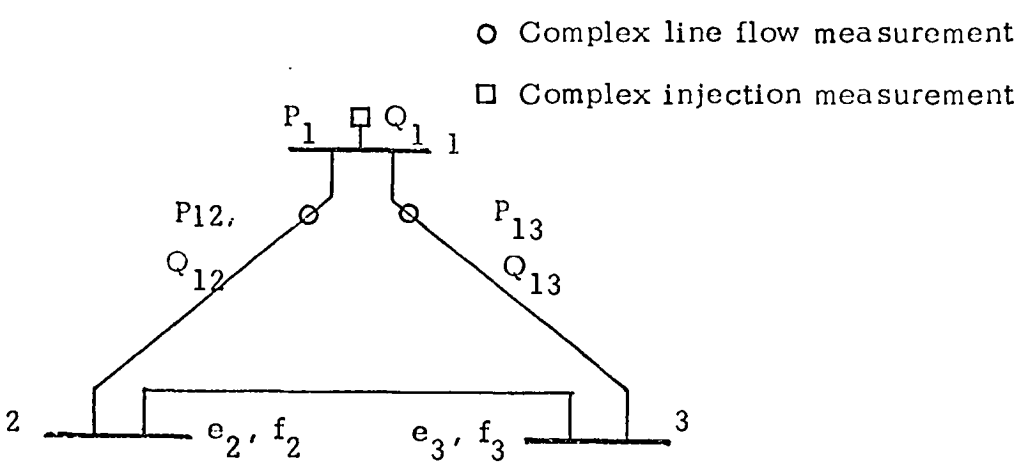

Fig. 4-3 Three node sample system.

is decomposed to a suitable number of subsystems and data which in each subsystem is collected by each local control centre. Information processed by the local estimators is interchanged with other information in a hierarchical manner. The buses of a given power system are classified into n blocks and the state vector is decomposed into n subvectors. The basic assumptions are: a) that the state vector is normally distributed and its variance-covariance matrix is known; b) the measurement equations can be linearized through a Taylor series expansion, and c) that the estimation process in each block is affected only by those elements which correspond to the buses connected to the other blocks through tie-lines. Again, the main disadvantage of the method is that it needs the interchange of information between neighbouring blocks. The exchange of phase angle information is useful for improving the convergence speed and accuracy of the phase angle estimation throughout all the blocks.

So far, the two methods described above require interchange of information between iterations, i.e., between partial solutions, something that is highly undesirable since it imposes a delay in obtaining the overall solution. In addition, high speed communication channels are demanded for this task.

4.3 Decomposed systems

4.3.1 System decomposition

A new method which overcomes the main difficulties encountered in prior suggestions is proposed using a very simple principle of independence.

It has been shown that the need for exchanging information between subsystems and the incorporation of an intermediate step to obtain overall convergence may require an optimization procedure followed by modification of the state vectors using the methods mentioned above.

The new approach takes advantage of the implicit solution of Kirchoff and Ohm laws given by the network and the corresponding information contained in the measurement set. Each measurement contains information for the unknown variables directly related to it. Fig. 4-3 shows a 3 node system having a complex injection measurement, and all complex line flows measured at node 1. The measurement of line 1 relates the complex voltage of nodes 1 and 2. The complex injection relates the complex voltages of all the nodes. So, having in mind the physical meaning of observability, it has been found possible to decompose the system into independent parts and solve them separately. This proposition does not require the imposition of a hierarchy unless it is necessary but even in this case, it will be shown that it is possible to find a decentralized solution procedure.

The decomposition of power system networks was proposed to solve the problem of load flow in very large systems. There is a good deal of literature suggesting ways in which to solve the load flow problem in partitioned networks (76,77,78). But we have to recall the distinction between the two problems (state estimation and load flows) which is the difference between a redundant and a non-redundant system of non-linear equations. This redundancy gives us flexibility and permits a fresh look at the decomposition problem as will become apparent later in this chapter.

4.3.2 Interpretation of systems decomposition

Before demonstrating approaches to the decomposed state estimation problem, we explain with block diagrams the ways a system can be decomposed. This idea was suggested by Mesarovic and Takahara (79) and a simplified variation of this proposition of general systems theory is given here (Fig. 4-4).

With reference to Fig. 4-4, it can be seen that some decompositions may be merged to give more complicated schemes but the main modules and interconnections needed are laid down. It is

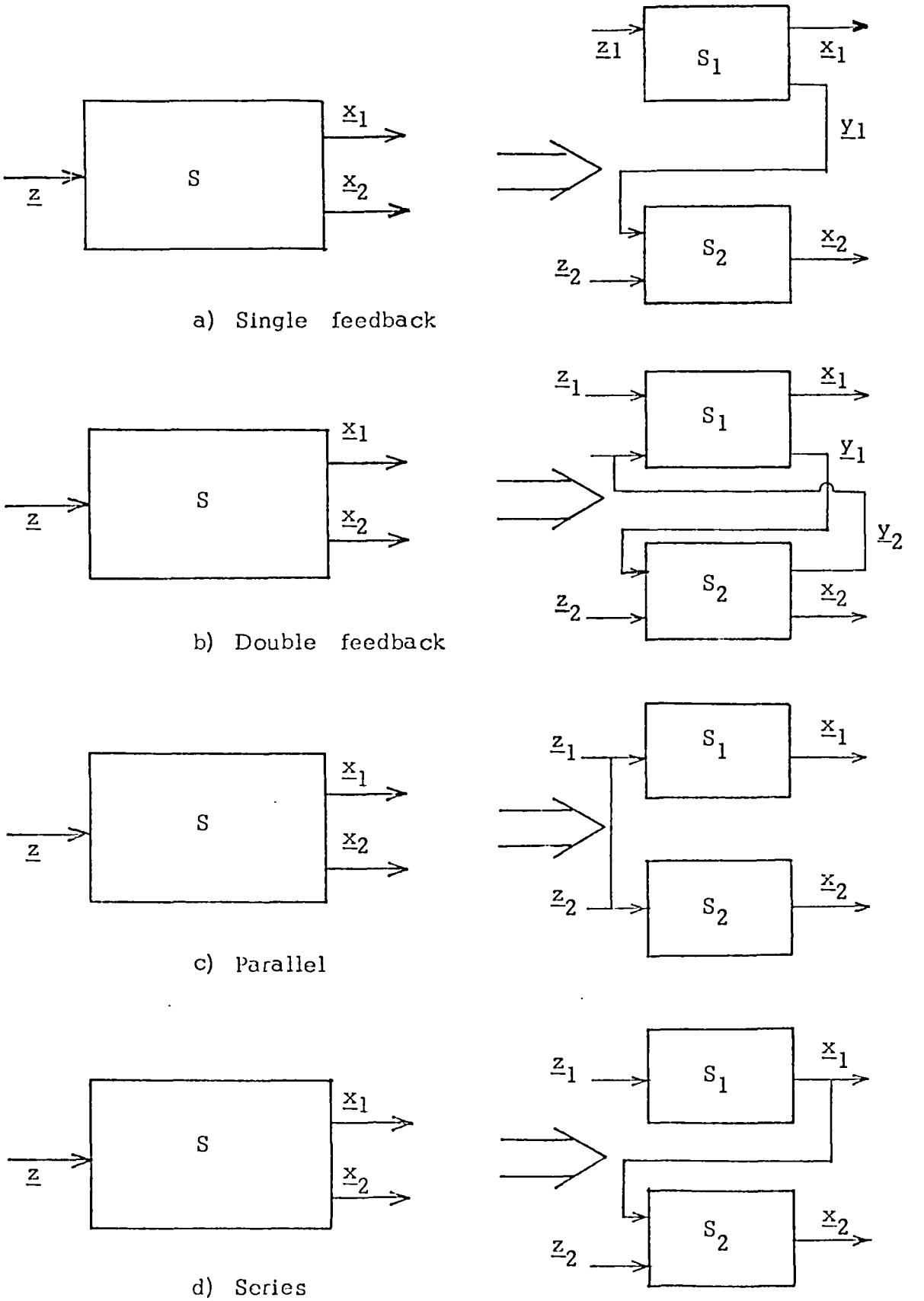

Fig. 4-4 Block diagram representation of system decomposition.

convenient to interpret these decompositions in terms of power systems state estimation.

Let us define a vector $\underline{z}$, the set of measurements which itself is formed by two subvectors $\underline{z}_1$ and $\underline{z}_2$ relating the subsets of measurements of area 1 and 2 respectively. The system S is the state estimation process and $\hat{\underline{x}}$ the estimated values of the state vector of the system composed of two subvectors $\hat{\underline{x}}_1$ and $\hat{\underline{x}}_2$ corresponding to areas 1 and 2 respectively and $\underline{y}_1$ and $\underline{y}_2$ are feedback vectors from each of the subsystems S_1 and S_2 which correspond to the estimation processes for areas 1 and 2.

Model 4-4 (a) corresponds to the case where independent sets of measurements exist for each area and feedback information (updating) is available from system 1 to system 2.

Model 4-4 (b) has the same properties as model (a) but there is additional feedback information from system 2 to system 1.

Model 4-4 (c) corresponds to the case of having common elements in the measurement set for both subsystems but the estimation for each area can be done locally without requiring any feedback between subsystems.

Finally, model 4-4 (d) is the case where we have independent sets of measurements for each area but we require the solution of the first one in order to proceed with the solution of the remainder. The main difference between this case and model 4-4 (a) is in the type of information sent between subsystems. For model 4-4 (d) the estimated value of the state vector from area 1 is required at area 2. In case 4-4 (a) however, it may be some type of processed information which may implicitly or explicitly carry information from the state vector in system 1.

4.4 An application example

In this section the interpretation of the block diagram for different decompositions will be explained.

Let us assume a network as depicted in Fig. 4-5. Its measurement

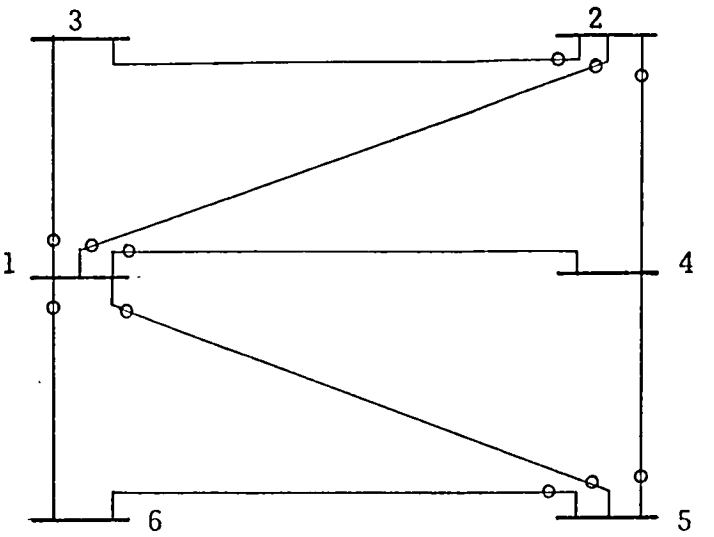

Fig. 4-5 One line diagram with measured points
o complex line flow measurement

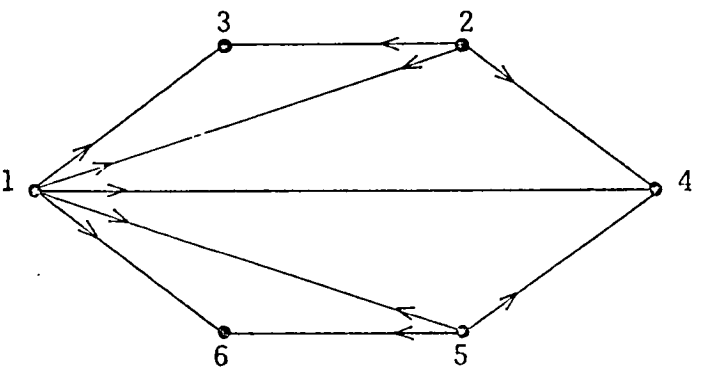

Fig. 4-6 Directed graph

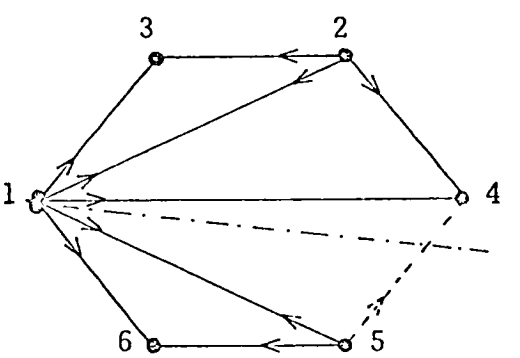

Fig. 4-7 System decomposition

incidence matrix is:

$$M = \begin{array}{c} \\ \text{Measurements} \end{array} \begin{array}{c} \begin{array}{cccccc} \multicolumn{6}{c}{\text{Nodes}} \\ 1 & 2 & 3 & 4 & 5 & 6 \end{array} \\ \begin{bmatrix} 1 & & -1 & & & \\ 1 & & & & -1 & \\ 1 & & & & & -1 \\ 1 & & & -1 & & \\ 1 & -1 & & & & \\ -1 & 1 & & & & \\ & 1 & & -1 & & \\ & 1 & -1 & & & \\ & & & -1 & & 1 \\ -1 & & & & & 1 \\ & & & & -1 & 1 \end{bmatrix} \end{array} \begin{array}{l} 1 \\ 2 \\ 3 \\ 4 \\ 5 \\ 6 \\ 7 \\ 8 \\ 9 \\ 10 \\ 11 \end{array} \qquad (4\text{-}1)$$

It shoul be noted that the structure of nonzero elements formed by submatrices of order 2×2 for the corresponding Jacobian matrix of the measurements is the same as the measurement incidence matrix, with the exception of the column corresponding to the reference node, node number one. This is illustrated in expression (3-22) and Fig. 3-3. The measurements for the former example are shown in the graph of Fig. 4-5.

Let us take node 1 as reference node, then the structure of the Jacobian is given by matrix S as follows, where x denotes nonzero elements.

$$S = \begin{array}{c} \\ \text{Measurements} \end{array} \begin{array}{c} \begin{array}{ccccc} 2 & 3 & 4 & 5 & 6 \end{array} \text{ Nodes} \\ \begin{bmatrix} & \times\times & & & \\ & \times\times & & & \\ & & & \times\times & \\ & & & \times\times & \\ & & & & \times\times \\ & & & & \times\times \\ & & \times\times & & \\ & & \times\times & & \\ \times\times & & & & \\ \times\times & & & & \\ \times\times & & & & \\ \times\times & & & & \\ \times\times & & \times\times & & \\ \times\times & & \times\times & & \\ \times\times & \times\times & & & \\ \times\times & \times\times & & & \\ & & \times\times & & \times\times \\ & & \times\times & & \times\times \\ & & & & \times\times \\ & & & & \times\times \\ & & & \times\times & \times\times \\ & & & \times\times & \times\times \end{bmatrix} \end{array} \begin{array}{c} 1 \\ 2 \\ 3 \\ 4 \\ 5 \\ 6 \\ 7 \\ 8 \\ 9 \\ 10 \\ 11 \end{array} \qquad (4\text{-}2)$$

Now, the crucial point of the solution procedure using the non-linear weighted least squares method in state estimation is the solution of the linear system of equations given by

$$J^T W J \Delta\underline{\hat{x}} = J^T W \underline{r} \qquad (4\text{-}3)$$

where J is the Jacobian matrix of the set of measurements, $\underline{r}$ the residuals vector at the current iteration and $\Delta\underline{\hat{x}}$ is the updating increment of the estimated state vector $\underline{\hat{x}}$.

To simplify the explanation of the decomposition there is no need to include the weighting matrix W since it is a diagonal matrix and it does not affect the nonzero elements structure of the Jacobian, so it is possible to use just the matrix S to illustrate the point.

Let us find $S^T S$:

$$S^T S = \begin{array}{c} \\ \text{Nodes} \\ 2 \\ 3 \\ 4 \\ 5 \\ 6 \end{array} \begin{array}{c} \begin{array}{ccccc} 2 & 3 & 4 & 5 & 6 \end{array} \\ \begin{bmatrix} \times\times & \times\times & \times\times & & \\ \times\times & \times\times & \times\times & & \\ \times\times & \times\times & & & \\ \times\times & \times\times & & & \\ \times\times & & \times\times & & \times\times \\ \times\times & & \times\times & & \times\times \\ & & & \times\times & \times\times \\ & & & \times\times & \times\times \\ & & \times\times & \times\times & \times\times \\ & & \times\times & \times\times & \times\times \end{bmatrix} \end{array} \qquad (4\text{-}4)$$

Looking at the matrix $S^T S$, it is readily seen that if we remove measurement 9 which links nodes 4 and 6 (dotted), the structure of the matrix $J^T W J$ is modified in such a way that after removing the row corresponding to measurement 9 in the system, the new structure is given by matrix $S'^T S'$ as:

$$S'^T S' = \begin{array}{c} \\ \text{Nodes} \\ 2 \\ 3 \\ 4 \\ 5 \\ 6 \end{array} \begin{array}{c} \begin{array}{ccccc} 2 & 3 & 4 & 5 & 6 \end{array} \\ \begin{bmatrix} \times\times & \times\times & \times\times & & \\ \times\times & \times\times & \times\times & & \\ \times\times & \times\times & & & \\ \times\times & \times\times & & & \\ \times\times & & \times\times & & \\ \times\times & & \times\times & & \\ & & & \times\times & \times\times \\ & & & \times\times & \times\times \\ & & & \times\times & \times\times \\ & & & \times\times & \times\times \end{bmatrix} \end{array} \qquad (4\text{-}5)$$

This changes the numerical value of block (4, 4) but the structure remains the same. The block diagonal structure of (4-5) clearly indicates that there are independent solutions for nodes 2, 3 and 4 with reference node at 1 and for nodes 5 and 6 with the same node one as reference node.

The variance-covariance matrix of the estimated state vector can be obtained using the properties for block diagonal matrices. So, it is possible to evaluate the variance-covariance matrix in separate forms, independently for each subsystem.

Let us put

$$\text{Cov}(\hat{x}) = (J^T W J)^{-1} \tag{4-6}$$

From (4-4), we can write

$$J = \begin{bmatrix} J_1 & 0 \\ 0 & J_2 \end{bmatrix} \quad ; \qquad W = \begin{bmatrix} W_1 & 0 \\ 0 & W_2 \end{bmatrix}$$

then we have in (4-5):

$$A^{-1} = (J^T W J)^{-1} = \left[\begin{bmatrix} J_1^T & 0 \\ 0 & J_2^T \end{bmatrix} \begin{bmatrix} W_1 & 0 \\ 0 & W_2 \end{bmatrix} \begin{bmatrix} J_1 & \\ & J_2 \end{bmatrix} \right]^{-1}$$

$$A^{-1} = \begin{bmatrix} J_1^T W_1 J_1 & 0 \\ 0 & J_2^T W_2 J_2 \end{bmatrix}^{-1} = \begin{bmatrix} A_1^{-1} & 0 \\ 0 & A_2^{-1} \end{bmatrix} \tag{4-7}$$

$$\text{Cov}(x_1) = A_1^{-1} \quad ; \tag{4-8}$$

$$\text{Cov}(x_2) = A_2^{-1} \tag{4-9}$$

Expressions (4-8) and (4-9) are the variance-covariance matrices for systems 1 and 2 respectively.

In Fig. 4-7 the parting arc is shown by the dotted line joining nodes 4 and 5. The subsystems are formed using node 1 as reference. The decomposed solution obtained can be related to the decomposition corresponding to model (c) in Fig. 4-4. The link in the input to each subsystem is the voltage at the reference node 1. Up to now we have not considered measurement number 9 which links the independent blocks of equations. Returning to Fig. 4-7, when measurement number 9 is used one additional piece of information, the complex voltage of node 4, is considered as another measurement. This procedure is the equivalent to the block diagram

d shown in Fig. 4-4.

If it is required to use all the measurements, another possibility is to handle the problem in a sequential manner, i.e., solve the problem for nodes 2, 3 and 4 as before, and afterwards solve the subsystem formed by nodes 5 and 6 with the addition of node 4, but without considering the measurements already used for the first subproblem.

It is important to emphasize that for both cases there is no need to exchange information between iterations. In the sequential solution case only the information from the state vector is needed, but its amount is quite small and it is not needed between iterations.

Another example extending these ideas showing a three subsystem case will be described in dealing with the principles to decompose the system in Section 5.4.

4.5 Numerical examples

The proposed method has been tested with different sets of measurements for two systems, the 14 node and 20 line (55) and the 23 node and 30 line (58), which are detailed in the Appendix 4. In both cases the systems were decomposed into two subsystems as indicated by the dotted line in figures 4-8 and 4-9. A common reference node at one of the partitioning points has been chosen. The sets of measurements corresponding to each case are shown by the arcs .

The results obtained for the state vector and its standard deviation are contained in tables 4-1 to 4-4. I t should be noted that values obtained for the state vector with the system solved together and the solutions obtained using the new decomposition are very close. The reason for the small difference is apparent from the expressions obtained for the covariance matrices in block diagonal forms. The voltages themselves are usually slightly different but this difference is diluted in the elements of the variance-covariance matrix $A = (J^T W J)^{-1}$. Looking at a particular element a(k,i) which is given by

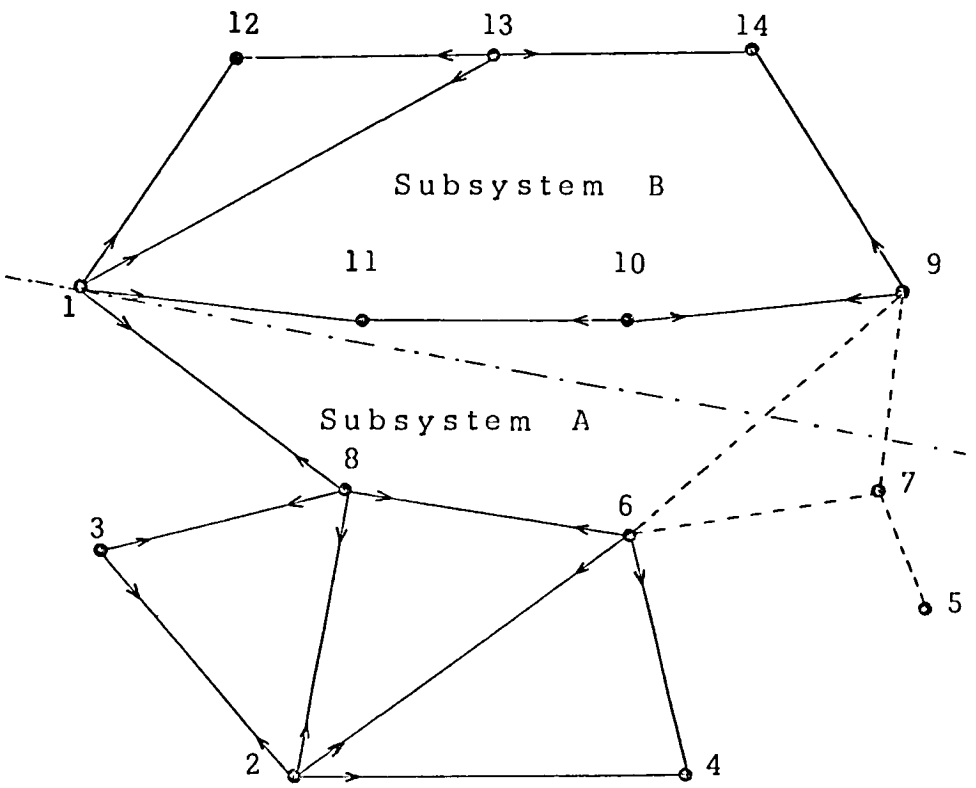

Fig. 4-8 Decomposition of the 14 node system

Table 4-1 Voltage values for the 14 node system, using a decentralized state estimator (see Fig. 4-8)
Reference voltage at node 1 = 1.06968 + j 0.0

Node No.	Solution E	Solution F	Standard Deviation 10^4 E	Standard Deviation 10^4 F
		(14 LM, 3 Inj.)		
2	1.03144	0.16743	3.53	9.55
3	1.02761	0.26034	4.27	10.61
4	1.00918	0.02643	3.94	11.03
5	- -	- -	-	-
6	1.01596	0.06850	3.28	9.36
7	- -	- -	-	-
8	1.01545	0.09617	3.03	8.29
		(16 LM, 1 Inj.)		
9	1.05584	-.01363	2.54	2.99
10	1.05066	-.01661	2.47	2.88
11	1.05633	-.01102	2.04	2.41
12	1.05416	-.01618	2.01	2.33
13	1.04999	-.01756	1.37	1.71
14	1.03465	-.03327	2.94	3.48
		(14 LM, 0 Inj.)		
2	1.03182	0.16935	3.91	11.93
3	1.02784	0.26047	4.55	12.80
4	1.00988	0.02840	4.17	12.37
5	- -	- -	-	-
6	1.01660	0.07018	3.53	10.90
7	- -	- -	-	-
8	1.01591	0.09729	3.45	10.56
		(10 LM, 1 Inj.)		
9	1.05596	-.01398	3.46	4.13
10	1.05078	-.01696	3.42	4.05
11	1.05650	-.01116	2.84	3.41
12	1.05412	-.01626	2.70	3.10
13	1.04995	-.01761	1.49	1.88
14	1.03466	-.03337	3.93	4.74

Table 4-2 Voltage values for the 14 node system, using a centralized state estimator (see Fig. 4-8).
Reference voltage at node 1 = 1.06968 + j0.0

Node No.	Solution E	Solution F	Standard Deviation 10^4 E	Standard Deviation 10^4 F
		(24 LM , 6 Inj.)		
2	1.03117	0.16798	3.53	9.54
3	1.02716	0.26108	4.27	10.59
4	1.00944	0.02657	3.94	11.03
5	1.09007	0.01689	7.05	4.89
6	1.01599	0.06877	3.28	9.36
7	1.06202	0.01618	3.23	4.32
8	1.01542	0.09653	3.03	8.28
9	1.05654	-.01292	3.46	4.13
10	1.05149	-.01571	3.42	4.05
11	1.05732	-.01030	2.84	3.40
12	1.05492	-.01565	2.69	3.10
13	1.05016	-.01715	1.49	1.88
14	1.03460	-.03336	3.92	4.73
		(24 LM , 8 Inj.)		
2	1.03125	0.16819	2.97	7.55
3	1.02744	0.26135	3.51	9.00
4	1.00924	0.02533	3.64	9.21
5	1.08977	0.01624	6.16	4.61
6	1.01597	0.06910	2.53	6.34
7	1.06161	0.01578	3.08	4.03
8	1.01543	0.09670	2.44	5.98
9	1.05591	-.01355	2.84	3.77
10	1.05067	-.01631	2.93	3.77
11	1.05625	-.01100	2.63	3.27
12	1.05430	-.01583	2.69	3.10
13	1.04989	-.01727	1.48	1.87
14	1.03459	-.03291	3.81	4.71
		(26 LM , 0 Inj.)		
2	1.03120	0.16667	3.91	11.94
3	1.02720	0.25993	4.56	12.80
4	1.00939	0.02604	4.18	12.39
5	1.08920	0.01619	7.27	14.73
6	1.01605	0.06861	3.53	10.91
7	1.06081	0.01571	5.51	14.25
8	1.01535	0.09602	3.45	10.58
9	1.05679	-.01331	3.47	4.14
10	1.05175	-.01610	3.43	4.06
11	1.05719	-.01034	2.84	3.41
12	1.05487	-.01628	2.70	3.15
13	1.05009	-.01723	1.88	2.39
14	1.03493	-.03345	3.97	4.77

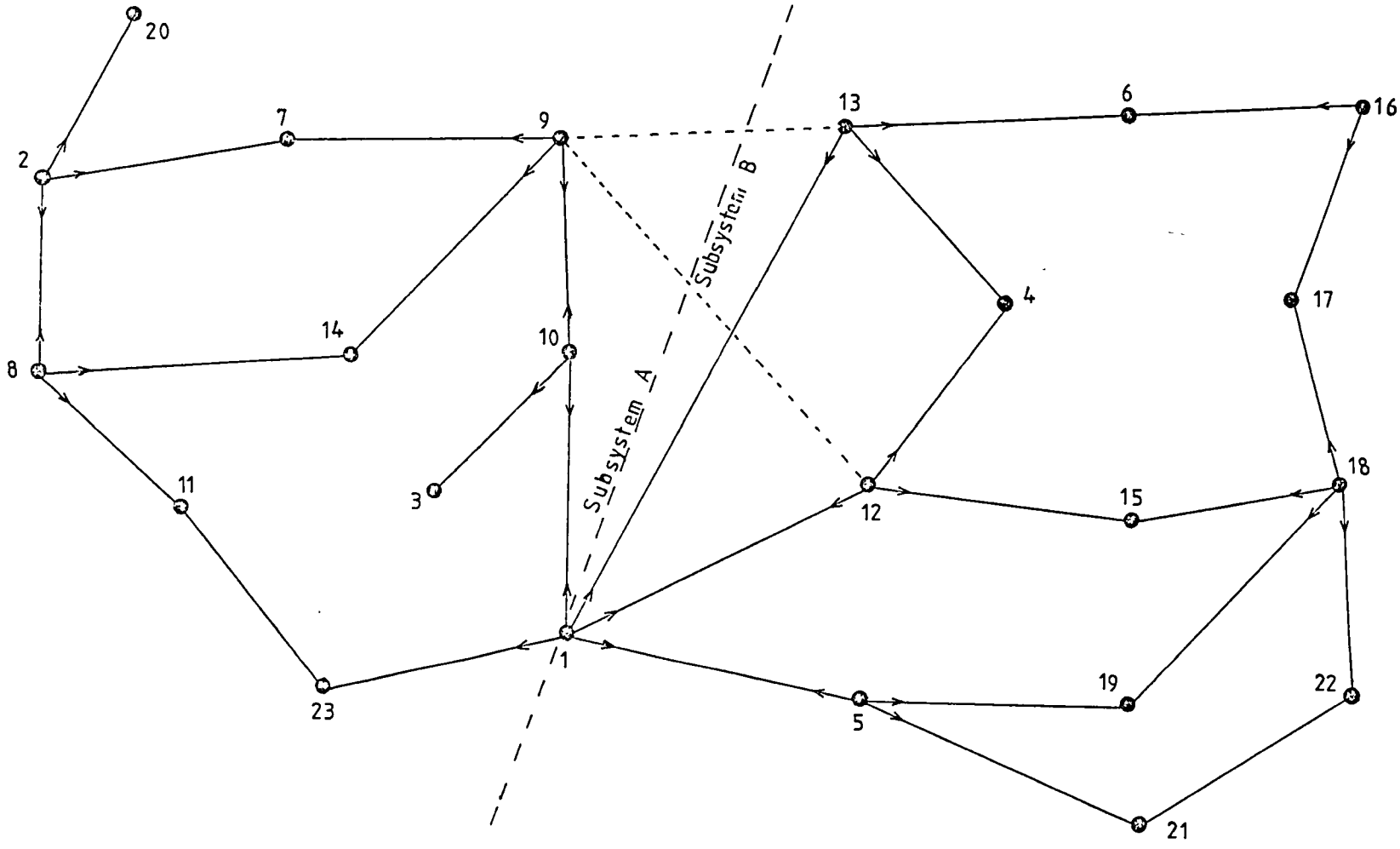

Fig. 4-9 Decomposition of the 23 node system.

Table 4-3 Voltage values for the 23 node system, using a decentralized state estimator (see Fig. 4-9).

Node No.	Total Solution		Decomposed Solution		Standard Deviation 10^4	
	E	F	E	F	E	F
2	1.00402	-.19804	1.00146	-.20103	8.11	11.39
3	1.03207	-.08234	1.03151	-.08431	7.48	12.74
4	1.04968	-.00573	1.04950	-.00563	2.12	2.52
5	1.04169	0.12948	1.04236	0.13232	1.44	6.72
6	1.03417	0.17953	1.03418	0.18028	1.78	9.66
7	0.98442	-.15895	0.98107	-.16219	7.53	10.84
8	1.00627	-.16819	1.00376	-.17145	7.80	11.22
9	0.99773	-.12748	0.99516	-.13005	6.79	10.24
10	0.97781	-.11588	0.97570	-.11863	6.35	9.81
11	1.00137	-.14406	0.99878	-.14747	8.23	11.55
12	1.03575	-.02648	1.03565	-.02709	0.86	2.30
13	1.03501	0.01264	1.03467	0.01218	1.61	1.62
14	0.99000	-.16000	0.98724	-.16300	7.51	10.97
15	1.01665	-.02801	1.01681	-.02861	1.94	2.38
16	1.01706	0.08345	1.01718	0.08428	2.00	6.17
17	1.01091	0.04692	1.01111	0.04761	2.12	6.18
18	1.01545	0.02590	1.01567	0.02647	2.00	5.33
19	1.01140	0.01866	1.01155	0.01945	2.10	5.53
20	0.96355	-.23073	0.96118	-.23318	9.63	12.37
21	1.02708	0.07072	1.02770	0.07307	2.63	10.50
22	1.02770	0.06798	1.02835	0.06946	2.46	8.05
23	0.98196	-.07996	0.98151	-.07945	5.49	10.75

Reference voltage at node 1 = 1.00049 + j 0.0

The number of measurements for the whole system is 32 LM and 6 Inj. Subsystem A: 14 LM and 3 Inj.; subsystem B: 18 LM and 3 Inj.

Table 4-4 Voltage values for the 23 node system, using a decentralized state estimator (see Fig. 4-9).

Node No.	Total Solution E	Total Solution F	Decomposed Solution E	Decomposed Solution F	Standard Deviation 10^4 E	Standard Deviation 10^4 F
2	1.00184	-.20054	1.00162	-.19972	8.44	11.93
3	1.03135	-.08673	1.03228	-.08402	8.24	12.89
4	1.05005	-.00515	1.04957	-.00517	2.12	2.52
5	1.04206	0.13049	1.04197	0.13075	1.55	7.17
6	1.03427	0.17836	1.03398	0.17942	1.97	11.69
7	0.98161	-.16194	0.98168	-.16086	7.68	11.22
8	1.00378	-.17139	1.00347	-.17081	8.10	11.75
9	0.99518	-.13033	0.99565	-.12900	6.96	10.66
10	0.97583	-.11896	0.97609	-.11757	6.51	10.26
11	0.99884	-.14702	0.99852	-.14644	8.46	11.94
12	1.03575	-.02665	1.03575	-.02673	0.86	2.30
13	1.03520	0.01276	1.03470	0.01230	1.62	1.62
14	0.98744	-.16302	0.98709	-.16245	7.70	11.39
15	1.01696	-.02802	1.01666	-.02814	1.97	2.39
16	1.01746	0.08412	1.01696	0.08269	2.11	7.66
17	1.01138	0.04693	1.01090	0.04633	2.15	6.54
18	1.01594	0.02644	1.01530	0.02511	2.09	6.15
19	1.01180	0.01921	1.01129	0.01811	2.16	6.21
20	0.96122	-.23275	0.96101	-.23198	10.24	13.17
21	1.02741	0.07118	1.02757	0.07148	2.70	11.05
22	1.02827	0.06893	1.02804	0.06699	2.55	8.21
23	0.98151	-.07945	0.98168	-.07923	5.49	10.75

Reference voltage at node 1 = 1.00049 + j 0.0

The number of measurements for the whole system is 32 LM and 0 Inj. Subsystem A: 14 LM and 0 Inj.; subsystem B: 18 LM and 0 Inj.

$$a(k,i) = \sum_{j=1}^{m} W_{ii} \frac{\partial f_j}{\partial x_i} \frac{\partial f_j}{\partial x_i} \qquad (4\text{-}10)$$

where W_{ii} is the same for the decomposed solution and for the complete one. It can be seen that the values of $\partial f_j / \partial x_i$ are the same, since only those elements that are directly related, i.e., the connected elements in the directed graph, have non-zero values and they are the only elements which have influence in the element a(k,i). This effect can be deduced from the graphs corresponding to the measured points.

For the 14 node system decomposition, the system was simplified by parting nodes 5 and 7, without any loss of generality. These nodes do not have a strong influence on the state vector and dropping them only affects injections at nodes 6 and 9. However, these are not considered since our main measurement cutting line is on the line that links node 6 and 9. The only common element that can be seen for both areas is the reference node. But it is important to note that this does not mean that the system itself is disconnected. The same idea applies to the measurements for the 23 node system. In its measurement directed graph, shown in Fig. 4-9, it can be seen how it splits clearly into two parts with a common reference node.

4.6 Comments

It has been shown how feasible the present approach is to the solution of the state estimation problem, solved in a decentralized manner. In practice it would be possible to use transformers as breaking points, as in our examples, since they are the natural choice for the splitting points, not only from the mathematical point of view but also from the natural division of voltage levels throughout the system. Thus we are faced with the problem: how can decomposition be achieved in a systematic way ? The works

already mentioned (50,73,75) do not provide an answer and in the next chapter this problem will be dealt with by a proposed possible procedure.

The advantages of the present approach to the decomposed state estimation are:

1. Large problems can be handled in smaller subproblems.
2. Smaller computer requirements, time and core storage.
3. Different, localized computers can solve the estimation problem of the area independently.
4. Smaller amount of information need to be interchanged between areas, implying savings on communication lines.
5. Increased reliability since the task of estimation is shared among several computers.

CHAPTER FIVE

DECOMPOSITION METHOD

5.1 Introduction

The size of the problems posed by the modern power system in terms of computer needs, has encouraged several researchers to try to find ways of decomposing the large problems into smaller subproblems with a systematic procedure. The aim is to obtain more tractable and efficient solutions. The power systems SEP is equivalent to a large system of redundant non-linear equations. An algorithm to find the main nodes (vertices) of the measuremcnts directed graph is proposed and use of reachability properties of directed graphs is made. A procedure to find the possible decentralized subsystems using an ordering algorithm is illustrated. This procedure is applied to the adjacency matrix structure of the power system network and several test systems were conducted to show the heuristics applied to obtain the final decomposition.

5.2 Decomposition and related problems

For some time there has been a widespread interest in finding an algorithm, which has the capabilities for the efficient solution of very large problems using a partitioned subsystem. Real-time operation of power systems in recent times has made this type of solution an urgent need due to the capabilities of core size and computing time available in a real-time environment. The application of mini-computers reduces the amount of data to be transmitted and increases the processing power of the local controller.

In the past, three problems have motivated the search for algorithms to decompose the power system network into smaller subnetworks. These problems are: load flow (78,85), economic dispatch (80) and network reduction (84,86).

The algorithms suggested to decompose the large problem into smaller subproblems can briefly be described in the following manner:

1) Form trees for each area, keeping the lines with the highest impedance to form the linking lines between subsystems (83). This proposal applies decomposition to those lines which produce least partitioning effects.
2) Find some combination of boundary nodes such that the number of lines radiating from the main system is kept to a minimum. This ensures that a minimum number of nodes are related to the outside areas (84,86). By these means, the minimum fill-in is obtained for the admittance matrix that is required in the area that is to be analized in detailed form.
3) Find some node permutation such that the system admittance matrix forms a set of diagonal blocks with the least number of connections between them (81,87). This produces diagonal blocks which will permit a sequential solution of the subproblem.

The above three procedures are oriented towards the solution of a set of n equations (linear or non-linear) in n unknowns. This limits the extent of searching the decomposed parts and forces all the parts to be connected in some manner.

The SEP possesses a special feature with respect to the problems mentioned above. It can be expressed as a redundant system of non-linear equations. Taking advantage of this redundancy, it is possible to solve the whole problem as several smaller, independent subproblems. These decentralized subsystem problems can then be solved without having to put the solution of these smaller subproblems together to form the solution of the original problem. Thus savings in execution time and the exchange of information is produced. However, the main hurdle is to find the cutting points so that the subsystems formed are independent and observable with acceptable degradation due to neglected measurements in the links between the subsystems.

To date, no criteria have been proposed to decompose the SEP in such a way that it is possible to find a localized set of measure-

ments that can be used by a local state estimator. It is true that for the diakoptics and piece-wise load flow approaches several criteria have been suggested and their results reported (81,83, 82). In these references, the solution of the whole problem is obtained by a set of subproblems which cover a subnetwork of a given size or some arbitrary number of nodes with the aim of having the least number of links between subsystems. All these criteria and some of those mentioned before for network decomposition, are not easily implemented. It is necessary to apply graph theory to determine the cutting points.

The decomposition, for state estimation, might make more stringent the local redundancy in the sense that for a local (decentralized) state estimator it is necessary to have enough local measurements to achieve independent subsystems without omitting any measurements. It is important to note that the process of achieving independent areas is not done by omission of unknown variables, relaxing them or fixing them to some value. On the other hand, it may require sometimes to duplicate some border node voltages and to handle them as measurements for a different area or simply compute them for each case, with their associated area measurements. Thus, independence between areas can be obtained by:

a) Neglecting some measurements, i.e., supressing some of the redundant information. This will imply either a small degradation from the overall optimum solution or none at all in some particular cases.
b) Estimating voltages at the boundary nodes twice using only the information contained on "each side" of the boundary system and
c) As in (b) but applying a series solution in which it is required to receive some information from the central control, for

example the reference angle from the cut border nodes, and then to use the known node voltage for the magnitudes. This corresponds to model (d) in Fig. 4-4.

5.3 Application of graph theory concepts

In the analysis of systems in general, it is useful to find some concepts which will help in clarifying our understanding of the interaction of the different elements that form a large system. In recent times there has been an increasing awareness of the need of developing a generalized systems theory (88) that takes into account the behaviour of the large power systems as a whole and using hierarchical systems theory to analize and to control the relatively smaller areas or elements in a decentralized manner without relaxing the overall control of the complete system. In this respect, graph theory provides a theoretical framework which permits us to take advantage of the structural properties of the power system. This approach brings with it a set of optimality criteria and algorithms which enhance the understanding of the power system problems. Algorithms associated with graph theory, such as maximum flow, shortest spanning tree, etc. can be described by using abstract concepts. Application of these concepts to a set of measurements makes apparent the potential of these ideas, as shown in Chapter 3 of this thesis.

The adjacency matrix provides a systematic representation of the measurements from a system. The crucial problem is now to find those measurements that decompose the directed graph into disconnected subgraphs which satisfy the requirements of a decentralized state estimator.

Initially, it is necessary that in any partitioning of the measurement set, relates all the unknown variables contained in each corresponding segment of the system. It is important to know which variables are observable (for the whole system) with the available

(non-decomposed) set of measurements. In Chapter 3, it was mentioned that the reachability matrix could be used to check this property.

Let us now consider the next graph theory concepts (62).

A graph G is strongly connected if there exists a path between every pair of distinct vertices. This definition is equivalent to saying that we can go or we can "see" from any vertex i to any other vertex j.

A graph is said to be "weakly connected" or "weak" if there is at least one chain joining every pair of distinct vertices. This can be illustrated by the example of Fig. 5-1 (b), which is a weak graph, since there is no path from x_1 to x_4; x_1 to x_5 and vice-versa.

If a graph is not strongly connected, the strongest components of G are the maximal strongly connected subgraphs of G. In the above mentioned example, the subgraph formed by vertices 4 and 5 is a strongly connected subgraph and these vertices form a strong component of graph G.

The vertices contained in a strong component can be found by selecting those vertices related to a vertex x_i, when this vertex x_i is taken to be both the initial and terminal vertices of a path. The vertices that can reach x_i and be reached from x_i, and also reach and be reached from each other, can be obtained in the set given by $R(x_i) \cap Q(x_i)$, where the operator $\cap$ means the common elements of the considered set. This can be computed by the special matrix operation $R \otimes Q$, where the operator $\otimes$ means the element by element binary multiplication of the two matrices. It is apparent that row x_i of the matrix $R \otimes Q$ contains values of 1 in those columns x_j for which x_i and x_j are mutually reachable and values of 0 in all other places. Thus, two vertices are in the same strong component if and only if their corresponding rows

(a)

Measurements:

Δ voltage magnitude

O complex line flow

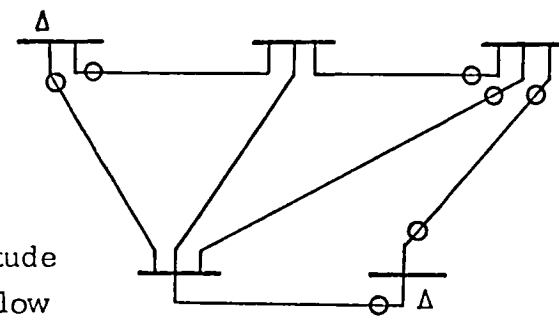

(b)

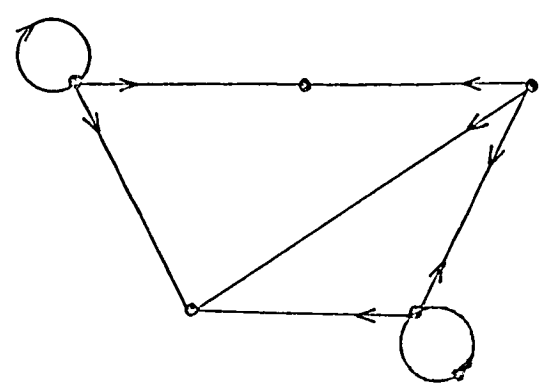

Fig. 5-1 Sample power system network. (a) One line diagram with measured points. (b) Its equivalent directed graph.

(or columns) are identical.

The next example will show this clearly.

Let us have the directed graph shown in Fig. 5-2 with its adjacency matrix as:

$$A = \begin{array}{c} \\ 1 \\ 2 \\ 3 \\ 4 \\ 5 \\ 6 \\ 7 \\ 8 \\ 9 \\ 10 \\ 11 \\ 12 \\ 13 \end{array} \begin{array}{c} \begin{array}{ccccccccccccc} 1 & 2 & 3 & 4 & 5 & 6 & 7 & 8 & 9 & 10 & 11 & 12 & 13 \end{array} \\ \left[\begin{array}{ccccccccccccc} & 1 & 1 & 1 & & 1 & & & & & & & \\ 1 & & 1 & 1 & 1 & & & & & & & & \\ & & & & & & & & & & & & \\ 1 & 1 & & & 1 & & 1 & 1 & & & & & \\ & & & & & & & & & & & & \\ 1 & & & & & & & & & 1 & & 1 & 1 \\ & & & & & & & & & & & & \\ & & & 1 & & & 1 & & 1 & & 1 & & \\ & & & & & & & & & & & & \\ & & & & & & & & & & & & \\ & & & & & & & & & & & & \\ & & & & & & & & & & & & \\ & & & & & 1 & & & & & & 1 & 1 & \end{array}\right] \end{array} \qquad (5\text{-}1)$$

Its reachability and reaching matrices are:

$$R = \begin{array}{c} \\ 1 \\ 2 \\ 3 \\ 4 \\ 5 \\ 6 \\ 7 \\ 8 \\ 9 \\ 10 \\ 11 \\ 12 \\ 13 \end{array} \begin{array}{c} \begin{array}{ccccccccccccc} 1 & 2 & 3 & 4 & 5 & 6 & 7 & 8 & 9 & 10 & 11 & 12 & 13 \end{array} \\ \left[\begin{array}{ccccccccccccc} 1 & 1 & 1 & 1 & 1 & 1 & 1 & 1 & 1 & 1 & 1 & 1 & 1 \\ 1 & 1 & 1 & 1 & 1 & 1 & 1 & 1 & 1 & 1 & 1 & 1 & 1 \\ & & 1 & & & & & & & & & & \\ 1 & 1 & 1 & 1 & 1 & 1 & 1 & 1 & 1 & 1 & 1 & 1 & 1 \\ & & & & 1 & & & & & & & & \\ 1 & 1 & 1 & 1 & 1 & 1 & 1 & 1 & 1 & 1 & 1 & 1 & 1 \\ & & & & & & 1 & & & & & & \\ 1 & 1 & 1 & 1 & 1 & 1 & 1 & 1 & 1 & 1 & 1 & 1 & 1 \\ & & & & & & & & 1 & & & & \\ & & & & & & & & & 1 & & & \\ & & & & & & & & & & 1 & & \\ & & & & & & & & & & & 1 & \\ 1 & 1 & 1 & 1 & 1 & 1 & 1 & 1 & 1 & 1 & 1 & 1 & 1 \end{array}\right] \end{array} \qquad (5\text{-}2)$$

Fig. 5-2 Directed graph of a 13 node system with 24 measurements.

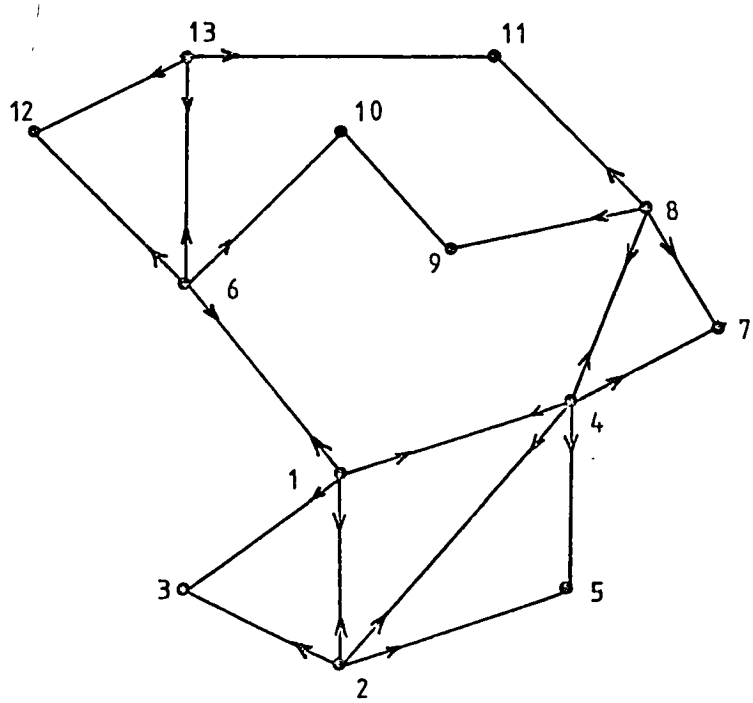

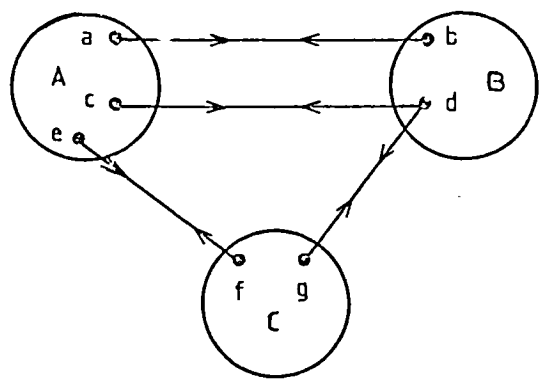

Fig. 5-3 System decomposed into three subsystems.

$$Q = \begin{array}{c} \\ 1 \\ 2 \\ 3 \\ 4 \\ 5 \\ 6 \\ 7 \\ 8 \\ 9 \\ 10 \\ 11 \\ 12 \\ 13 \end{array} \begin{array}{c} \begin{array}{ccccccccccccc} 1 & 2 & 3 & 4 & 5 & 6 & 7 & 8 & 9 & 10 & 11 & 12 & 13 \end{array} \\ \left[\begin{array}{ccccccccccccc} 1 & 1 & & 1 & & 1 & & 1 & & & & & 1 \\ 1 & 1 & & 1 & & 1 & & 1 & & & & & 1 \\ 1 & 1 & 1 & 1 & & 1 & & 1 & & & & & 1 \\ 1 & 1 & & 1 & & 1 & & 1 & & & & & 1 \\ 1 & 1 & & 1 & 1 & 1 & & 1 & & & & & 1 \\ 1 & 1 & & 1 & & 1 & & 1 & & & & & 1 \\ 1 & 1 & & 1 & & 1 & 1 & 1 & & & & & 1 \\ 1 & 1 & & 1 & & 1 & & 1 & & & & & 1 \\ 1 & 1 & & 1 & & 1 & & 1 & 1 & & & & 1 \\ 1 & 1 & & 1 & & 1 & & 1 & & 1 & & & 1 \\ 1 & 1 & & 1 & & 1 & & 1 & & & 1 & & 1 \\ 1 & 1 & & 1 & & 1 & & 1 & & & & 1 & 1 \\ 1 & 1 & & 1 & & 1 & & 1 & & & & & 1 \end{array}\right] \end{array} \qquad (5\text{-}3)$$

$$R \otimes Q = \begin{array}{c} \\ 1 \\ 2 \\ 3 \\ 4 \\ 5 \\ 6 \\ 7 \\ 8 \\ 9 \\ 10 \\ 11 \\ 12 \\ 13 \end{array} \begin{array}{c} \begin{array}{ccccccccccccc} 1 & 2 & 3 & 4 & 5 & 6 & 7 & 8 & 9 & 10 & 11 & 12 & 13 \end{array} \\ \left[\begin{array}{ccccccccccccc} 1 & 1 & & 1 & & 1 & & 1 & & & & & 1 \\ 1 & 1 & & 1 & & 1 & & 1 & & & & & 1 \\ & & 1 & & & & & & & & & & \\ 1 & 1 & & 1 & & 1 & & 1 & & & & & 1 \\ & & & & 1 & & & & & & & & \\ 1 & 1 & & 1 & & 1 & & 1 & & & & & 1 \\ & & & & & & 1 & & & & & & \\ 1 & 1 & & 1 & & 1 & & 1 & & & & & 1 \\ & & & & & & & & 1 & & & & \\ & & & & & & & & & 1 & & & \\ & & & & & & & & & & 1 & & \\ & & & & & & & & & & & 1 & \\ 1 & 1 & & 1 & & 1 & & 1 & & & & & 1 \end{array}\right] \end{array} \qquad (5\text{-}4)$$

Now, we obtain the strong components of the directed graph by doing the binary matrix multiplication of equation (5-4). From the results it is apparent that the strong component of this example is made up with vertices 1, 2, 8 and 13. With this information it is not very difficult to decide how to choose the vertices so as to form each of the composed parts. However, it is necessary to proceed further with a limited concept of reachability. The idea is to reflect in the partial reachability matrix the nearest nodes to a

particular node, making easier the detection of cutting elements. The limited reachability matrix will show the vertices that can be "seen" with 2, 3, ... q arcs away from any node, equivalent to finding the possible paths of cardinality less than or equal to q leading from node x_i to x_j. Let us now consider a limited strong components matrix given by

$$\text{Limited strong components} = R^q \otimes Q^q \tag{5-5}$$

Let us illustrate this with an example:

Using the graph in Fig. 5-2, the limited reachability and reaching matrices of

$$R^2 = \begin{array}{c} \\ 1 \\ 2 \\ 3 \\ 4 \\ 5 \\ 6 \\ 7 \\ 8 \\ 9 \\ 10 \\ 11 \\ 12 \\ 13 \end{array} \begin{array}{c} \begin{array}{ccccccccccccc} 1 & 2 & 3 & 4 & 5 & 6 & 7 & 8 & 9 & 10 & 11 & 12 & 13 \end{array} \\ \left[\begin{array}{ccccccccccccc} 1 & 1 & 1 & 1 & 1 & 1 & 1 & 1 & & 1 & & 1 & 1 \\ 1 & 1 & 1 & 1 & 1 & 1 & 1 & 1 & & & & & \\ & & 1 & & & & & & & & & & \\ 1 & 1 & 1 & 1 & 1 & 1 & 1 & 1 & 1 & & 1 & & \\ & & & & 1 & & & & & & & & \\ 1 & 1 & 1 & 1 & 1 & 1 & & & & 1 & 1 & 1 & 1 \\ & & & & & & 1 & & & & & & \\ 1 & 1 & & 1 & 1 & & 1 & 1 & 1 & & 1 & & \\ & & & & & & & & 1 & & & & \\ & & & & & & & & & 1 & & & \\ & & & & & & & & & & 1 & & \\ & & & & & & & & & & & 1 & \\ 1 & & & & & 1 & & & & 1 & 1 & 1 & 1 \end{array}\right] \end{array} \tag{5-6}$$

$$Q^2 = \begin{array}{c} \\ 1 \\ 2 \\ 3 \\ 4 \\ 5 \\ 6 \\ 7 \\ 8 \\ 9 \\ 10 \\ 11 \\ 12 \\ 13 \end{array} \begin{array}{c} \begin{array}{ccccccccccccc} 1 & 2 & 3 & 4 & 5 & 6 & 7 & 8 & 9 & 10 & 11 & 12 & 13 \end{array} \\ \left[\begin{array}{ccccccccccccc} 1 & 1 & & 1 & & 1 & & 1 & & & & & 1 \\ 1 & 1 & & 1 & & 1 & & 1 & & & & & \\ 1 & 1 & 1 & 1 & & 1 & & & & & & & \\ 1 & 1 & & 1 & & 1 & & 1 & & & & & \\ 1 & 1 & & 1 & 1 & 1 & & 1 & & & & & \\ 1 & 1 & & 1 & & 1 & & & & & & & 1 \\ 1 & 1 & & 1 & & & 1 & 1 & & & & & \\ 1 & 1 & & 1 & & & & 1 & & & & & \\ & & & 1 & & & & 1 & 1 & & & & \\ 1 & & & & & 1 & & & & 1 & & & 1 \\ & & & 1 & & 1 & & 1 & & & 1 & & 1 \\ 1 & & & & & 1 & & & & & & 1 & 1 \\ 1 & & & & & 1 & & & & & & & 1 \end{array}\right] \end{array} \tag{5-7}$$

and the limited strong components of cardinality 2 is given by $R^2 \otimes Q^2$ as follows:

$$R^2 \otimes Q^2 = \begin{array}{c} \\ 1 \\ 2 \\ 3 \\ 4 \\ 5 \\ 6 \\ 7 \\ 8 \\ 9 \\ 10 \\ 11 \\ 12 \\ 13 \end{array} \begin{array}{c} \begin{array}{ccccccccccccc} 1 & 2 & 3 & 4 & 5 & 6 & 7 & 8 & 9 & 10 & 11 & 12 & 13 \end{array} \\ \left[\begin{array}{ccccccccccccc} 1 & 1 & & 1 & & 1 & & 1 & & & & & 1 \\ 1 & 1 & & 1 & & 1 & & 1 & & & & & \\ & & 1 & & & & & & & & & & \\ 1 & 1 & & 1 & & 1 & & 1 & & & & & \\ & & & & 1 & & & & & & & & \\ 1 & 1 & & 1 & & 1 & & & & & & & \\ & & & & & & 1 & & & & & & \\ 1 & 1 & & 1 & & & & 1 & & & & & \\ & & & & & & & & 1 & & & & \\ & & & & & & & & & 1 & & & \\ & & & & & & & & & & 1 & & \\ & & & & & & & & & & & 1 & \\ 1 & & & & & 1 & & & & & & & 1 \end{array}\right] \end{array} \tag{5-8}$$

From inspection of the strong components matrix with cardinality 2, we can choose the nodes from 1 to 7 to form one subgraph and use node 6 as reference. The rest is left to form another subgraph. This leaves us with two sets of measurements which can be solved independently and in parallel.

It is important to note that there is a need for certain ordering of the nodes which will permit an easier visual inspection of the limited strong components matrix. However, at this stage there is no obvious procedure to "tell" the computer how to choose the main nodes and links that permit the splitting of the system into separate subsystems. But the application of the limited reachability concept provides us with a simple systematic procedure to find those nodes from the network with special properties like the matrix structure of those nodes that are connected only three or fewer lines away from any particular node.

Before coming to the practical implementation, the symmetric case is considered, i.e., a non-directed graph (e.g. the structure of the bus admittance matrix). Clearly this is a strong graph, since it is possible to go from any vertex i to any vertex j. The reachability matrix is the same as the reaching matrix, consisting of a matrix full of 1's. Most problems in power systems have a symmetric structure, e.g the admittance matrix, the Jacobian matrix for the solution of the load flow problem using Newton's method. The matrix H given by

$$H = J^T W J \tag{5-9}$$

is needed for the solution of the SEP as explained in Chapter 2.

The symmetric graph case requires special handling and since it is very important later, it will be illustrated in the next section.

5.4 An ordering algorithm

It has already been shown that the strong elements of a graph do not necessarily provide an easy way of finding the cutting elements and, moreover, in the symmetric case the situation is more complicated.

Now, the matrix structure of the measurements adjacency matrix might appear in a disordered grouping, the reordering of the nodes will help in finding the possible self-sufficient areas and in spotting the cutting elements. It is important that such reordering will not affect the sparsity of the network structure and tends to maintain local redundancy since this ordering will concentrate the measurements that relate a particular group of unknown voltages in the same portion of the network.

The main objectives that might be considered by an algorithm to decompose the system are:

i) Find those vertex (node) groupings with few arcs between them, such that the least number of measurements is affected.

ii) Find a reference node which will permit a parallel solution of the subsystems that may be formed.

iii) If it is not possible or extremely difficult to comply with ii), it is necessary to find a mixed solution with some partially sequential solutions and possibly duplicating some nodes in different areas.

Obviously these strategies are simple to state and easy to apply by someone with a little insight and experience into the problem. But to develop a computer program with those criteria is considerably difficult. The next example will clarify these criteria.

Suppose a system can be agrouped in such a way so that the subsystem as depicted in Fig. 5-3 is obtained. We assume that the subsystems are internally observable.

Firstly, criterion (i) can be achieved by neglecting measurements at lines a-b and e-f. Secondly, criterion (ii) is achieved by using

node d as reference node and incorporating it into each subsystem, considering only the measurements related to that subsystem, i.e., subsystem A will only consider measurements at line c-d , subsystem C will only consider measurements g-d and both subsystems will consider node d as a subsystem node.

Case (iii) can occur in many ways. If node a is chosen as reference node, subsystems A and B can be solved in parallel but subsystem C will require one of the solutions to solve its own problem using either node d or e as reference node. Another possible solution is provided if we have a voltage measurement at the node e and/or d. Using one of these voltage magnitudes as reference and setting its angle to zero, it is possible to find the solution for subsystem C and obtain its state vector. Once the solution is obtained for subsystem A or B and the angle at node d or e is known then we only have to add algebraically this angle to the angles obtained in the solution for subsystem C in order to have a reference common to the whole system.

There could be a large number of ways in which a graph with n nodes can be divided to form subsystems. One of the critical problems in implementing these objectives is the identification of those nodes that comply with the points (i) and (ii). The main objective must be to obtain a permutation where the number of boundary nodes is usefully small,but it is possible to reach some cases which are not minimal but contain certain number of border nodes relating different possible partitions. One of these nodes could provide the reference node to the subsystem, provided a voltage measurement is available. However, to implement all the criteria mentioned to split the system is a difficult task for the following reasons: i) the number of different possible permutations for large n is also large. This has motivated a simplified procedure described hereunder which may be applied to detect the possible groupings; ii) the problem of the computer "seeing"

those connected subgraphs with few arcs between them and detecting the probable reference node is extremely difficult. But, although the simplified procedure may not give the optimal solution, it can give useful guide lines for an insight into the structure of the graph, the corresponding network and the system of equations representing it. The following simplified algorithm is proposed which can be integrated into an interactive procedure and, by visual inspection and judgement,can provide several alter native solutions.

1) Initiate renumbering with the given starting node and assign to it the new node number 1.
2) Assign new node numbers to all the nodes directly connected to the starting node.
3) Look for those nodes directly connected to the already renumbered nodes that have not been considered, and renumber them. Increase counters accordingly.
4) Check if the No. of renumbered nodes is equal to the No. of nodes. If not, go to step (3); if yes, go to step (5).
5) Is there a new starting node ? If not, stop; if yes, go to step (1).

5.5 Application examples

Several systems were used to test the algorithm described above. These systems were the 23 node and 30 line from reference (58), the 30 node and 41 line and the 57 node and 78 line from reference (55). Their data structure is contained in Appendix 7.

Only symmetric cases were chosen for analysis, where the equivalent graph has measurements for each line end. This symmetry makes this case the most difficult, since it has the largest number of possible permutations that can be generated. The corresponding adjacency matrices before and after re-ordering for example cases are shown in figures 5-4 (a) and (b) (23 node), 5-5 (a), (b), (c) and (d) (30 node) and 5-6 (a), (b), (c) and (d) (57 node). In these matrices, the dots represent the existence of the corresponding

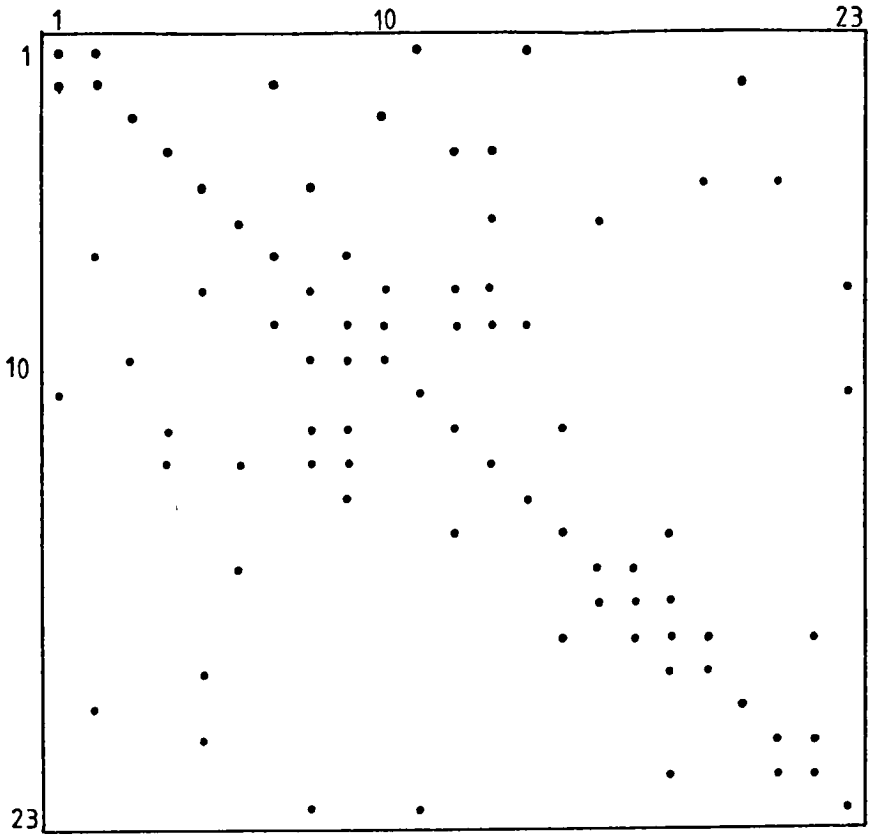

Fig. 5-4 (a) Adjacency matrix of the 23 node system network.

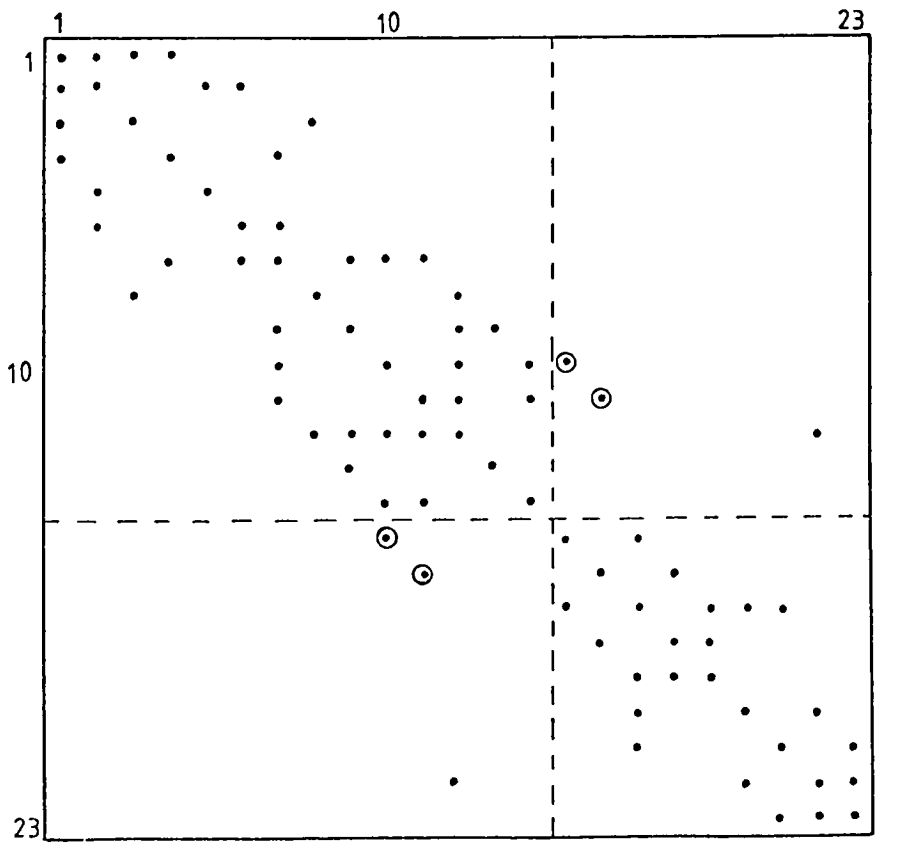

Fig. 5-4 (b) Re-ordered adjacency matrix(starting node:1).

arc, i.e., a 1 in binary representation. Tables 5-1, 5-2 and 5-3 contain the re-ordered node numbers for the systems tested. The 30 and 57 node systems have been run with three different starting nodes. Table 5-4 shows execution time for the algorithms. The figures in brackets correspond to the running time obtained, excluding printing of the old and new node numbers, on a Cyber 7314 machine.

Thus, with respect to the 23 node system, the initial ordering does not produce an obvious formation of subsystems as can be seen in the corresponding matrix of Fig. 5-4 (a). After the node re-ordering, it is clear from Fig. 5-4 (b) that two subsystems may be formed, having a common reference node (provided there is a voltage measurement in this node) for both subsystems. Any node from 10, 11 or 12 can be chosen as is apparent from Fig. 5-4 (b), the re-ordered adjacency matrix. It is possible to cut the arcs that are formed by the encircled elements, which will form one subsystem of 14 nodes and another of 10, a total of 24 nodes because the reference node appears in both subsystems. Using the new node 12 (old 8) as reference node, the dotted line on the adjacency matrix in Fig. 5-4 (b) , indicates the portions into which the system is split into two independent blocks once the arcs corresponding to the encircled elements are withdrawn.

For the 30 node system, using the initial ordering, it is possible to split the system into three subsystems that can be solved in parallel having node 10 as a reference. The three subsystems are formed as follows: the first one is made with nodes 1 to 11; the second one is composed of node 10 and nodes 12 to 20 and the third is integrated with node 10 and nodes 21 to 30. All subsystems are clearly shown in Fig. 5-5 (a) separated by the dotted line. The arcs represented by the encircled elements are either supressed or considered with the nodes in other subsystems and permit the system to be split satisfactorily. It is important to

Table 5-1 Re-ordering for the 23 node system, with node 1 as starting node.

Old	1	2	3	4	5	6	7	8	9	10	11	12
New	1	2	13	14	22	16	6	12	7	9	3	10
Old	13	14	15	16	17	18	19	20	21	22	23	
New	11	4	15	18	19	17	20	5	23	21	8	

Table 5-2 Node re-ordering for the 30 node system.

	starting node				starting node		
Old	1	6	13	Old	1	6	13
1	1	3	28	16	21	21	16
2	2	2	26	17	15	15	11
3	3	6	27	18	22	22	17
4	4	4	3	19	24	24	19
5	5	5	29	20	14	14	10
6	6	1	4	21	16	16	12
7	8	8	30	22	17	17	13
8	9	9	5	23	23	23	18
9	10	10	7	24	25	25	20
10	11	11	9	25	26	26	21
11	13	13	8	26	27	27	22
12	7	7	2	27	28	28	23
13	18	18	1	28	12	12	6
14	19	19	14	29	29	29	24
15	20	20	15	30	30	30	25

Table 5-3 Node reordering for the 57 node system .

	starting node				starting node		
Old	1	20	40	Old	1	20	40
1	1	48	27	30	36	11	48
2	2	51	30	31	40	17	52
3	6	52	31	32	41	18	53
4	7	53	32	33	42	19	54
5	8	54	33	34	43	20	55
6	9	55	34	35	44	21	3
7	11	15	36	36	45	22	2
8	12	56	37	37	46	23	4
9	14	47	26	38	32	7	5
10	15	43	25	39	48	25	6
11	16	33	15	40	47	24	1
12	17	57	39	41	21	32	14
13	18	41	23	42	53	31	13
14	23	37	19	43	22	34	16
15	3	36	18	44	49	26	8
16	4	49	28	45	26	35	17
17	5	50	29	46	25	39	21
18	10	3	35	47	54	38	20
19	27	2	41	48	50	28	10
20	28	1	42	49	24	27	9
21	29	4	43	50	55	40	22
22	30	5	7	51	20	42	24
23	31	6	44	52	39	16	51
24	33	8	45	53	56	44	56
25	34	9	46	54	57	45	57
26	35	10	47	55	19	46	40
27	37	12	49	56	52	30	12
28	38	13	50	57	51	29	11
29	13	14	38				

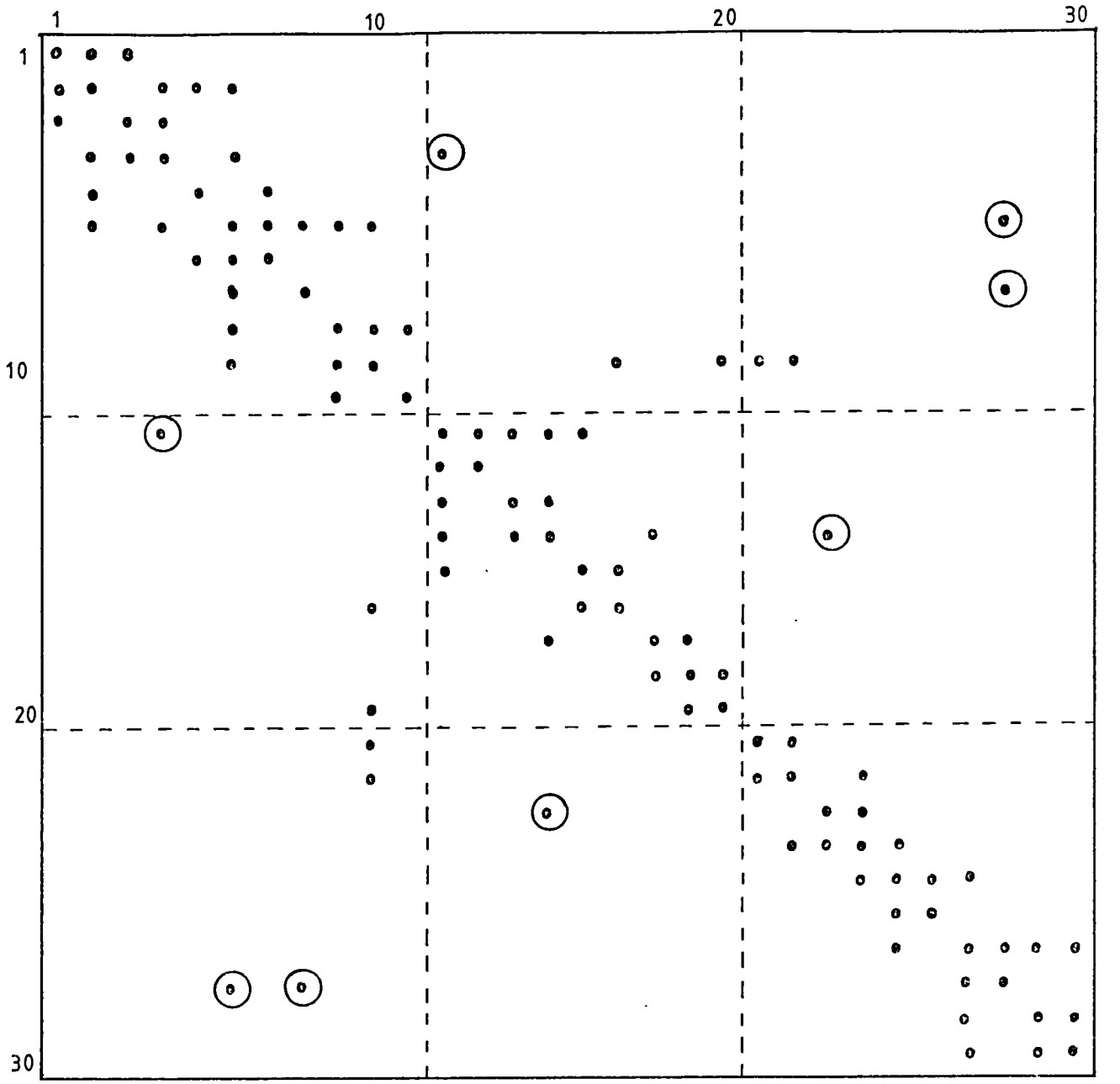

Fig. 5-5 (a) Adjacency matrix of the 30 node system network.

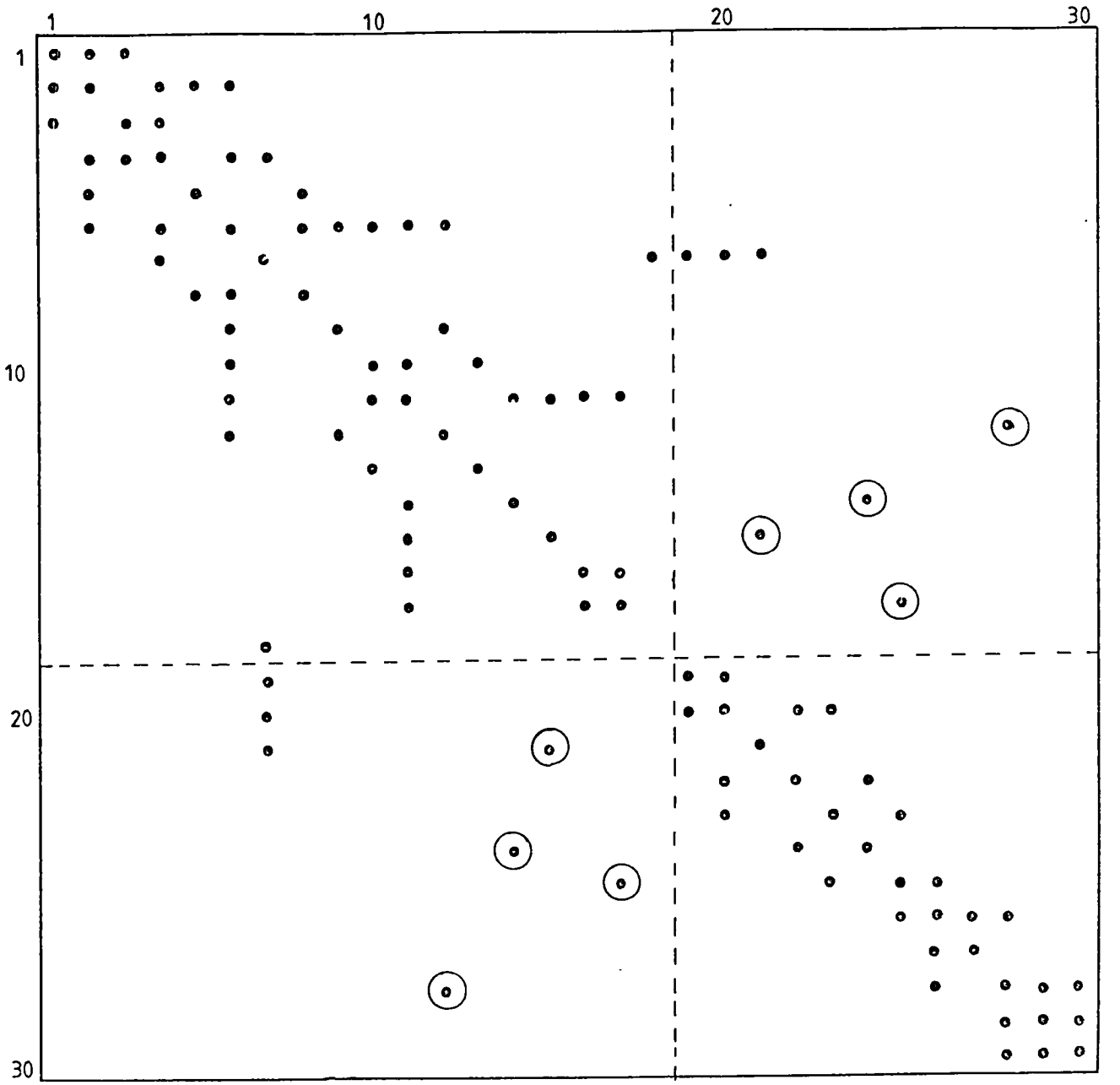

Fig. 5-5 (b) Re-ordered adjacency matrix(starting node:1).

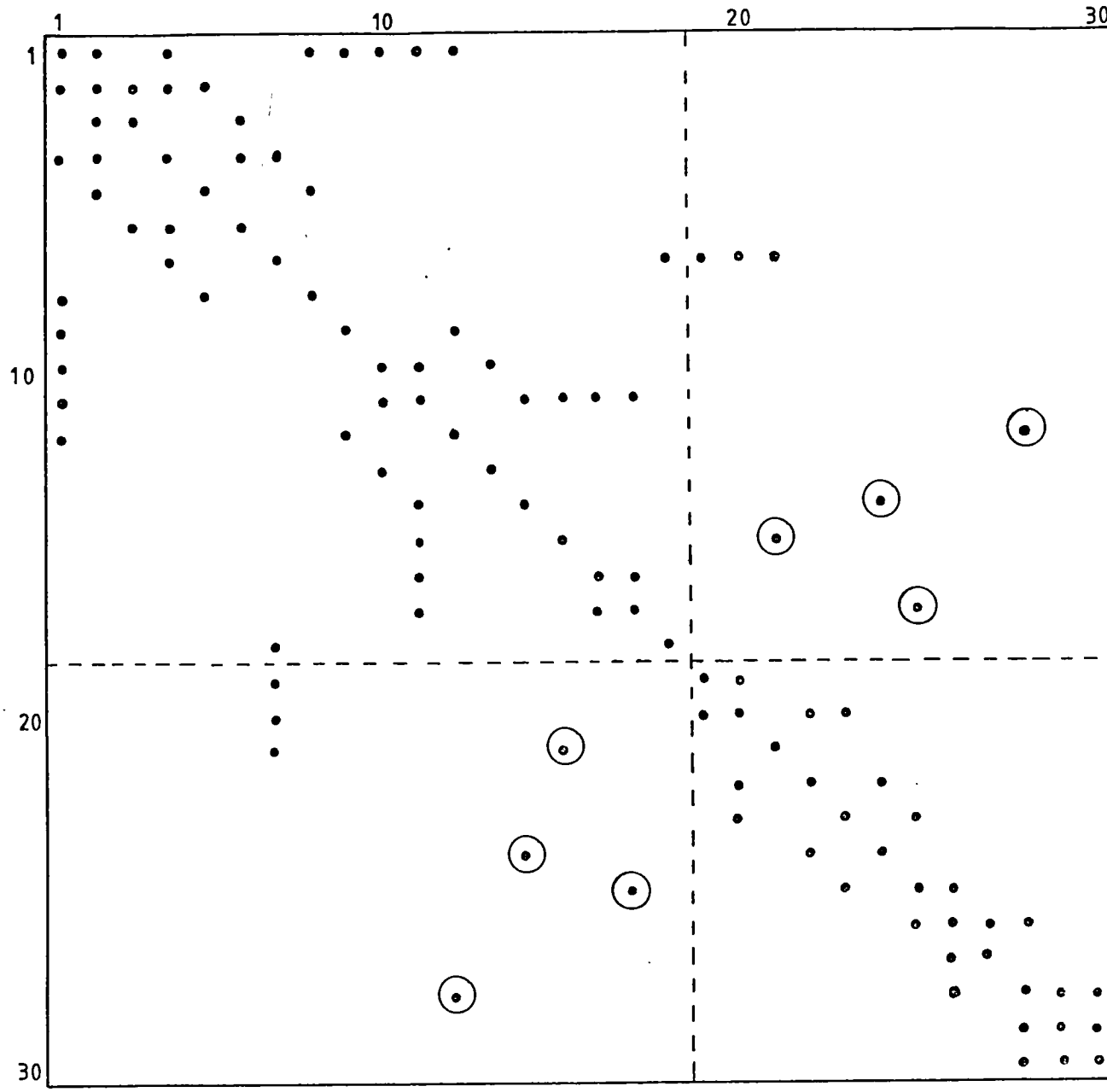

Fig. 5-5 (c) Reordered adjacency matrix(starting node:6).

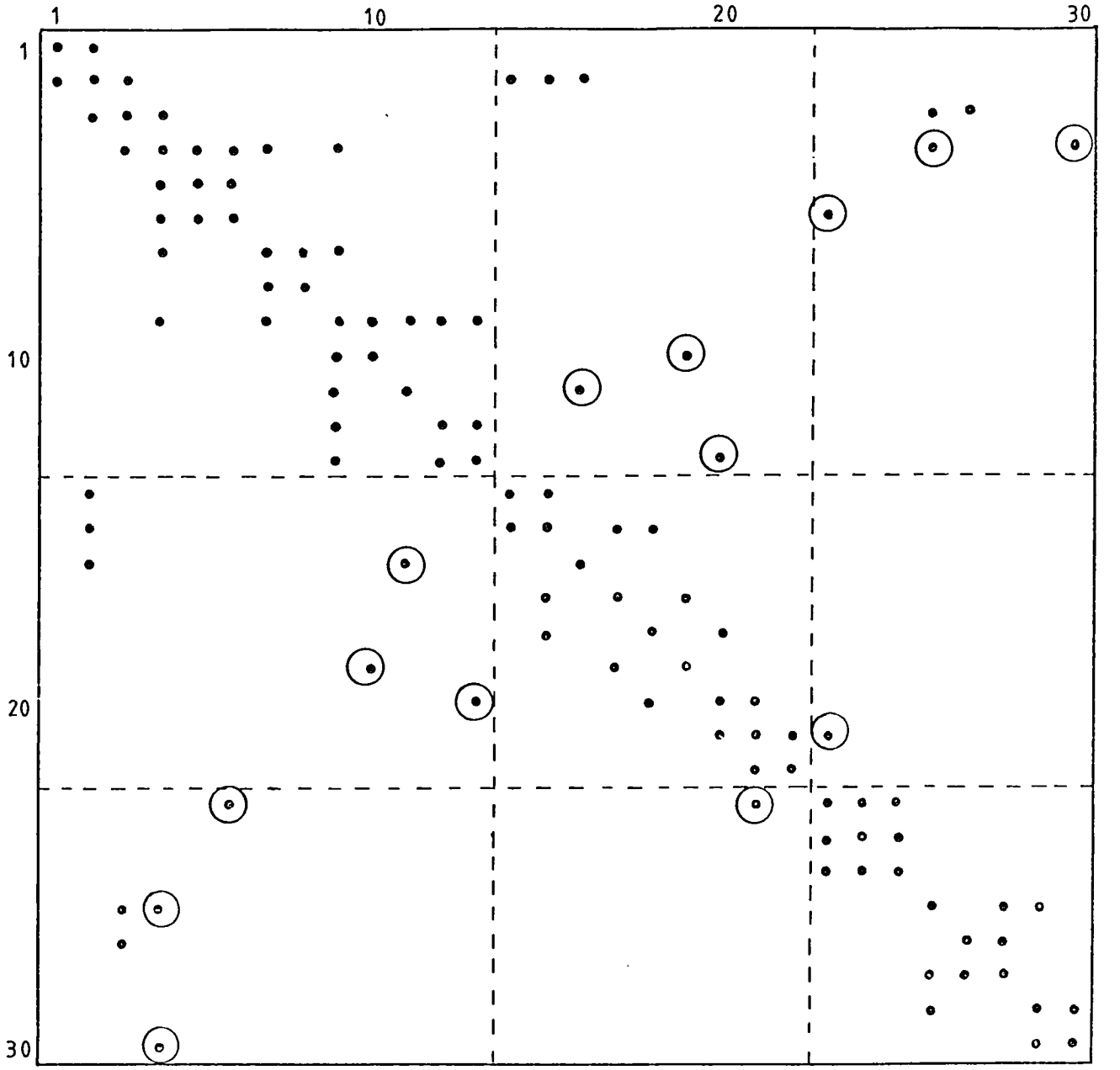

Fig. 5-5 (d) Re-ordered adjacency matrix (Starting node:13).

note that the initial ordering complies more or less with the procedure of the ordering algorithm. The three cases, run with old numbered starting nodes 1, 6 and 13 are shown by their re-ordered adjacency matrices in figures 5-5 (b), (c) and (d), respectively. From node 1, the re-ordered matrix shows the possibility of splitting the system into two subsystems, as shown by the line dividing the adjacency matrix in Fig. 5-5 (b). These subsystems can be solved in parallel using the new node 7 as reference node. The subsystems formed are composed of nodes 1 to 18 for the first system and node 7, 19 to 30 for the second system. Starting with node 6 is basically the same.

Finally, with starting node 13, shows how the algorithm is influenced by the starting node. In this test, three subsystems can be formed, the first with nodes 1 to 13, the second with node 2 and nodes 2 to 22 and the third with node 3 and nodes 23 to 30. This splitting of the system does not provide a parallel solution and the third subsystem has to receive the angle reference for the whole system, either from the first subsystem through the common node 3 or from subsystem 2 through the common link within nodes 23 and 21. For this 30 node system, the best arrangement is that given by the initial ordering. This initial ordering permits the parallel solution which offers the best method by taking advantage of the reduced need for centralized control.

The initial ordering in the 57 node system provides two possible divisions. The first splits the system into two, as is shown in Fig. 5-6 (a) by the full line. Node 11 is considered as reference and one subsystem is formed by nodes 1 to 29 and the second with node 11 and nodes 30 to 57. The number of links between subsystems is 8. The second possibility, which is more interesting since smaller subsystems are produced, has three subsystems which can be solved in parallel. These are composed of nodes 1

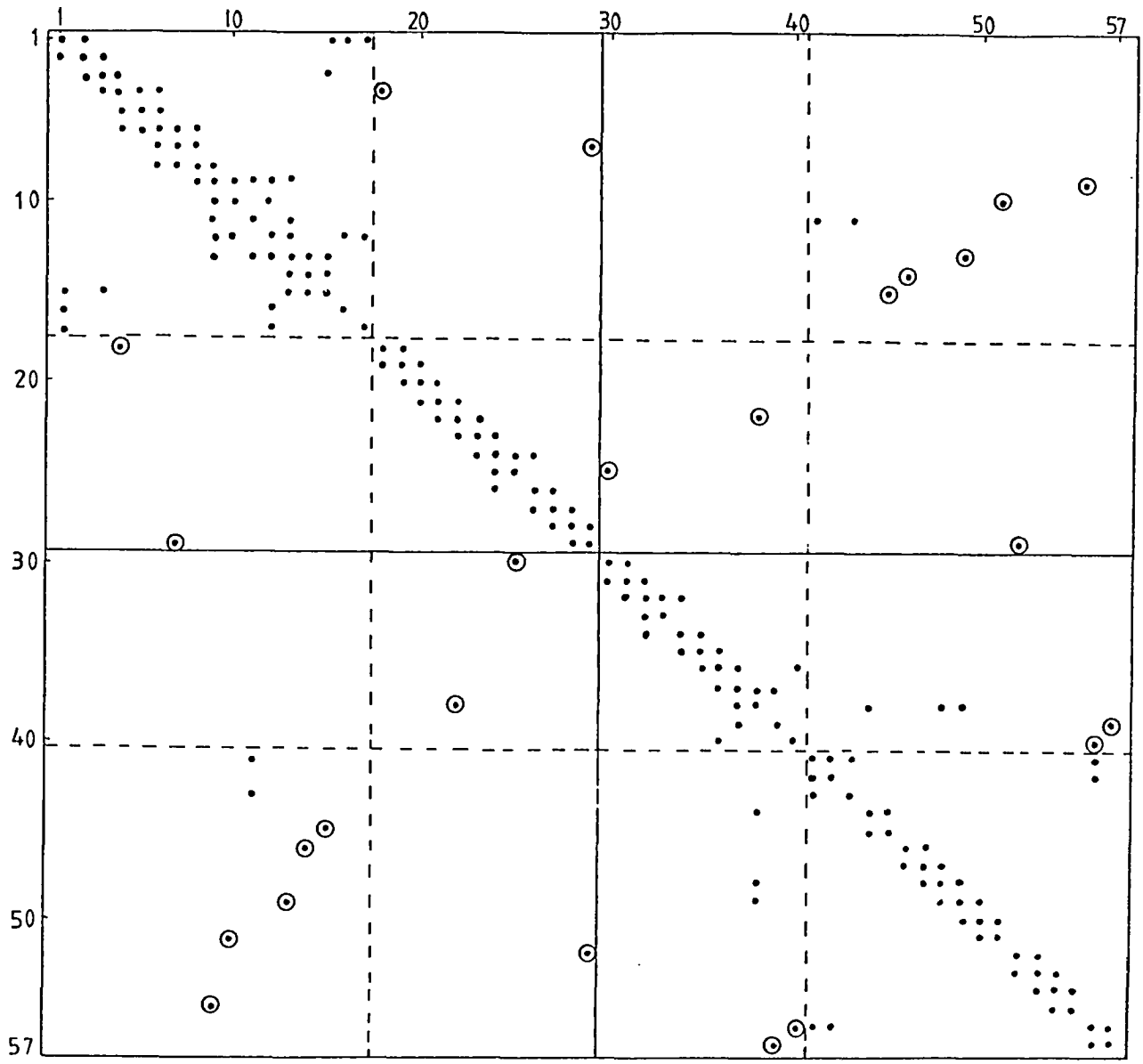

Fig. 5-6 (a) Adjacency matrix of the 57 node system network.

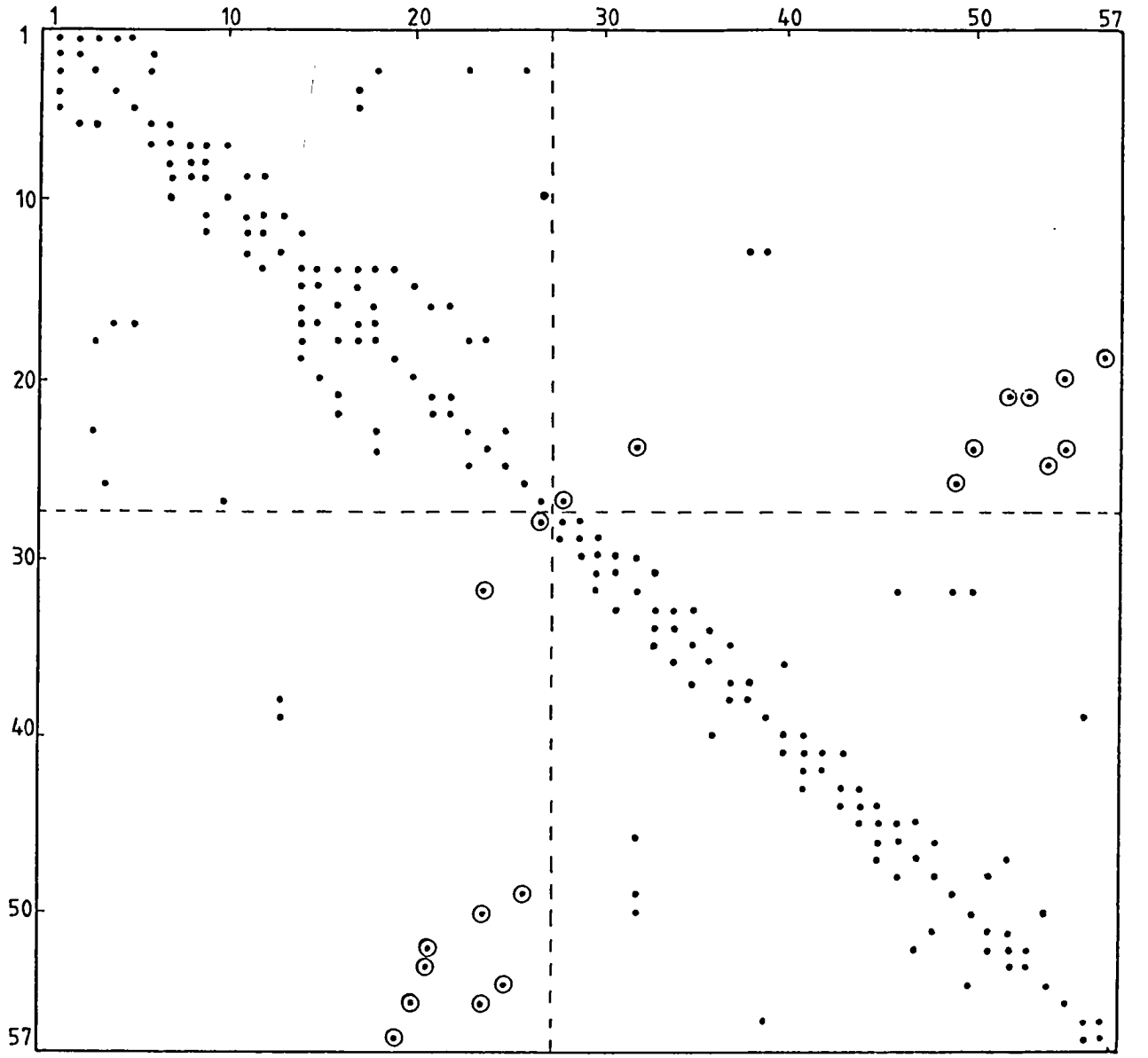

Fig.5-6 (b) Re-ordered adjacency matrix(starting node:1).

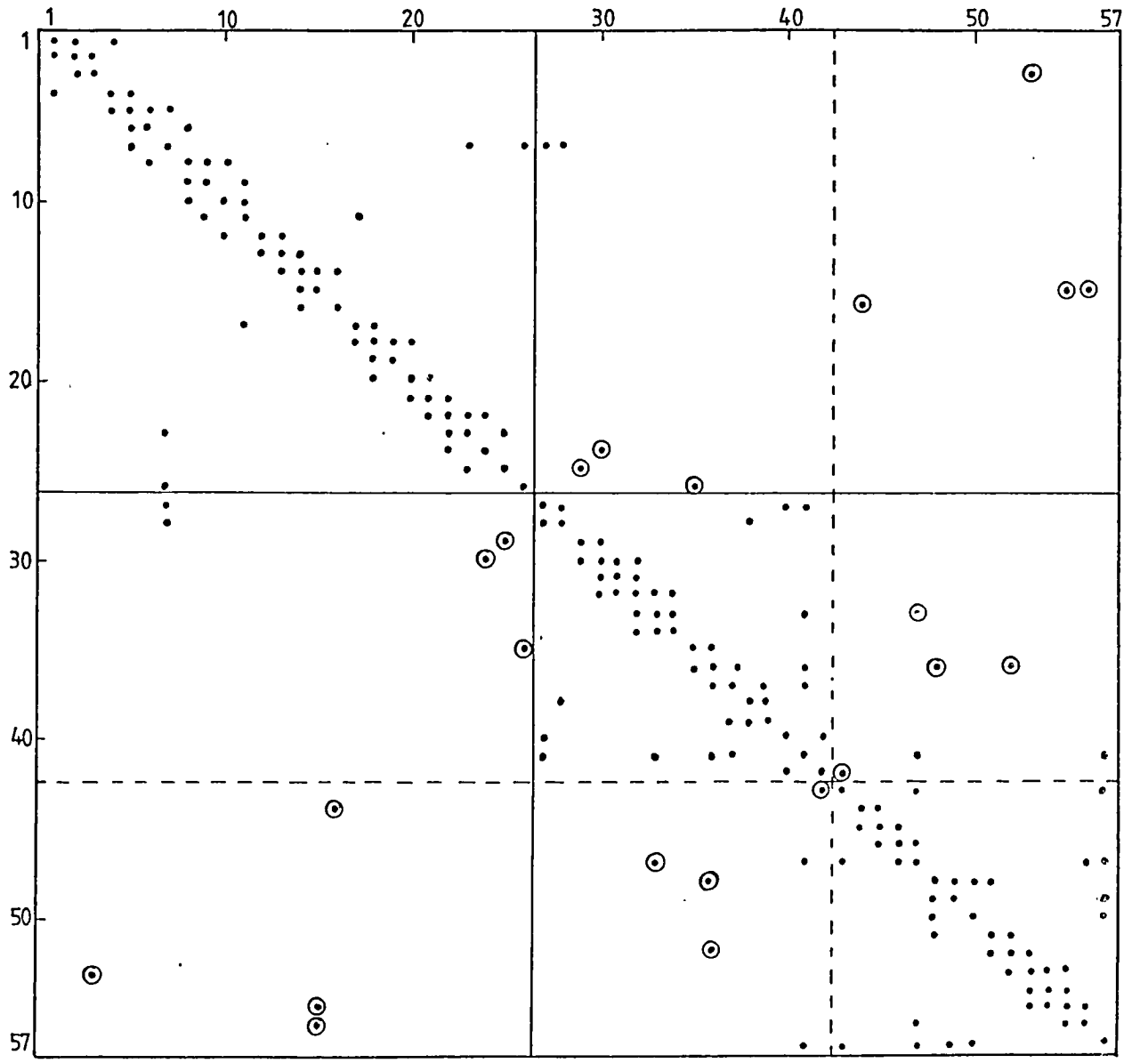

Fig. 5-6 (c) Reordered adjacency matrix (starting node:20).

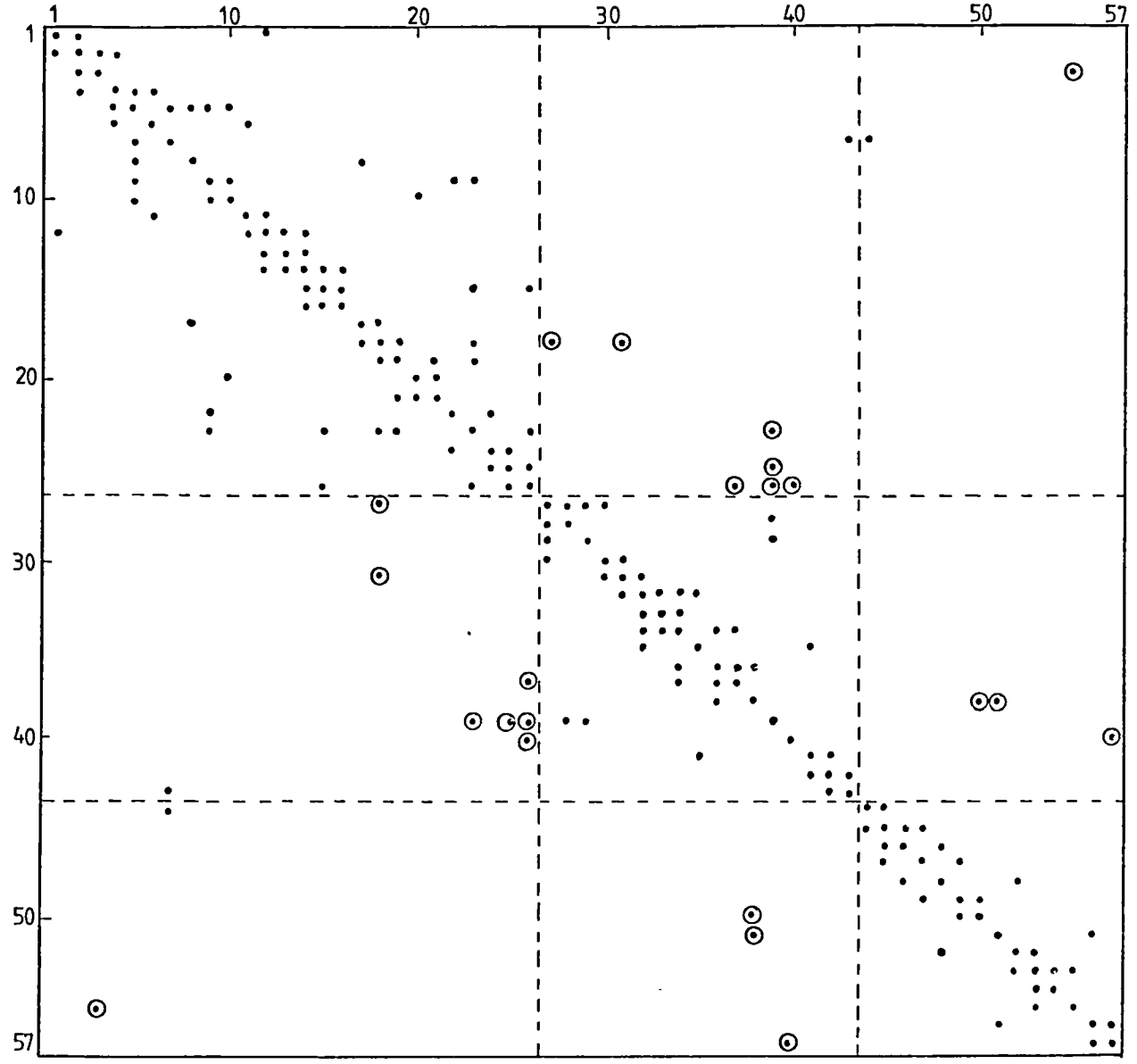

Fig. 5-6 (d) Re-ordered adjacency matrix(starting node: 40).

to 17 and 41 to 57 having as reference the node 11. Another way of solving in parallel is the subsystems formed by nodes 18 to 40 and 41 to 57 having node 38 as reference. The reference angle is now obtained from node 11 and its links with nodes 41 and 43. The No. of links between subsystems is 12.

The test shown in Fig. 4-6 (b), using node 1 as starting node, does not improve the partition provided by the initial ordering. The case of Fig. 5-6 (c) with starting node 20, provides a little improvement since only one link is reduced. However, the case of Fig. 5-6 (d) provides a further improvement because the system can be solved in parallel and the number of links between subsystems is less. The system splits into three blocks with 11 links between them. The reference is node 7. The three subsystems are composed by nodes 1 to 26, node 7 and node 27 to 43 and node 7 and nodes 44 to 57. It is worthwhile mentioning that there is a reduction of core storage for the 57 node solution assuming full symmetric matrices. For the whole system, $n(n+1)/2 = 1653$ memory positions are needed; the initial ordering needs 624 memory positions and the positions for the 12 links joining the subsystems. For the re-ordered system obtained using node 40 as starting node, 642 memory positions are required to store the three subsystems structure and an additional store for the 11 links joining the subsystem. One extra consideration for the initial ordering case, is the need of additional information to handle the sequential part of the solution and the time delay involved.

5.6 Comments

An algorithm to order the nodes of the network has been implemented. Several criteria are applied by visual inspection and the feasibility of decomposing the SEP for the symmetric graph case shown. A decomposition procedure has a strong dependence on the user objectives.

It has been shown that the starting node has a definite influence

on the node ordering,but no attempt was made to define the properties or features of the starting node. Not only was the number of links between subsystems affected but the starting node also affected the selection of the number of nodes for the chosen subsystems.

One useful property of ordering is that the node grouping may help in finding the interdependence of the various elements of the whole system as well as giving insight into localized properties or features and groups of variables that are only related to certain portions of the network.

The concept of limited reachability can be useful in showing the interaction between the closest nodes of the network and in spotting the main variables related to them.

Although it may not be possible to formulate an algorithm that rigorously applies defined criteria, for example the objectives attained with the application of examples by visual inspection after re-ordering, simpler algorithms can provide useful guidelines in obtaining decentralized estimation processes to accomplish the desired results. They are useful in facilitating the task of visualisation and judgement when only two or three subsystems are desirable.

Furthermore,by visual inspection of the adjacency matrix with ordering as has been proposed,the most likely common variables can be found.

The results obtained so far greatly encourage the use of a simple algorithm which does not require much computing and offers two or three alternatives using different starting nodes.

It is important to note that the subsystems formed maintain the original sparsity of the system and are not affected by the splitting of the system whatever way the nodes are grouped.

The main virtue of the proposed method is in providing parallel solutions for self-sufficient decentralized estimation. With parallel solutions, it is possible to solve large scale problems with greater speed than by solving the whole problem in the conventional way.

The re-ordering algorithm computing time requirements are very small, as is shown in Table 5-4. This is mainly because no numerical operations are required, only logical variables and operations are used. With simple modifications, the method can be extended to comply with certain requisites such as a fixed number of nodes per subsystem or that certain nodes must be constrained to lie in a particular subsystem.

Table 5-4 Timing of the ordering algorithm.

System (nodes)	Starting node No.	Time: execution & printing	Time: execution
23	1	0.025	0.007
30	1	0.031	0.008
	6	0.033	0.008
	13	0.063	0.016
57	1	0.058	0.012
	20	0.110	0.023
	40	0.113	0.023

CHAPTER SIX

MEASUREMENT SYSTEM OPTIMIZATION

6.1 Introduction

In the planning stage of an on-line monitoring system it is required to determine the best distribution of measurement points in the power system network and to design the data acquisition, transmission and reception arrangements. This step requires the analysis of several factors like: i) how and where the measurements are to be taken, ii) measurement accuracy, iii)redundancy and iv) type of estimator.

The especification of an optimal or near optimal measurement point selection is posed as several different problems, depending on their modelling. This selection problem is expressed in terms of graph theory and a suboptimal procedure is used which guarantees the spanning of the network locating the measured points. A further extension is that of finding the solution to the minimum number of collecting nodes in terms of a plant location problem.

6.2 Problem description

There are many factors which influence the selection of a set of measurements for state estimation: observability and its condition number, the number of measurements that provide better solution, cost of the measurements, load conditions, performance of the measurement system in practical conditions, the parameters of the network associated with the measurements, the covariance matrix changing with the voltage profile and with changes in the network, etc. All these factors make the assessment of a particular set of measurements and the simulation of the different practical conditions, a very difficult task.

Large computational requirements are demanded to assess all the possible combinations of conditions and to find an optimal meas-

urement system for a particular or a general situation of the power network.

One of the first questions that arise in choosing a measurement configuration is: which quantities can and should be measured ? The solution will have to take into account the features of the particular power system network being analized. For example, when a relatively large number of generation nodes exists, a combination of node voltage, line flow measurements and injection measurements will be chosen.

Another question is: what accuracy of measurement is required? A total error of about 3% in a power measurement whose value ranges between 40 and 100% of the full scale of the meter will provide an acceptable estimated voltage assuming a redundancy of around 2 for the whole network. On the other hand, if we try to optimize the meter configuration keeping to strict levels of accuracy it is impossible to simulate all or most of the different load levels and posible configurations of the measurement system that may arise in practical conditions. The results obtained with this approach by Koglin (90) provide a solution for a set of particular conditions of the system, which is constrained to a desired level of accuracy and does not provide a general solution for a wide range of conditions of the measurement system, network structure, voltage profile, etc.

A better approach is proposed by Handschin and Bongers (89) where the observability condition is checked first for any meter configuration. The main criterion is reliability and the solution is obtained for a measurement configuration with a "good" local redundancy that provides a certain level of probability that guarantees the bad data detection step. It is pointed out that the local redundancy is much more important than the overall redundancy for the reliability of the estimator, especially in the bad data detection and identifi-

cation step. This effect can be visualized in Section 3.4.2 .

Although attempts to optimize the cost of the measurement system are made in (89), there is no proposal for a mathematical model to represent the problem of the measurement optimization.

6.3 Cost function modelling

From the practical point of view there are many factors to be considered in the optimization of the measurement system, the main factor being cost which can be affected by many parameters such as the length of transmission between two points, the gathering of data in a power station or a substation, the complexity of the equipment, etc. It is therefore very difficult to provide the whole spectrum of possible factors that can influence the choice of measurements and points.

A simplified procedure has been developed by making several assumptions which will permit the conversion of the problem of optimal allocation of measurements into a weighted graph problem. This problem is defined in terms of a linear cost function subject to the restriction of covering all the nodes of the network . Each measurement has an associated cost and a weighted graph is made in the same manner as the measurement directed graph described in Chapter 3. There are several advantages in expressing the problem in terms of a weighted graph. Among these are the availability of a theoretical framework and a number of algorithms which can be applied and the fact that it is fairly simple to incorporate different criteria and factors so as to reflect certain features on the selection of measurements. This is made apparent in the application examples to follow.

The following assumptions are made in order to model the problem:

i) The general cost function is linear, and

ii) the cost of each measurement is related to the associated data transmission cost.

The cost function for optimization is expressed as follows:

$$C = \sum_{i \in I} c_i Z_i \tag{6-1}$$

where c_i is the associated cost of measurement i. Z is set to 1 if the measurement i is chosen, or to zero otherwise.

$$I = \{1, 2, \ldots, m\}$$

where m is the total number of feasible measurements.

The cost function is subject to the next set of constraints:

$$\sum |a_{ji}| Z_i \geq 1 \tag{6-2}$$

where a_{ji} is an element of the transpose of the node incidence measurement matrix. This set of constraints forces each node to be related to a measurement at least once. There are other possible additional constraints that may be formulated. For example, if for a given line it is desired not to have both ends measured, this constraint can be expressed as:

$$Z_i + Z_j \leq 1 \tag{6-3}$$

where Z_i is the corresponding element in the unknown vector which corresponds to one end measurement, and Z_j to the opposite end. This has the effect of excluding one of the line ends.

Other types of constraint that can be constructed is, for example, to force a set of measurements to concentrate in a given node, etc.

It is worthwhile to point out that the cost function as expressed is quite a general one. It is possible to relate the costs to the importance of the measurement in the network, for example taking into account the structure of the system which, as shown in Chapter 3, has a definite influence in the condition number and in the sensitivity matrix used in (89). The usefulness of this approach is exhibited in the systematic formulation of the measurement optimization problem. There are general algorithms to solve this problem, but some variations of the problem are now explained taking into

account certain features of the power system network.

The formulation contained in expressions (6-1) to (6-3) only accounts for the cost of individual measurements and considers them, to a certain extent, independent between themselves. There are other formulations which lead to a simplified mathematical model of the problem. A minimal spanning $\text{tree}_{\Lambda}^{(SST)}$(92) approach will now be considered.

Assuming that the most costly part of equipment is the data acquisition and transmission devices, as many measurements as possible should be made at nodes in the system, since the cost increases only marginally with additional measurements. Thus, it is possible to have the next cost expression for each node as:

$$c_j = a_j + \sum_{i \in I} b_{ij} \qquad (6\text{-}4)$$

where c_j is the total cost at node j ; a_j the cost of installing the data acquisition and transmission system, and b_{ij} the cost of measurement i at node j.

Modifying the cost of each measurement at node j in order to build up a graph (weighted graph) with link costs given by:

$$c_j' = c_j/\text{No. of measurements at node } j \qquad (6\text{-}5)$$

Then the link cost of a line measurement will be equal to the lowest of the two end costs.

Once we have the corresponding weighted graph of the measurement system, the minimal spanning tree of this graph can be obtained and the final node selection is then computed by choosing the cheapest end node of every link forming the SST. These nodes will then be the measured nodes, i.e., all lines going out from them will be measured. With this approach there is no guarantee that the overall optimum is found, but the solution to this problem is very easy and well known. By definition, all the node variables

of the network are covered by the SST. The corresponding algorithm requires a short computer time, is easy to implement and has a very wide range of applications.

In this approach it is possible to include a weight (cost) according to the structure of the network, the importance of the node (at small cost if measuring equipment already exists), etc.

6.3.1 Trees and the Shortest Spanning Tree

A nondirected tree (62) is a connected graph of n vertices and n-1 links. If G = (X,A) represents a nondirected graph of n vertices, then a spanning tree of G is defined as a partial graph of G which forms a tree according to the definition above. Thus, if G is represented in the graph of Fig. 6-1 (a), then the graph of Fig. 6-1 (b) is a spanning tree of G.

One particular tree is of great interest: the tree that spans the network with the minimum cost. This basic problem can be stated as follows:

Consider a connected nondirected graph G(X,A) with costs c_{ij} associated with its links (x_i, x_j). Of the many possible spanning trees of G, we want to find the one whose sum of link costs is a minimum. This problem appears in communications, pipelines and electric networks. The shortest spanning tree can be used to optimize certain properties of the network like distance, reliability and cost.

In our case the main point is to find all those links which provide the SST and from this to assign the nodes where measurements are to be made.

The finding of the SST of a graph can be done by an algorithm originated by Prim (92). This algorithm produces a SST, Ts by growing only one subtree containing more than a single vertex and considering the remaining single vertices to form one subtree each. Subtree Ts is then grown continuously by adjoining

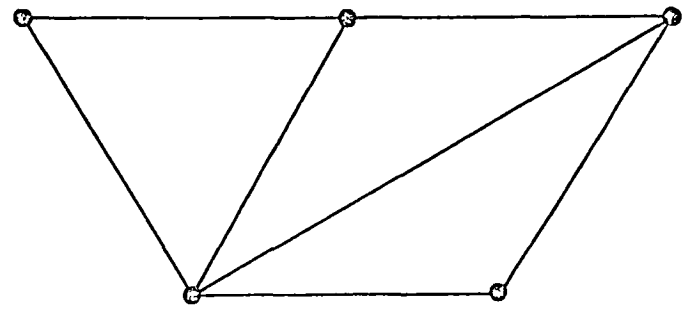

(a)

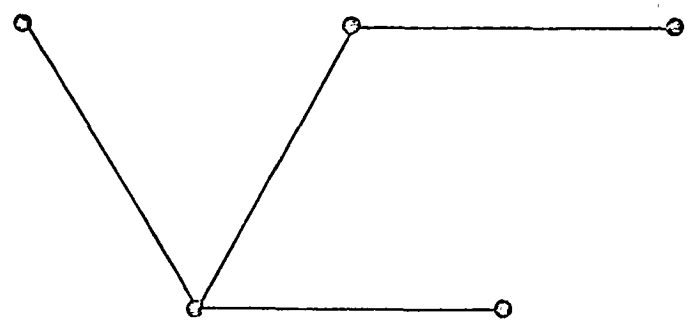

(b)

Fig. 6-1 (a) Graph G. (b) A spanning tree of the graph.

the link (x_i, x_j), $x_i \in Ts$, $x_j \notin Ts$ with the minimum cost c_{ij} until (n-1) links are added and Ts becomes the required SST. An efficient technique for its implementation is given in (94).

6.3.2 Minimal number of collection nodes

Assuming all the nodes have measurement equipment (or have already been selected) and considering the data transmission line as the most expensive item, cost being proportional to its length, and that information coming from neighbouring nodes can be gathered at any node or passed onto another one, thus making better use of the data transmission links without capacity constraints, we wish to minimize the total data transmission cost and the number of collection centres. This problem can be stated as a plant location problem (95) and is expressed as follows:

Minimize

$$C = \sum_{i \in I} \sum_{j \in J} g_{ij} Z_{ij} + \sum_{k \in K} f_k y_k \qquad (6\text{-}6)$$

subject to

$$\sum_{j \in J} Z_{ij} = d_j \qquad (6\text{-}7)$$

$$Z_{ij} \geq 0 \qquad (6\text{-}8)$$

$$i \in I; \quad j \in J$$

and

$$y_k = 0 \text{ or } 1 \qquad (6\text{-}9)$$

$$k \in K$$

where,

$$I = \{ i = 1, \ldots, n \} \; ; \; J = \{ j = 1, \ldots, n \} \; ; \; K = \{ k = 1, \ldots, p \}$$

The model represents a network with p collection centres to install and n nodes; d_j is the number of measurements at node j, f_i is a positive cost associated with the installation of the collection centre k and g_{ij} is a positive cost per unit of the data transmission between node i and j. The variables Z_{ij} and y_i

represent the number of measurements transmitted between i and j, whether a collection centre is installed ($y_i = 1$) or not ($y_i = 0$).

Thus, we are left with the problem of minimizing the number of collection centres and the data transmission costs. To simplify the problem, the number of collection centres can be fixed and the corresponding cost obtained. This procedure is repeated for a series of collection centres and the resulting costs compared.

Thus, the objective is now to minimize the transmission costs and the allocation of collection centres. This problem is identical to the one expressed by the generalized p-median problem (62).

In practice, f_k in (6-6) represents the fixed costs associated with building the facility at node k. If we consider f_k to be the same for all the nodes ($f_k = f$) and since the number of measurement centres has been fixed at exactly p, the cost function becomes

$$C = \sum \sum g_{ij} Z_{ij} + \varrho f \qquad (6\text{-}10)$$

Then the fixed costs need not be considered in the formulation of the plant location problem and only the equivalent pure p-median problem (93) is left to be solved. This p-median problem consists of locating p facilities on a network, so that the sum of shortest distances from each of the nodes of the network to its nearest facility is minimized (fixed costs are assumed not to vary with the location of the facility).

Equations (6-6) to (6-9) correspond to the integer programming formulation of the plant location problem. With the simplification described above, this problem can be stated as follows:

Minimize

$$C = \sum_{i \in I} \sum_{j \in J} d_{ij} Z_{ij} \qquad (6\text{-}11)$$

subject to

$$\sum_{i \in I} Z_{ij} = 1 \qquad (6\text{-}12)$$

$$\sum_{i \in I} Z_{ii} = p \qquad (6\text{-}13)$$

$$Z_{ij} \leq Z_{ii} \qquad i \in I, \quad j \in J, \quad i \neq j \tag{6-14}$$

$$Z_{ij} = \begin{cases} 1 & \text{if node } j \text{ is allocated to facility } i \\ 0 & \text{otherwise} \end{cases}$$

where

$$J = \{j = 1, \ldots, n\} \quad ; \quad I = \{i = 1, \ldots, n\}$$

$$Z_{ii} = \begin{cases} 1 & \text{if a facility is located at node } i \\ 0 & \text{otherwise} \end{cases}$$

Since there are no capacity restrictions and no economies of scale are made, no node will need to be associated with more than one centre. Hence, $Z_{ij} \in \{0, 1\}$ for all i and j; $Z_{ii} \in \{1, 0\}$ indicates that the centre is installed or not.

The solution to the p-median problem has been studied extensively and several methods of solution have been proposed (62,93). In the present work, a direct tree search algorithm (62,96) is used.

The basic pronciple involved in tree search methods is the partitioning of an initial problem P_o into a number of subproblems P_1, $P_2, \ldots, P_k$, whose totality represent the original problem and which are easier to solve than P_o.

To solve a subproblem means

either i) find an optimal solution,

or ii) show that the value of the optimal solution of the subproblem is worse than the best solution obtained so far,

or iii) show that the subproblem is infeasible.

If, after the initial partition, it is still impossible to solve the subproblem P_1, it is further partitioned into yet smaller subproblems $P_{i1}, P_{i2}, \ldots, P_{ik}$.

This branching is repeated for every subproblem which cannot be solved.

To deal in detail with the algorithm is outside the scope of this

work but a complete description of the algorithm and some other methods of solution to the p-median problem can be found in (93).

6.4 Power systems network applications

6.4.1 Shortest spanning tree approach

In order to convert the original problem into one of a shortest spanning tree, preliminary calculations are made.

For a given node i, the cost of measuring k lines and the cost of corresponding equipment is given by equation (6-4).

The matrix cost containing the link costs is built up from:

$$w_{ij} = \min (c'_i , c'_j) \quad \text{and}$$

$$w_{ij} = w_{ji}$$

Several tests were made for different values of fixed costs and variable measurement costs.

One set of simulated costs was obtained with the fixed cost at a fictitious value of 500 units and the arc costs were simulated at 0, 200, 500, 600 and 800 units. The extreme case of fixed zero cost and the arc cost of 100 was also considered. The results are shown in tables 6-1 and 6-2 for the systems of 14, 23, 30 and 57 nodes. The redundancy was computed with the expression:

$$\text{Redundancy} = \frac{\text{No. of complex measurements}}{\text{No. of nodes} - 1}$$

The resultant number of measurements is approximately equal to the number of links plus the number of nodes minus one. This means that at least one additional measured point is available at each node, which may be an injection or a voltage measurement.

In most cases the overall redundancy is approximately equal to or greater than 2.

As shown in Table 6-1, the same node selection was obtained

Table 6-1 Results with the shortest spanning tree approach for different systems .

No. of nodes	fixed costs = 500 ; arc costs = 200,500,600,800 Selected nodes	No. of measurements	Redundancy	fixed cost = 0 ; arc cost = 100 Selected nodes	No. of measurements	Redundancy
14	3, 6, 7, 8, 9	24	1.85	3,6,7,8,9,2,11,13	37	2.85
23	1,2,5,8,9,10,12,13,16, 18	45	2.05	1,2,5,6,8,9,10,12,13, 16,18,21,23	54	2.45
30	2,4,6,9,10,12,15,19,24, 25,27	55	1.90	3,4,5,6,9,10,12,15,17, 19,20,22,25,27,28,29	73	2.52
57	1,4,6,9,10,11,12,13,14, 15,19,20,22,24,27,29,30, 32,34,36,37,38,41,48,49, 53,54,56	123	2.20	1,3,4,6,7,9,10,11,12, 13,14,15,19,20,22,24,25, 27,28,29,30,32,34,36,37, 38,41,44,46,48,49,51,53, 54,55,56,57	152	2.71

Table 6-2 Timing for the node selection using the shortest spanning tree approach

System:	14 node	23 node	30 node	57 node
Time (secs) :	0.026	0.106	0.229	1.48

Note.- Time shown corresponds to algorithm execution time only, using a Cyber 7314 machine.

with all the different fictitious cost values used, with the exception of the extreme case where the fixed cost equals zero and the arc cost equals 100, which is shown in Table 6-1.

It should be noted that this procedure leads to a suboptimal result, since we are forcing all possible measurements to be made only at those nodes contained in the shortest spanning tree of the network.

6.4.2 The p-median approach

Two main networks have been used to test the model:

i) The 14 node and its reduced 10 node network, and

ii) the 23 node and its reduced 20 node network.

This was done considering that each resulting node is in fact a substation, i.e., a single location.

The reduced 10 node network was derived by grouping together nodes 3 and 8 into a single node and nodes 5, 6, 7 and 9 into another one.

The reduced 20 node network was obtained in a similar manner, this time grouping nodes 8, 9, 12 and 13 into a single node.

For our case, to give importance to the nodes with greater number of lines, the arc costs were assigned values proportional to the number of links existing at the corresponding end node.

Tables 6-3 to 6-6 show the values of the cost function, i.e., the minimum sum of link costs corresponding to different numbers of collection centres.

The total minimum can be obtained by adding the fixed costs pf to the minimum cost of the corresponding p-median shown in the third column of tables 6-3 to 6-6.

An example will illustrate this point.

Let us assume that f is equal to 10 units and the total costs are those shown in Table 6-7. The underlined numbers will then be the

Table 6-3 Results of the application of the p-median algorithm to the 14 node system.

No. of centres	No. of solutions	minimum cost	time * secs.
1	1	68	1.13
2	1	43	2.11
3	1	31	3.27
4	2	25	3.42
5	2	20	2.88
6	1	16	1.93
7	1	13	1.47
8	6	11	1.45

Table 6-4 Results of the application of the p-median algorithm to the 10 node system.

No. of centres	No. of solutions	minimum cost	time * secs.
1	1	33	0.48
2	1	19	0.53
3	1	15	0.45
4	1	12	0.53
5	6	10	0.70
6	15	8	0.99
7	20	6	1.12
8	15	4	0.95

* The time shown includes data reading, execution and data and solution printing, using a Cyber 7314 machine.

Table 6-5 Results of the application of the p-median algorithm to the 23 node system.

No. of centres	No. of solutions	minimum cost	time* secs.
1	1	141	5.03
2	1	92	18.55
3	1	70	56.97
4	1	56	79.27
5	2	48	100.17
6	2	42	105.08
7	3	37	98.68
8	1	32	72.89
9	6	28	48.01
10	3	24	24.62

Table 6-6 Results of the application of the p-median algorithm to the 20 node system.

No. of centres	No. of solutions	minimum cost	time* secs.
4	2	36	16.45
5	1	31	21.28
6	4	27	21.34
7	3	23	21.74
8	27	21	22.05

* The time shown includes data reading, execution and data and solution printing, using a Cyber 7314 machine.

minimum costs.

Table 6-7 Total costs, with f=10.

No. of centres	23 nodes	20 nodes	14 nodes	10 nodes
1	151		78	43
2	112		63	39
3	100		61	45
4	96	76	65	52
5	98	81	70	60
6	102	87	76	68
7	107	93	83	76
8	112	101	91	84
9	118			
10	124			

It can clearly be seen that there is a point (minimum) beyond which any further increase in the number of collection centres will not reduce the total cost.

6.5 Comments

Two mathematical models that complement each other were formulated for the solution of the measurement optimization problem. Although this mathematical modelling is well known in other fields, operational research for example, improvements to the model remain in power systems, for example, the use of realistic costs.

It can be observed that the SST solution provides coverage of the network with partial reachability of cardinality 1, which is similar to the p-median solution for this particular case, corresponding to the number of nodes selected with the SST approach.

Of no less importance is to have a technique for reducing the size of the network, especially when dealing with large networks, since the computer time is considerably reduced when the number

of nodes reduces. This is shown in tables 6-3 to 6-6.

A further extension may be the use of the two mathematical models in a sequential manner. First, the SST approach is used to obtain the nodes where measurements are to be made, and then to these nodes the p-median algorithm is applied to locate the optimized collection centres.

It is apparent that for the solution of extreme cases, like fixed cost = 0 and arc cost = 0, very simple rules can be applied but, for the general case, the SST approach offers a computationally attractive procedure.

CHAPTER SEVEN

CONCLUSIONS

7.1 General comments

The on-line state estimation problem has been widely studied and various approaches have been suggested towards its solution.

In the present work the proper weighting factors of the measurement residuals in the cost function have been assessed, especially for the case when bad data errors (gross measurements) are present. As shown in Chapter 2, the scale weighting provides a more consistent performance than the one provided by the reciprocal of the variance weighting method, especially when the gross measurement error is negative. This is a desirable property since scale overshooting is a type of error easy to detect. This illustrates the importance of properly modelling the variance of the measurements and judiciously selecting the weighting factors. It is important to note the well behaved properties of the performance cost function as proved by the linearity test for the examples tested with different weighting factors. There is a close relationship between these well behaved properties and the value of the condition number in the corresponding system of linear equations.

In general, it can be said that the observability of the system is determined by the structural and numerical properties associated to a given set of measurements. However, from the linearity test and condition number obtained, it can be concluded that for most cases the observability of the system is more dependent on the structure of the set of measurements (i.e., the covering of the network), than on the numerical process.

The partial observability concept leads us to the solution of partially observed networks. Its relationship with the singular case was illustrated and methods of solution for this situation were described. The equivalence and invariance of the solution is a characteristic important to emphasize.

It is possible to solve the singular case along the lines of Chapter 3 by using the standard methods, employing a rank reduced system and giving the trivial solution values to the unobserved variables of the network.

With the grounds established above, the decentralized state estimation problem is solved by using the partially observed networks obtained by applying the concept of independent blocksof equations and taking advantage of the redundancy of the system. The results obtained are highly encouraging. The local estimators have the properties of a centralized estimator, with the following additional advantages:

i) The large scale state estimation problem can be solved with smaller computer requirements.

ii) The subproblems can be solved in parallel.

iii) Different control areas can solve the state estimation problems in an independent manner.

iv) There is no need of a master control as in the case of the hierarchical approach.

v) The amount of data to be transmitted is reduced.

The disadvantages, though not crucial are:

i) Local redundancy is made more stringent.

ii) A slight degradation of the estimation process occurs, especially at the common nodes.

iii) Voltage measurements are required at various portions of the network.

The need to apply decentralized structures has arisen due to the high cost of communication lines and the impracticality of telemetering all the data required for a centralized controller.

The currently used decomposing criteria for solving the state estimation problem require a coordination process, which by itself reduces the efficiency of this solution. Schemes like the one proposed in this

work are highly desirable since they best suit the on-line needs.

The forming of subsystems, as shown in Chapter 4, may be useful in the analysis and design of large scale systems, large systems of non-linear equations and similar problems where knowledge of the interaction between different elements and/or parts of the whole system is required.

The mathematical modelling of the measurement system is the first step to provide algorithms to optimize it. Two models were tested which had a strong bias towards the nodes with a large number of connecting lines. The results of the measurement optimization problem shown in Chapter 6, exhibit a pattern of node clustering which favours network decomposition.

A more rigorous model, though not implemented, is suggested for future research, which expresses the problem as a set covering problem that can be solved by using a set covering algorithm or a general integer programming algorithm. The latter may comprise other type of constraints, as the forcing of all measurements of a given node to be chosen, etc.

In our models, no attempt was made to minimize the level of error or any related function but our generalized modelling could allow for it since it is possible to give weight, cost, etc. to the nodes and/or measurements to reflect the degree of accuracy, importance of a certain measurement, etc.

7.2 Possible areas for further research

7.2.1 System decomposition

Research is required to further develop the re-ordering algorithm so as to automatically produce the splitting of the system into subsystems with parallel solutions, giving the corresponding node (state variable) selection for each subsystem.

7.2.2 Decentralized dynamic state estimation

Application of the developed decomposition principles to the dynamic state estimation of the electrical power systems is required. This

will provide the basis for the determination of control actions by the local controller to prevent (or cope with) dynamic instability of the system. The idea is to find out the sets of equations that can be grouped together in order to decompose the whole problem into smaller subproblems and be able to obtain independent estimators accordingly. Each subproblem may be linked to the rest of the system only through the electrical reference angle at the selected boundary point(s), i.e., the boundary variable.

7.2.3 Individual measurement optimization

Implementation of the solution is needed to obtain the general case of individual measurement allocation using a mathematical model which is equivalent to a set covering problem (62). This approach will include several types of possible cost functions and/or constraints (106).

The measurement allocation problem can be modelled as follows:

Minimize

$$C = \sum_{i \in I} c_i Z_i \tag{7-1}$$

subject to

$$\sum_{i \in I} a_{ji} Z_i \geq 1 \tag{7-2}$$

$j \in J$

and

$$Z_i = 1 \text{ or } 0 \tag{7-3}$$

$i \in I$

where

$$I = \{i = 1, \ldots, m\}$$

$$J = \{j = 1, \ldots, n\}$$

n is the number of nodes,

m is the number of possible (or starting) measured points,

c_i is the cost of measurement i,

$a_{ji} = 1$ means measurement i relates node j,

$a_{ji} = 0$ " measurement i does not relate node j,

$Z_i = 1$ " measurement i is chosen, and

$Z_i = 0$ " measurement i is not chosen.

The units on the RHS of the inequalities cause all nodes to be covered. The greater than or equal sign permits redundant measurements. Other constraints that can be put in the form of equation (7-2) may be added.

APPENDIX 1

Least Squares Estimator (34)

Let us have a sequence of measurements $y_1, y_2, \ldots, y_m$, where m is the number of measurements. The measurements can be written as: measurement = true value + noise. Or:

$$\underline{y} = \underline{y}_t + \underline{\eta} \tag{A1-1}$$

and the expected value:

$$E\{\underline{y}\} = \underline{y}_t \tag{A1-2}$$

Now, the feature of the linear estimator is that we have a linear relationship between the state unknowns $\underline{x}$ which are to be estimated.

$$\underline{y}_t = A\underline{x}_t \tag{A1-3}$$

We also want that our linear estimates be unbiased; this means:

$$E\{\underline{\eta}\} = \underline{0} \tag{A1-4}$$

and its covariance matrix:

$$R = E\{\underline{\eta}\,\underline{\eta}^T\} \tag{A1-5}$$

The theory states (34) that the least squares linear unbiased estimate of $\underline{x}$ is defined as the vector $\underline{\hat{x}}$, which minimizes the quadratic risk function with respect to $\underline{x}$:

$$J(\underline{x}) = (\underline{y} - A\underline{x})^T(\underline{y} - A\underline{x}) \tag{A1-6}$$

We have to note that the matrix A^TA has to be non-singular. To minimize (A1-6), differentiate with respect to $\underline{x}$, and equating the derivative to zero, we have:

$$\nabla_{\underline{x}} J(\underline{x})\Big|_{\underline{x}=\underline{\hat{x}}} = -2A^T\underline{y} + 2A^TA\,\underline{\hat{x}} = \underline{0} \tag{A1-7}$$

and

$$\underline{\hat{x}} = (A^TA)^{-1}A^T\underline{y} \tag{A1-8}$$

To show that it is a minimum point, we write the risk function in

the form of the squared norm:

$$d = \left\| \underline{y} - A\underline{x} \right\|^2 \qquad \text{(A1-9)}$$

If $\underline{y} = A\hat{\underline{x}}$,

$$d = \left\| \underline{y} - A\underline{x} \right\|^2 \geq \left\| \underline{y} \right\|^2 - \left\| A\hat{\underline{x}} \right\|^2 \qquad \text{(A1-10)}$$

Then J has a minimum if and only if $\underline{x} = \hat{\underline{x}}$, where $\hat{\underline{x}}$ is given by (A1-7).

The next step is to show that $\hat{\underline{x}}$ is an unbiased estimate .

Let us write:

$$\begin{aligned} E\left\{\hat{\underline{x}} - \underline{x}_t\right\} &= E\left\{(A^TA)^{-1}A^T\underline{y}\right\} - \underline{x}_t \\ &= (A^TA)^{-1}A^T E\left\{\underline{y}\right\} - \underline{x}_t \\ &= (A^TA)^{-1}A^TA\underline{x}_t - \underline{x}_t \\ &= \underline{x}_t - \underline{x}_t = 0 \end{aligned}$$

This means that $\hat{\underline{x}}$ approaches $\underline{x}_t$ and we do not have any deviation of this value. Therefore, $\hat{\underline{x}}$ is an unbiased estimate of $\underline{x}$.

The covariance matrix of $\hat{\underline{x}}$ can be written as follows:

$$\begin{aligned} \text{Cov}\,(\hat{\underline{x}}) &= E\left\{(\hat{\underline{x}} - \underline{x}_t)(\hat{\underline{x}} - \underline{x}_t)^T\right\} \\ &= E\left\{\hat{\underline{x}}\hat{\underline{x}}^T\right\} - \left[E\left\{\hat{\underline{x}}\right\}\right]^2 \\ &= E\left\{(A^TA)^{-1}A^T\underline{y}\,\underline{y}^TA\,(A^TA)^{-1}\right\} - \underline{x}_t\,\underline{x}_t^T \end{aligned}$$

Define

$$B = (A^TA)^{-1}A^T \;; \qquad B^T = A(A^TA)^{-1}$$

$$\text{Cov}\,(\hat{\underline{x}}) = E\left\{B\underline{y}\,\underline{y}^TB^T\right\} - \underline{x}_t\,\underline{x}_t^T$$

$$E\left\{B\,\underline{y}\,\underline{y}^TB^T\right\} = BE\left\{\underline{y}\,\underline{y}^T\right\}B^T = B\left[A\underline{x}_t\,\underline{x}_t^TA^T + E\left\{\eta\eta^T\right\}\right]B^T$$

$$= BA\underline{x}_t\,\underline{x}_t^TA^TB^T + BE\left\{\eta\eta^T\right\}\;B^T$$

$$= I\,\underline{x}_t\,\underline{x}^T I + B E\left\{\underline{\eta}\,\underline{\eta}^T\right\} B^T \qquad \text{(A1-11)}$$

Then

$$\text{Cov}(\underline{\hat{x}}) = \underline{x}_t\,\underline{x}_t^T + B E\left\{\underline{\eta}\,\underline{\eta}^T\right\} B^T - \underline{x}_t\,\underline{x}_t^T$$

$$= (A^T A)^{-1} A^T E\left\{\underline{\eta}\,\underline{\eta}^T\right\} A (A^T A)^{-1} \qquad \text{(A1-12)}$$

Weighted Least Squares Linear Estimator

Most of the times we wish to assign a relative importance to the measurements. Then, we assign some weighting factors to the risk function associated with the different measurements. Thus, we can write:

$$J(\underline{x}) = (\underline{y} - A\underline{x})^T W^{-1} (\underline{y} - A\underline{x}) \qquad \text{(A1-13)}$$

In practical situations, we generally have that W^{-1} is a symmetric and positive-definite matrix.

The estimate $\underline{\hat{x}}$, which produces a minimum of the risk function, can be established by operating on J, as follows:

$$\nabla_{\underline{x}} J(\underline{x}) = \underline{0} \qquad \text{(A1-14)}$$

$$\nabla_{\underline{x}} J(\underline{x})\Big|_{\underline{x}=\underline{x}} = \nabla_{\underline{x}} (\underline{y}^T - \underline{x}^T A^T) W^{-1} (\underline{y} - A\underline{x})\Big|_{\underline{x}=\underline{x}}$$

$$= -2A^T W^{-1} \underline{y} + 2A^T W^{-1} A\underline{x} = \underline{0}$$

$$A^T W^{-1} A\,\underline{\hat{x}} = A^T W^{-1} \underline{y} \qquad \text{(A1-15)}$$

$$\underline{\hat{x}} = (A^T W^{-1} A)^{-1} A^T W^{-1} \underline{y} \qquad \text{(A1-16)}$$

The proof that (A1-16) yields an absolute minimum requires some mathematical manipulations that are out of our present objectives. Reference (34) deals with it in detail.

The covariance matrix of the estimate is:

$$\text{Cov}(\underline{\hat{x}}) = E\left\{\underline{\hat{x}}\,\underline{\hat{x}}^T\right\} - \left[E\left\{\underline{\hat{x}}\right\}\right]^2 \qquad \text{(A1-17)}$$

$$E(\underline{\hat{x}}) = \underline{x}_t \quad ; \quad E\left[\left\{\underline{x}\right\}\right]^2 = \underline{x}_t\,\underline{x}_t^T \qquad \text{(A1-18)}$$

$$E\left\{\hat{\underline{x}}\,\hat{\underline{x}}^T\right\} = E\left\{(A^TW^{-1}A)^{-1}A^TW^{-1}\,\underline{y}\,\underline{y}^TW^{-1}A(A^TW^{-1}A)^{-1}\right\}$$

By analogy with (A1-11) and writing

$$C = (A^TW^{-1}A)^{-1}A^TW^{-1} \quad ,$$

$$E\left\{\hat{\underline{x}}\,\hat{\underline{x}}^T\right\} = C\left[A\,\underline{x}_t\,\underline{x}_t^TA^T + E\left\{\eta\,\eta^T\right\}\right]C^T \qquad \text{(A1-19)}$$

Substituting (A1-17) and (A1-18) into (A1-19):

$$\begin{aligned}
\text{Cov}(\hat{\underline{x}}) &= (A\underline{x}_t\,\underline{x}_t^TA^TC^T + CE\left\{\eta\,\eta^T\right\}\quad C^T - \underline{x}_t\underline{x}_t^T \\
&= I\,\underline{x}_t\,\underline{x}_t^T\,I + CE\left\{\eta\,\eta^T\right\}\quad C^T - \underline{x}_t\,\underline{x}_t^T \\
&= CE\left\{\eta\,\eta^T\right\}C^T \\
&= (A^TW^{-1}A)^{-1}A^TW^{-1}E\left\{\eta\,\eta^T\right\}\,W^{-1}A(A^TW^{-1}A)^{-1}
\end{aligned} \qquad \text{(A1-20)}$$

We now choose $W = E\left\{\eta\,\eta^T\right\}$, which will provide the minimum variance estimator (34). In other words, any other weighting matrix would give us a greater covariance matrix for the estimated values. Then, substituting $W = E\left\{\eta\,\eta^T\right\}$ into (A1-20) we have:

$$\begin{aligned}
\text{Cov}(\hat{\underline{x}}) &= (A^TW^{-1}A)^{-1}A^TW^{-1}W\,W^{-1}A(A^TW^{-1}A)^{-1} \\
&= (A^TW^{-1}A)^{-1}A^TW^{-1}IA(A^TW^{-1}A)^{-1} \\
&= (A^TW^{-1}A)^{-1}(A^TW^{-1}A)(A^TW^{-1}A)^{-1} \\
&= (A^TW^{-1}A)^{-1}\,I \\
\text{Cov}(\hat{\underline{x}}) &= (A^TR^{-1}A)^{-1}
\end{aligned} \qquad \text{(A1-21)}$$

Now, if $W_1 \neq R$, we state, without proof, that the covariance matrix is:

$$\text{Cov}(\hat{\underline{x}}_1) = C_1R^{-1}C_1^T \qquad \text{(A1-22)}$$

where

$$C_1 = (A^T W_1^{-1} A)^{-1} A^T W_1^{-1}$$

is greater than the matrix (A1-21). Then, we write:

$$C_1 R^{-1} C_1^T \geq (A^T R^{-1} A)^{-1}$$

Thus, our choosing of $W = R$ gives us the minimum variance estimate. This expression is of more theoretical than practical use, because in practical applications the exact values of the elements of the covariance matrix of the errors are seldom known. However, it gives us the possibility to state that we use some values as close as possible to the true but unknown elements of the covariance matrix.

APPENDIX 2

Elementary Concepts of Graph Theory (62)

A graph G is a collection of points or vertices $x_1, x_2, \ldots, x_n$ (denoted by the set X), and a collection of lines $a_1, a_2, \ldots, a_m$ (denoted by the set A) joining some or all of these points. The graph G is then fully described and denoted by the doublet (X,A).

If the lines in A have a direction -which is usually shown by an arrow- , they are called arcs and the resulting graph is called a directed graph (Fig. A2-1). If the lines have no orientation they are called links and the graph is non-directed (Fig. A2-2).

The arc is denoted by the pair of its initial and final vertices, its direction is given from the first vertex to the second. Thus, in Fig. A2-1, (x_1,x_2) refers to arc a_1 and (x_2,x_1) to arc a_2.

A path in a directed graph is any sequence of arcs where the final vertex of one is the initial vertex of the next one.

Thus, in Fig. A2-3 the sequence of arcs:

$$a_1, a_6, a_5, a_9 \qquad \text{(A2-1)}$$

is a path.

Arcs $a = (x_i,x_j)$, $x_i \neq x_j$ which have a common terminal vertex are called adjacent. Also, two vertices x_i and x_j are called adjacent if either arc(x_i,x_j) or arc (x_j,x_i) or both exist in the graph. Thus, in Fig. A2-3 arcs a_1, a_{10}, a_3 and a_6 are adjacent and so are the vertices x_5 and x_3; on the other hand, arcs a_1, and a_5 or vertices x_1 and x_4 are not adjacent.

Another way of describing a directed graph G, is by specifying the set of vertices and a correspondence H which shows how the vertices are related to each other. H is called a mapping of the set X in X and the graph is described by the doublet $G = (X,H)$.

In the example of Fig. A2-1 we have:

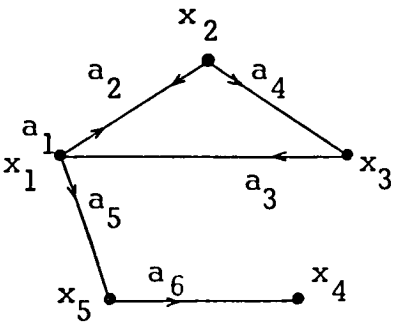

Fig. A2-1 Directed graph.

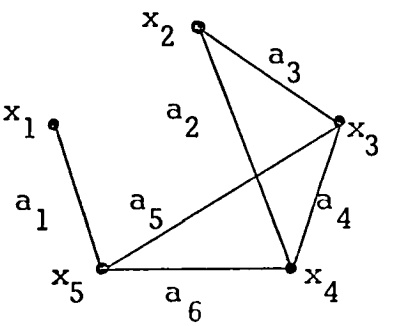

Fig. A2-2 Nondirected graph.

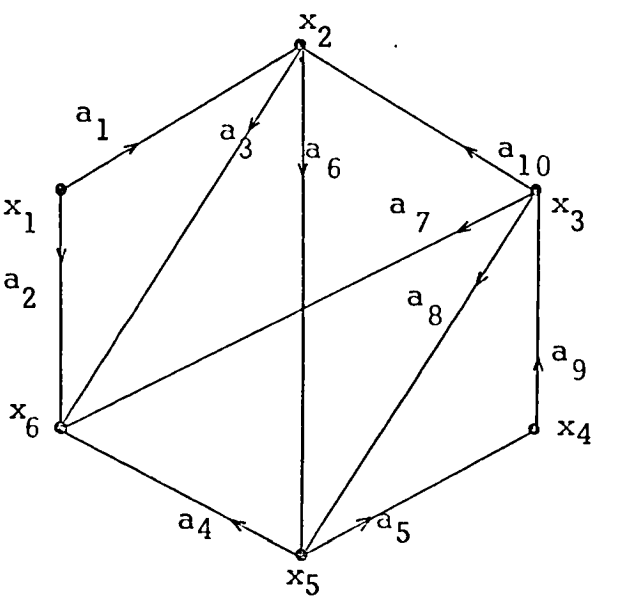

Fig. A2-3 Sample graph.

$$H(x_1) = \{x_2, x_5\}$$

i.e., x_2 and x_5 are the final vertices of arcs whose initial vertex is 1.

$$H(x_4) = \emptyset \quad , \text{ the null or empty set.}$$

When the correspondence H does not operate on a single vertex but on a set of vertices such as $X_q = \{x_1, x_2, \ldots, x_q\}$, then $H(X_q)$ is taken to mean:

$$H(X_q) = H(x_1) \cup H(x_2) \cup \ldots \cup H(x_q)$$

i.e., $H(X_q)$ is the set of those vertices $x_j \in X$ for which at least one arc (x_i, x_j) exists in G, for some $x_i \in X_q$. Thus, for the graph of Fig. A2-1,

$$H(\{x_2, x_5\}) = \{x_1, x_3, x_4\}$$

and

$$H(\{x_1, x_3\}) = \{x_2, x_5, x_1\} \quad .$$

The double correspondence $H(H(x_i))$ is written as $H^2(x_i)$. Similarly the triple correspondence $H(H(H(x_i)))$ is written as $H^3(x_i)$ and so on. Thus, the graph in Fig. A2-1 :

$$H^2(x_1) = H(H(x_1)) = H(\{x_2, x_5\}) = \{x_1, x_3, x_4\}$$

The relation $H^{-1}(x_i)$, the set of those vertices x_k for which an arc (x_k, x_i) exists in G, is called the inverse correspondence. Thus in Fig. A2-1 we have:

$$H^{-1}(x_1) = \{x_2, x_3\}$$

It is apparent that for a non-directed graph,

$$H^{-1}(x_i) = H(x_i) \quad \text{for all} \quad x_i \in X.$$

A simple path is a path which does not use the same arc more than once.

An elementary path is a path which does not use the same vertex more than once.

A chain is the nondirected counterpart of the path and applies to graphs with the direction of its arcs disregarded. Thus a chain is a sequence of links in which every link, except perhaps the first and last links, is connected to the links $\bar{a}_{i-1}$ and $\bar{a}_{i+1}$ by its two terminal vertices.

$$\bar{a}_2, \bar{a}_4, \bar{a}_8, \bar{a}_{10} \qquad \text{(A2-2)}$$

is a chain (Fig A2-3) where a bar above the symbol of an arc means that its direction is disregarded, i.e., it is to be considered as a link.

A simple chain is a chain which does not use the same link more than once.

An elementary chain is a chain which does not use the same vertex more than once.

A path or a chain may also be represented by the sequence of vertices that form it. This representation is often more useful when one is concerned with finding elementary paths or chains.

A number c_{ij} may sometimes be associated with an arc (x_i, x_j). The numbers are called weights, lenghts or costs and the graph is then called arc-weighted. Also a weight v_i may sometimes be associated with a vertex x_i and the resulting graph is then called vertex-weighted. If a graph is both arc and vertex weighted it is simply called weighted.

Considering a path μ represented by the sequence of arcs $(a_1, a_2, \ldots, a_q)$, the length (or cost) of the path 1 (μ) is taken to be the sum of the arc weights on the arcs appearing in μ, i.e.,

$$l(\mu) = \sum_{(x_i,x_j) \text{ in } \mu} c_{ij} \qquad \text{(A2-3)}$$

The cardinality of the path μ is q, i.e., the number of arcs appearing in the path.

A loop is an arc whose initial and final vertices are the same.

A circuit is a path $a_1, a_2, \ldots, a_q$, in which the initial vertex of a_1 coincides with the final vertex of a_q.

A cycle is the nondirected counterpart of the circuit. Thus, a cycle is a chain $x_1, x_2, \ldots, x_q$ in which the beginning and end vertices are the same, i.e., in which $x_1 = x_q$.

The number of arcs which have a vertex x_i as their initial vertex is called the outdegree of vertex x_i, and similarly the number of arcs which have x_i as their final vertex is called the indegree of vertex x_i.

For a nondirected graph the degree of a vertex x_i is defined in a similar way.

Given a graph $G = (X,A)$, a partial graph G_p of G is the graph (X,A_p) with $A_p \subset A$. Thus, a partial graph is a graph with the same number of vertices but with only one subset of the arcs of the original graph.

Given a graph $G = (X,H)$, a subgraph G_s is the graph (X_s,H_s) with $X_s \subset X$; and for every $x_i \in X_s$, $H_s(x_i) = H(x_i) \cap X_s$. Thus, a subgraph has only a subset X_s of the set of vertices of the original graph but contains all the arcs whose initial and final vertices are both within this subset.

APPENDIX 3

The AEP Algorithm (2,3)

Given S_m, a vector of line flow measurements only, it can be modelled as follows:

$$\underline{S_m} = \underline{S} + \underline{\eta} \tag{A3-1}$$

and

$$E\{\underline{\eta}\} = \underline{0} \tag{A3-2}$$

$$R = E\{\underline{\eta}\,\underline{\eta}^T\} \tag{A3-3}$$

where $E\{\underline{\eta}\}$ represents the expected value of the m-dimensional vector $\underline{\eta}$, the "noise" of the measurement, and R is a m×m diagonal variance-covariance matrix.

The line power flow of line j can be expressed as:

$$s_j = ((E_p - E_q)Y_{pq})^* E_p + E_p^2 Y_{pj}^* \tag{A3-4}$$

Where E_p and E_q are the voltages at nodes p and q respectively; Y_{pq} is the admittance of the line j between nodes p and q; Y_{pj} is the shunt admittance of line j at node p, and * represents the conjugate operator. Expression (A3-4) can be re-written as:

$$s_j = V_{pq}^* Y_{pq}^* E_p + E_p^2 Y_{pj}^* \tag{A3-5}$$

Using the "measured" values of V, the voltage across the line p-q and substituting $Z_j = 1/Y_{pq}$, we have:

$$s_{mj} = (V_{mj}/Z_j)^* E_p + E_p^2 Y_{pj}^* \tag{A3-6}$$

Substituting (A3-5) and (A3-6) into (A3-1):

$$(V_{mj}/Z_j)^* E_p + E_p^2 Y_{pj}^* = (V_j/Z_j)^* E_p + E_p Y_{pj}^* + \eta_j \tag{A3-7}$$

Multiplying (A3-7) by Z_j^*/E_p:

$$V^*_{mj} = V^*_j + \frac{Z^*_j}{E_{pj}} \eta_j \qquad \text{(A3-8)}$$

Defining

$$\epsilon_j = \frac{Z_j}{E^*_{pj}} \eta^*_j \qquad \text{(A3-9)}$$

we can then write:

$$V_{mj} = V_j + \epsilon_j \qquad \text{(A3-10)}$$

From the structure of the network we have that:

$$\underline{V} = B\underline{E} \qquad \text{(A3-11)}$$

where B is a matrix with 0, 1, -1 valued elements. Then

$$\underline{V}_m = B\underline{E} + \underline{\epsilon} \qquad \text{(A3-12)}$$

The cost function is given by:

$$J(\underline{E}) = \left[\underline{V}_m - \underline{V} \right]^{*T} D \left[\underline{V}_m - \underline{V} \right] \qquad \text{(A3-13)}$$

Minimizing (A3-13), as in Appendix 1, we have:

$$\hat{\underline{E}} = (B^T D B)^{-1} B^T D \underline{V}_m \qquad \text{(A3-14)}$$

We now choose D to be: $D = Q^{-1}$, where Q is equal to:

$$Q = E\left\{ \epsilon \epsilon^{*T} \right\}$$

$$Q = \left[q_{ij} \right] = \left[\frac{|Z_j|^2}{|E_{pj}|^2} E\left\{ \eta_i \eta_j \right\} \right] \qquad \text{(A3-15)}$$

$$Q = \text{diag} \left[\frac{|Z_j|^2}{|E_{pj}|^2} E\left\{ \eta_j^2 \right\} \right] \qquad \text{(A3-16)}$$

$$d_j = \left[\frac{|E_{pj}|^2}{|Z_j|^2} \frac{1}{\sigma_j^2} \right] = \left[\frac{|E_{pj}|^2}{|Z_j|^2} \right] W_j \qquad \text{(A3-17)}$$

where σ_j^2 is the variance of the jth measurement.

Expression (A3-14) is used iteratively to compute the node voltages and the process is stopped when a tolerance criterion is reached.

APPENDIX 4

Table A4-1 Line data for the 5 node and 7 line system.

line from node	to node	line admittance in series G	B	shunt admittance (1/2) B
1	2	5.0000	-15.0000	0.030
1	3	1.2500	- 3.7500	0.025
2	3	1.6667	- 5.0000	0.020
2	4	1.6667	- 5.0000	0.020
2	5	2.5000	- 7.5000	0.015
3	4	10.0000	-30.0000	0.010
4	5	1.2500	- 3.7500	0.025

Table A4-2 Load conditions for the 5 node and 7 line system.

node No.	P	Q
1	1.295	-.075
2	0.200	0.200
3	-.450	-.150
4	-.400	-.050
5	-.600	-.100

Table A4-3 Line data for the 10 node and 13 line system.

line from node	to node	line admittance in series G	B	shunt admittance (1/2) B
1	2	4.0489	-19.8346	0.0506
1	3	2.6008	- 7.1400	0.0506
1	4	1.9028	-12.5282	0.0759
1	8	3.5631	-17.3481	0.0506
2	4	4.0489	-19.8346	0.0253
3	7	3.7591	-14.7136	0.0759
4	6	3.0305	-19.9948	0.0253
4	7	3.6098	-14.4372	0.0759
4	8	1.2480	- 4.9012	0.0506
4	10	9.7371	-48.6855	0.0506
5	9	1.9028	-12.5282	0.0759
6	9	4.3677	-14.6158	0.0506
8	9	1.2480	- 4.9012	0.0506

Note.- All power and line data are in per unit form, on 100-MVA base.

Table A4-4 Load conditions for the system of 10 nodes and 13 lines.

node No.	P	Q
1	4.2139	0.4774
2	3.8400	-.2465
3	-.3800	0.5011
4	-4.6599	1.7651
5	0.0600	0.0806
6	-.1951	0.5792
7	-.9000	-.4000
8	-2.6000	-1.5500
9	-1.0000	-.5000
10	1.9200	-.8000

Table A4-5 Load conditions for the system of 14 nodes and 20 lines.

node No.	P	Q
1	2.3230	-.1690
2	0.1831	0.2962
3	-.1118	0.0466
4	-.9419	0.0435
5	0.0000	0.1732
6	-.4780	0.0390
7	0.0000	0.0000
8	-.0760	-.0160
9	-.2950	-.1660
10	-.0900	-.0580
11	-.0350	-.0180
12	-.0610	-.0160
13	-.1350	-.0580
14	-.1490	-.0500

Note.- All power data are in per unit form, on 100-MVA base.

Table A 4-6 Line data for the 14 node and 20 line system.

line from node	to node	line admittance in series G	line admittance in series B	shunt admittance (1/2) B	
1	2	4.9991	-15.2631	0.0264	
1	8	1.0259	- 4.2350	0.0246	
2	4	1.1358	-4.78340	0.0219	
2	6	1.6860	-5.11580	0.0187	
2	8	1.7011	- 5.1939	0.0170	
3	8	0.0000	- 4.2575	0.2895	(-.3106)
3	11	1.9550	- 4.0941	0.0000	
3	12	1.5260	- 3.1760	0.0000	
3	13	3.0989	- 6.1028	0.0000	
4	6	1.9860	- 5.0688	0.0173	
5	7	0.0000	- 5.6770	0.0000	
6	7	0.0000	- 4.8895	-.1100	(0.1076)
6	8	6.8410	-21.5786	0.0064	
6	9	0.0000	- 1.8555	-.0594	(0.0575)
7	9	0.0000	- 7.0901	0.0000	
9	10	3.9021	-10.3654	0.0000	
9	14	1.4240	- 3.0291	0.0000	
10	11	1.8809	- 4.4029	0.0000	
12	13	2.4890	- 2.2520	0.0000	
13	14	1.1370	- 2.3150	0.0000	

Note.- All line data are in per unit form, on 100-MVA base. Figures in brackets correspond to those shunt admittances whose values are different at each end of the line.

Table A 4-7 Line data for the 23 node and 30 line system.

line from node	to node	line admittance in series		shunt admittance (1/2)	
1	2	0.0625	- 4.9992	0.0000	
1	11	6.9111	-15.4214	0.0059	
1	14	5.3671	-12.0369	0.0076	
2	20	4.2448	- 9.3301	0.0099	
2	7	2.0482	- 5.3953	0.0171	
3	10	7.3159	-16.1389	0.0228	
4	12	3.4386	-28.0688	0.1187	
4	13	3.4386	-28.0688	0.1187	
5	19	3.3817	-27.2039	0.1226	
5	21	7.6932	-63.1656	0.0528	
5	8	5.3427	-11.6553	0.0079	
6	16	7.3271	-60.0821	0.0555	
6	13	1.6910	-13.6799	0.2436	
7	9	7.4725	-16.4460	0.0056	
8	23	3.7015	- 8.3242	0.0109	
8	10	2.8624	- 6.3050	0.0146	
8	12	0.3161	-11.5295	-.3805	(0.3683)
8	13	0.3110	-11.3429	-.5671	(0.5401)
9	14	4.7436	-12.4832	0.0074	
9	10	2.8624	- 6.3050	0.0146	
9	12	0.1042	- 7.3245	-.3662	(0.3488)
9	13	0.3345	-12.2004	0.2904	(-.2975)
11	23	2.1800	- 5.7528	0.0160	
12	15	3.9710	-32.0818	0.1039	
15	18	4.1583	-34.2169	0.0976	
16	17	15.3846	-123.0769	0.0272	
17	18	7.4126	-58.9481	0.0567	
18	19	9.7650	-77.5099	0.0431	
18	22	6.4103	-51.2821	0.0649	
21	22	10.6125	-86.4160	0.0385	

Note.- All line data are in per unit form, on 100-MVA base. Figures in brackets correspond to those shunt admittances whose values are different at each end of the line.

Table A 4-8 Load conditions for the system of 23 nodes and 30 lines.

node No.	P	Q
1	-.1214	0.5116
2	0.2413	0.3579
3	1.0291	0.5639
4	0.2040	0.5857
5	9.0300	1.6621
6	8.5097	1.1806
7	-.4800	-.1200
8	-.0360	0.0000
9	-1.4972	-.3800
10	-1.7700	-.4500
11	0.0000	-.0100
12	0.0438	0.0000
13	0.0471	0.0000
14	-.4700	-.1300
15	-2.0100	-.5000
16	-1.3200	-.3300
17	-3.4400	-.8600
18	-1.0400	-.2600
19	-3.7600	-.9400
20	-.5100	-.1300
21	-3.7500	-.9400
22	2.1000	0.5200
23	-.4100	-.1000

Note.- All power data are in per unit form, on 100-MVA base.

APPENDIX 5

Linear Least Squares Solutions by Householder Transformations (64)

Let A be a given m×n real matrix with m≥n and of rank n and $\underline{b}$ a given vector. We wish to determine a vector $\hat{\underline{x}}$ such that

$$\left\| \underline{b} - A\hat{\underline{x}} \right\| = \min.$$

where $\|...\|$ indicates the Euclidean norm . Since the Euclidean norm is unitarily invariant

$$\left\| \underline{b} - A\underline{x} \right\| = \left\| \underline{c} - QA\underline{x} \right\|$$

where $\underline{c} = Q\underline{b}$ and $Q^T Q = I$. We choose Q so that

$$QA = R = \begin{bmatrix} U \\ .. \\ 0 \end{bmatrix} \begin{matrix} \\ \\ \} (m-n)\times n \end{matrix} \qquad \text{(A5-1)}$$

and U is an upper triangular matrix. Clearly,

$$\hat{\underline{x}} = U^{-1} \underline{c}_1$$

where $\underline{c}_1$ denotes the first n components of $\underline{c}$.

A very effective method to realize the decomposition (A5-1) is via Householder transformations. Let $A = A^{(1)}$, and let $A^{(2)}$, $A^{(3)}$, ... $A^{(n+1)}$ be defined as follows:

$$A^{(k+1)} = P^{(k)} A^{(k)} \qquad (k = 1, 2, \ldots, n).$$

$P^{(k)}$ is a symmetric, orthogonal matrix of the form

$$P^{(k)} = I - \beta_k \underline{u}^{(k)} \underline{u}^{(k)T}$$

where the elements of $P^{(k)}$ are derived so that

$$a_{i,k}^{(k+1)} = 0$$

for $i = k+1, \ldots, m$. $P^{(k)}$ is generated as follows:

$$\sigma_k = \left[\sum_{i=k}^{m} (a_{i,k}^{(k)})^2 \right]^{\frac{1}{2}} ,$$

$$\beta_k = \left[\sigma_k \left(\sigma_k + \left| a_{k,k}^{(k)} \right| \right) \right]^{-1},$$

$$u_i^{(k)} = 0 \quad \text{for} \quad i<k,$$

$$u_k^{(k)} = \operatorname{sgn}(a_{k,k}^{(k)}) \left(\sigma_k + \left| a_{k,k}^{(k)} \right| \right),$$

$$u_i^{(k)} = a_{i,k}^{(k)} \quad \text{for} \quad i>k.$$

The matrix $P^{(k)}$ is not computed explicitly. Rather we note that

$$A^{(k+1)} = (I - \beta_k \underline{u}^{(k)} \underline{u}^{(k)T}) A^{(k)}$$

$$= A^{(k)} - \underline{u}^{(k)} \underline{y}_k^T$$

where

$$\underline{y}_k^T = \beta_k \underline{u}^{(k)T} A^{(k)}.$$

In computing the vector $\underline{y}_k$ and $A^{(k+1)}$, one takes advantage of the fact that the first (k-1) components of $\underline{u}^{(k)}$ are equal to zero.

At the k^{th} stage the column of $A^{(k)}$ is chosen which will maximize $\left| a_{k,k}^{(k+1)} \right|$. Let

$$s_j^{(k)} = \sum_{i=k}^{m} (a_{i,j}^{(k)})^2 \qquad j=k, k+1, \ldots, n.$$

Then since $\left| a_{k,k}^{(k+1)} \right| = \sigma_k$, one should choose that column for which $s_j^{(k)}$ is maximized. After $A^{(k+1)}$ has been computed, one can compute $s_j^{(k+1)}$ as follows:

$$s_j^{(k+1)} = s_j^{(k)} - (a_{k,j}^{(k+1)})^2$$

since the orthogonal transformations leave the column lengths invariant.

Let $\underline{\bar{x}}$ be the initial solution obtained, and let $\underline{\hat{x}} = \underline{\bar{x}} + \underline{e}$. Then

$$\left\| \underline{b} - A\underline{\hat{x}} \right\| = \left\| \underline{r} - A\underline{e} \right\|$$

where

$$\underline{r} = \underline{b} - A\underline{\bar{x}}, \text{ the residual vector.}$$

Thus the correction vector $\underline{e}$ is itself the solution to a linear least squares problem. Once A has been decomposed, and if the transformations have been saved, then it is a simple matter to compute $\underline{r}$ and solve for $\underline{e}$. The iteration process is continued until convergence.

APPENDIX 6

Singular Value Decomposition (65)

To compute the singular value decomposition of a given matrix A, a real m×n matrix with m≥n, the algorithm described below is suggested which first uses Householder transformations to reduce A to bidiagonal form, and then the QR algorithm to find the singular values of the bidiagonal matrix. The two phases properly combined produce the singular value decomposition of A.

Two finite sequences of Householder transformations are constructed as follows:

$$P^{(k)} = I - 2x^{(k)}x^{(k)T} \qquad (k=1,2,\ldots,n)$$

and

$$Q^{(k)} = I - 2y^{(k)}y^{(k)T} \qquad (k=1,2,\ldots,n-2)$$

(where $x^{(k)T}x^{(k)} = y^{(k)T}y^{(k)} = 1$) such that

$$P^{(n)}\ldots P^{(1)}AQ^{(1)}\ldots Q^{(n-2)} = \begin{bmatrix} q_1 & e_2 & 0 & \cdots & 0 \\ & q_2 & e_3 & \ddots & \vdots \\ & & \ddots & \ddots & 0 \\ & & & & e_n \\ & & & & q_n \\ \hline & & 0 & & \end{bmatrix} \equiv J^{(0)},$$

$(m-n)\times n$

an upper bidiagonal matrix. If we let $A^{(1)} = A$ and define

$$A^{(k+\frac{1}{2})} = P^{(k)}A^{(k)} \qquad (k=1,2,\ldots,n)$$
$$A^{(k+1)} = A^{(k+\frac{1}{2})}Q^{(k)} \qquad (k=1,2,\ldots,n-2)$$

then $P^{(k)}$ is determined such that

$$a_{ik}^{(k+\frac{1}{2})} = 0 \qquad (i=k+1,\ldots,m)$$

and $Q^{(k)}$ such that

$$a_{kj}^{(k+1)} = 0 \qquad (j=k+2,\ldots,n).$$

The singular values of $J^{(0)}$ are the same as those of A. Thus, if the singular value decomposition of

$$J^{(0)} = G D H^T$$

then

$$A = P G D H^T Q^T$$

so that $U = PG$, $V = QH$ with $P \equiv P^{(1)} \ldots P^{(n)}$, $Q \equiv Q^{(1)} \ldots Q^{(n-2)}$.

Singular Value Decomposition of the Bidiagonal Matrix

By a variant of the QR algorithm, the matrix $J^{(0)}$ is iteratively diagonalized so that

$$J^{(0)} \longrightarrow J^{(1)} \longrightarrow \cdots \longrightarrow D$$

where

$$J^{(i+1)} = S^{(i)T} J^{(i)} T^{(i)},$$

and $S^{(i)}$, $T^{(i)}$ are orthogonal. The matrices $T^{(i)}$ are chosen so that the sequence $M^{(i)} = J^{(i)T} J^{(i)}$ converges to a diagonal matrix while the matrices $S^{(i)}$ are chosen so that all $J^{(i)}$ are of the bidiagonal form.

For notational convenience, we drop the suffix and use the notation

$$J \equiv J^{(i)}, \quad \bar{J} \equiv J^{(i+1)}, \quad S \equiv S^{(i)}, \quad T \equiv T^{(i)}, \quad M \equiv J^T J, \quad \bar{M} \equiv \bar{J}^T \bar{J}.$$

The transition $J \rightarrow \bar{J}$ is achieved by application of Givens rotations to J alternately from the right and the left. Thus

$$\bar{J} = \underbrace{S_n^T S_{(n-1)}^T \cdots S_2^T}_{S^T} J \underbrace{T_2 T_3 \cdots T_n}_{T} \qquad (A6\text{-}1)$$

where

$$S_k = \begin{bmatrix} & & & (k-1) & (k) & & \\ 1 & 0 & & & & & \\ 0 & \ddots & & & & & \\ & & 1 & & & & \\ & & & \cos\theta_k & -\sin\theta_k & & \\ & & & \sin\theta_k & \cos\theta_k & & \\ & & & & & 1 & \\ & & & & & & \ddots \; 0 \\ & & & & & & 0 \; 1 \end{bmatrix} \begin{matrix} \\ \\ \\ (k-1) \\ (k) \\ \\ \\ \end{matrix}$$

and T_k is defined analogously to S_k with φ_k instead of θ_k.

Let the first angle, φ_2, be arbitrary while all the other angles are chosen so that $\bar{J}$ has the same form as J. Thus,

T_2 annihilates nothing, generates an entry $\{J\}_{21}$,

S_2^T annihilates $\{J\}_{21}$, generates an entry $\{J\}_{13}$,

T_3 annihilates $\{J\}_{13}$, generates an entry $\{J\}_{32}$,

and
finally

S_n^T annihilates $\{J\}_{n,n-1}$, and generates nothing.

This is shown in Fig. A6-1.

This process is frequently described as "chasing". Since $\bar{J} = S^T J T$,

$$\bar{M} = \bar{J}^T \bar{J} = T^T M T$$

and $\bar{M}$ is a tri-diagonal matrix just as M is. We show that the first angle, φ_2, which is still undetermined, can be chosen so that the transition $M \rightarrow \bar{M}$ is a QR transformation with a given shift s.

The usual QR algorithm with shifts is described as follows:

$$\begin{aligned} M - sI &= T_s R_s \\ R_s T_s + sI &= \bar{M}_s \end{aligned} \qquad \text{(A6-2)}$$

where $T_s^T T_s = I$ and R_s is an upper triangular matrix. Thus $\overline{M}_s = T_s^T M T_s$. It is not necessary to compute (A6-2) explicitly but it is possible to perform this shift implicitly. Let T be for the moment an arbitrary matrix such that

$$\{T_s\}_{k,1} = \{T\}_{k,1} \qquad (k=1,2,\ldots,n),$$

(i.e., the elements of the first column of T_s are equal to the first column of T) and

$$T^T T = I.$$

Then we have the following theorem: If

i) $\overline{M} = T^T M T$,

ii) $\overline{M}$ is a tri-diagonal matrix,

iii) the sub-diagonal elements of M are non-zero,

it follows that $\overline{M} = V \overline{M}_s V$ where V is a diagonal matrix whose diagonal elements are ± 1.

The transition (A6-1) is equivalent to the QR transformation of $J^T J$ with a given shift s.

The shift parameter is determined by an eigenvalue of the lower 2×2 minor of M.

Test for Convergence

If $|e_n| \leq \delta$, a prescribed tolerance, then $|q_n|$ is accepted as a singular value, and the order of the matrix is dropped by one. If, however, $|e_k| \leq \delta$ for $k \neq n$, the matrix breaks into two, and the singular values of each block may be computed independently.

If $q_k = 0$, then at least one singular value must be equal to zero. In the absence of round-off error, the matrix will break if a shift of zero is performed. Now, suppose at some stage

$$|q_k| \leq \delta$$

At this stage an extra sequence of Givens rotations is applied from the left to J involving rows $(k, k+1), (k, k+2), \ldots, (k, n)$ so that

e_{k+1} $\{J\}_{k,k+1}$ is annihilated, but $\{J\}_{k,k+2}$, $\{J\}_{k+1,k}$ are generated,

$\{J\}_{k,k+2}$ is annihilated, but $\{J\}_{k,k+3}$, $\{J\}_{k+2,k}$ are generated,

and finally

$\{J\}_{k,n}$ is annihilated, and $\{J\}_{n,k}$ is generated.

The matrix thus obtained has the form

$$\bar{J} = \begin{bmatrix} q_1 & e_2 & & & & & \\ & \ddots & \ddots & & & & \\ & & & e_k & & & \\ & & & \bar{q}_k & & & \\ & & & \delta_{k+1} & \bar{q}_{k+1} & \bar{e}_{k+2} & \\ & \bigcirc & & \vdots & & \ddots & \bar{e}_n \\ & & & \delta_n & & & \bar{q}_n \end{bmatrix} \begin{matrix} \\ \\ \\ \\ (k) \\ \\ \end{matrix}$$

$$\qquad\qquad\qquad\qquad\qquad\qquad\qquad\qquad\qquad\qquad\qquad\qquad\qquad\qquad\qquad\qquad (k)$$

Note that by orthogonality

$$\bar{q}_k^2 + \delta_{k+1}^2 + \cdots + \delta_n^2 = q_k^2 \leq \delta^2$$

Thus choosing $\delta = \left\| J^{(0)} \right\|_\infty \varepsilon_\circ$ ($\varepsilon_\circ$, the machine precision) ensures that all δ_k are less in magnitude than $\varepsilon_\circ \left\| J^{(0)} \right\|_\infty$. Elements of $\bar{J}$ not greater than this are neglected. Hence $\bar{J}$ breaks up into two parts which may be treated independently.

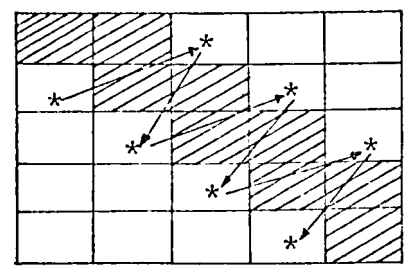

Fig. A6-1

APPENDIX 7

Table A7-1 Data structure for the 14 and 10 node network.

14 nodes			10 nodes		
link No.	node	to node	link No.	node	to node
1	1	2	1	1	2
2	1	8	2	1	3
3	2	4	3	1	5
4	2	6	4	1	7
5	2	8	5	1	8
6	3	8	6	1	9
7	3	11	7	2	3
8	3	12	8	2	4
9	3	13	9	2	5
10	4	6	10	4	5
11	5	7	11	5	6
12	6	8	12	5	10
13	6	7	13	6	7
14	6	9	14	8	9
15	7	9	15	9	10
16	9	10			
17	9	14			
18	10	11			
19	12	13			
20	13	14			

Table A7-2 Data structure for the 23 and 20 node network.

23 Nodes			23 Nodes		
link No.	node	to node	link No.	node	to node
1	1	2	1	1	2
2	1	11	2	1	3
3	1	14	3	1	6
4	2	7	4	2	4
5	2	20	5	2	5
6	3	10	6	3	9
7	4	12	7	5	10
8	4	13	8	6	10
9	5	8	9	7	8
10	5	19	10	7	10
11	5	21	11	9	10
12	6	13	12	10	11
13	6	16	13	10	12
14	7	9	14	10	13
15	8	10	15	10	14
16	8	12	16	11	20
17	8	13	17	13	18
18	8	23	18	14	15
19	9	10	19	14	16
20	9	12	20	15	17
21	9	13	21	16	18
22	9	14	22	17	18
23	11	23	23	18	19
24	12	15	24	19	20
25	15	18			
26	16	17			
27	17	18			
28	18	19			
29	18	22			
30	21	22			

Table A7-3 Data structure for the 30 node network.

link No.	node	to	node	link No.	node	to	node
1	1		2	22	12		13
2	1		3	23	12		14
3	2		4	24	12		15
4	2		5	25	12		16
5	2		6	26	14		15
6	3		4	27	15		18
7	4		12	28	15		23
8	4		6	29	16		17
9	5		7	30	18		19
10	6		7	31	19		20
11	6		8	32	21		22
12	6		9	33	22		24
13	6		10	34	23		24
14	6		28	35	24		25
15	8		28	36	25		26
16	9		11	37	25		27
17	9		10	38	27		28
18	10		20	39	27		29
19	10		17	40	27		30
20	10		21	41	29		30
21	10		22				

Table A7-4 Data structure for the 57 node network.

link No.	node	to	node	link No.	node	to	node
1	1		2	40	22		23
2	1		15	41	22		38
3	1		16	42	23		24
4	1		17	43	24		25
5	2		3	44	24		26
6	3		4	45	25		30
7	3		15	46	26		27
8	4		5	47	27		28
9	4		6	48	28		29
10	4		18	49	29		52
11	5		6	50	30		31
12	6		7	51	31		32
13	6		8	52	32		33
14	7		8	53	32		34
15	7		29	54	34		35
16	8		9	55	35		36
17	9		10	56	36		37
18	9		11	57	36		40
19	9		12	58	37		38
20	9		13	59	37		39
21	9		55	60	38		44
22	10		12	61	38		48
23	10		51	62	38		49
24	11		13	63	39		57
25	11		41	64	40		56
26	11		43	65	41		42
27	12		13	66	41		43
28	12		16	67	44		45
29	12		17	68	46		47
30	13		14	69	47		48
31	13		15	70	48		49
32	13		49	71	49		50
33	14		15	72	50		51
34	14		46	73	52		53
35	15		45	74	53		54
36	18		19	75	54		55
37	19		20	76	56		41
38	20		21	77	56		42
39	21		22	78	56		57

BIBLIOGRAPHY

1. Schweppe, F.C. et al.; "Power system static state estimation", IEEE, PAS 89, 120, 1970.
2. Dopazo, J.F., Klitin, O.A., Stagg, G.W. and VanSlyck, L.S.; "State calculation of power systems from line flow measurements", IEEE, PAS 89, 1698, 1970.
3. Dopazo, J.F., Klitin, O.A. and VanSlyck, L.S.; "State calculation of power systems from line flow measurements", Part II, IEEE, PAS 91, 145, 1972.
4. Debs, A.S. and Larson, R.E.; "A dynamic estimator for tracking the state of a power system", IEEE, PAS 89, 1670, 1970.
5. Debs, A.S. and Larson, R.E.; "Experimental evaluation of tracking state estimation", Proc. 7th PICA Conf., 1971.
6. Johnson, S.L.; "An algorithm for state estimation in power systems", Proc. 8th PICA Conf., 1973.
7. Bubenko, J.A. et al.; "On-line state estimation", IEEE Summer Meeting, Paper C-74 321-6, 1974.
8. Debs, A.S.; "State and parameter estimation for power systems in the steady state", Proc. Nat. Elcctronics Conf. 29, 1974.
9. Marquardt, D.W.; "An algorithm for least squares estimation of non-linear parameters", SIAM J. 11, 431, 1963.
10. Fletcher, R.; "A modified Marquardt subroutine for non-linear least squares", R. 6799, AERE, 1971. Harwell, England.
11. Debs, A.S., Larson, R.F., Hajdu, L.P.; "On-line sequential state estimation for power systems", Paper 3.3/7, PSCC, 1972.
12. Dopazo, J.F., Klitin, O.A., Ehrmann, S.T. and Sasson, A.M.; "Justification of the AEP real time load flow project", IEEE, PAS 92, 1501, 1973.
13. Svoen, J., Fismen, S.A., Faanes, H.H. and Johannessen, A.; "The on-line closed loop approach for control of generation and overall protection at Tokke power plants", Paper 32-06, CIGRE 1972.

14. Debs, A.S. and Litzenberger, W.H.;"Implementation of the BPA on-line state estimator", PSCC Paper 2.3/10, 1975.

15. Lecture notes of the symposium "Implementation of real-time power system control by digital computer", Imperial College of of Science and Technology, Electrical Eng. Dept., 1973.

16. Handshin, E.;"Real-time data processing using state estimation" in Real-Time Control of Electric Power Systems. Proc. of the Symposium held in Baden, Switzerland. Elsevier Pub., 1972.

17. Schweppe, F.C. and Handshin , E.J.;"Static state estimation", Proc. of the IEEE , 62, 972, 1974.

18. Van Meeteren, H.P., Feyen, A.R. and Michelis, E.J.;"Comparative study of two different types of state estimation including bad data identification methods", PSCC Paper 2.3/4, 1975.

19. Bard, Y.;"Comparison of gradient methods for the solution of non-linear parameter estimation problems", SIAM J. Numerical Analysis 7, 157, 1970.

20. Petterson, L.O.;"State estimation in the Swedish TIDAS", PSCC Paper 2.3/6, 1975.

21. Suzuki, H., Kawakami, J. and Sekine, Y.;"Power system state determination with minimum information". Elec. Eng. in Japan 93, 98, 1973.

22. Fetzer, E.E. and Anderson, P.M.;"Observability on the state estimation of power systems", IEEE, PAS 94, 1981, 1975.

23. Stagg, G.W. and El-Abiad, E.H.;"Computer methods in power system analysis" , McGraw-Hill, Tokyo, 1968.

24. Elgerd, O.I.; Electric Energy Systems Theory , McGraw-Hill, India, 1971.

25. Ariatti, F., Castagnoli, V., Marzio, L. and Ricci, P.;"Methods for electric power system state estimation: comparative analysis of computing simulations based upon generalized load flow, tracking and least squares methods", 4th PSCC, Paper 3.3/10, 1972.

26. Sasson, A.M.; "Non-linear programming solutions for load flow, minimum loss and economic dispatching problems", IEEE, PAS 88, 399, 1969.

27. Tsypkin, Y.Z.; Adaptation and Learning in Automatic Systems. Academic Press, London, 1971.

28. Tinney, W.F. and Hart, C.E.;"Power flow solution by Newton's method", IEEE, PAS 86, 1449, 1967.

29. Schweppe, F.; "Role fo the system identification in electric power systems", 4th PSCC, Paper 3.3/1, 1972.

30. Debs, A.S.; "Estimation of steady-state power system model parameters", IEEE Winter Power Meeting, T 74 153-3, 1974.

31. Masiello, R.D. and Schweppe, F.; "A tracking static state estimator", IEEE, PAS 90, 1025, 1971.

32. Himmelblau, D.M.; Applied Nonlinear Programming. McGraw-Hill, USA, 1972.

33. Allam, M. and Laughton, M.A.; "A general algorithm for estimating power system variables and network parameters", IEEE Summer Power Meeting, C 74 331-5, 1974.

34. Deutsch, R.; Estimation Theory. Prentice-Hall, New Jersey, 1965.

35. Neuenswander, J.R.; Modern Power Systems. Scranton, PA, International Textbook Co., 1971.

36. Jodoin, R. and Houle, J.; "Calcul en temps reel de l'ecoulment d'energie dans de grands reseaux", Canadian IEEE Power Conf., 169, 1974.

37. Fletcher, R.; "A new approach to variable metric algorithms", Computer Journal 13, 317, 1970.

38. Gill, P.E. and Murray, W.; "Quasi-Newton methods for unconstrained optimization", J. of the Inst. of Maths. and its Applications 9, 91, 1972.

39. Hartley, H.O.; "The modified Gauss-Newton method for the fitting of non-linear regression functions by least squares", Technometrics 3, 269, 1961.

40. Levenberg, K.;"A method for the solution of certain non-linear problems in least squares", Quart. Appl. Math. 2, 164, 1944.

41. Jacoby, S.L.S., Kowalik, J.S. and Pizzo, J.T.;"Iterative methods for non-linear optimization problems". Prentice-Hall, New Jersey, 1972.

42. Reid, J.K.;"Least squares solution of sparse systems of non-linear equations by modified Marquardt algorithm", in Decomposition of Large-scale Problems; p. 437; Ed. Himmelblau, D.M., Elsevier Pub. Co., 1973.

43. Larson, H.J.; Introduction to Probability Theory and Statistical Inference. J.Wiley, USA, 1969.

44. Stuart, T.A.;"Optimal ordering of network buses for weighted least squares state estimation", IEEE Winter Power Meeting, Paper C 74 152-5, 1974.

45. Zollenkopf, K.;"Bi-factorization-basic computational algorithm and programming techniques", in Large Sparse Sets of Linear Equations; Ed. Reid, J.K., Academic Press, London, 1971.

46. Tinney, W.F.;Discussion in reference 54.

47. Stagg, G.W., Dopazo, J.F., Klitin, O.A. and VanSlyck, L.S.; "Techniques for the real-time monitoring of power system operations", IEEE, PAS 89, 545, 1970. Discussion by Jazwinski, A.H.

48. Gross, G. and Luini, J.F.;"Effective control of convergence of the Newton load flow", IEEE-PICA, 41, 1975.

49. Schweppe, F.C. ; Uncertain Dynamic Systems. Prentice-Hall, New Jersey, 1973.

50. Kobayashi, H., Narita, S. and Hammam, M.S.A.A.; "Model coordination method applied to power system control and estimation problems", Proc. IFAC/IFIP Conf. Dig. Comp. Applications to Process Control, 1974.

51. Kohli, N.P., Sharma, J. and Ray, L.M.; "Optimal reactive power allocation", IEEE-PICA Conf. Proc., 216, 1975.

52. Kuppurajulu, A., Raman, N.;"Optimal load flow- a reformulation of the load flow problem", Elektrotech. Z. (ETZ) Ausgabe A, 93, 586, 1972.

53. Dopazo, J.F., Klitin, O.A., Sasson, A.M.; "Stochastic load flows", IEEE, Paper T74 308-3, Summer Power Meeting, 1974.

54. Sasson, A.M., Treviño, C. and Aboytes, F.; "Improved Newton's load flow through a minimization technique", IEEE-PICA , 1971.

55. Freris, L.L., Sasson, A.M.; "Investigation of the load-flow problem", Proc. IEE 115, 1459, 1968.

56. Bard, Y.; Non-linear Parameter Estimation. Academic Press, 1974.

57. CIGRE-1972. "Optimization studies for the operation of power systems", Paper 32-19.

58. Shen, C.M., Laughton, M.A.; "Determination of optimum power system operating conditions under constraints", Proc. IEE, 116, 225, 1969.

59. Aboytes, F.; "Computer methods for state estimation and security assessment in the electrical power systems", Ph.D. Thesis, Imperial College, Univ. of London, 1974.

60. Allam, M.F.; "Static and dynamic algorithms for power system state variables and parameters estimation", Ph.D. Thesis, Queen Mary College, Univ. of London, 1974.

61. Borkowska, B.;"Application of the pseudo-inverse to state estimation", International Conference on On-line Operation and Optimization of Transmission and Distribution Systems; London, 1976.

62. Christofides, N.; Graph Theory, an Algorithmic Approach. Academic Press, London, 1975.

63. Fadeeva, V.N. and Fadeev, D.K.; Computational Methods of Linear Algebra. W.H. Freeman and Co., San Francisco, 1963.

64. Businger, P. and Golub, G.H.; "Linear least squares solutions by Householder transformations", Numer. Math., 7, 269, 1965.

65. Golub, G.H. and Reinsch, C.; "Singular value decomposition and least squares solutions", Handbook for Automatic Computation, II, 134. Linear Algebra, Springer-Verlag, Berlin, 1971.

66. Peters, G. and Wilkinson, J.H.; "The least squares problem and pseudo-inverses", The Computer Journal, 13, 309, 1970.

67. Penrose, R.; "A generalized inverse for matrices", Proc. Cambridge Phil. Soc., 51, 406, 1955.

68. Pringle, R.M. and Rayner, A.A.; Generalized Inverse Matrices. Griffin, London, 1971.

69. Milne, R.D.; "An oblique matrix pseudoinverse", SIAM J. Appl. Math., 16, 931, 1968.

70. Forsythe, G.E. and Moler, C.B.; Computer Solution of Linear Algebraic Syatems. Prentice-Hall, New Jersey, 1967.

71. Mesarovic, M.D., Macko, D. and Takahara, Y.; Theory of Hierarchical Multilevel Systems. Academic Press, New York, 1970.

72. Fallside, F. and Perry, P.F.; "Hierarchical optimization of a water-supply network", Proc. IEE, 122, 202, 1975.

73. Arafeh, S.A. and Sage, A.P.; "Hierarchical system identification of states and parameters in interconnected power systems", Int. J. Systems Science, 5, 817, 1974.

74. Smith, N.J. and Sage, A.P.; "A sequential method for system identification in hierarchical structure", Automatica, 9, 677, 1973.

75. Ishi, S. and Fukao, T.; "Decentralized state estimation in power systems", Elec. Eng. in Japan, 95, 53, 1975.

76. Happ, H.H.; Diakoptics and Networks. Academic Press, New York, 1971.

77. Sasson, A.M.; "Decomposition techniques applied to the non-linear programming load-flow method", IEEE Trans., PAS 89, 78, 1970.

78. Bosarge, W.E., Jordan, J.A. and Murray, W.A.; "A non-linear block SOR-Newton load flow algorithm", IEEE Summer Meeting, Paper C73 644-5, 1973.

79. Mesarovic, M.D. and Takahara, Y.; General Systems Theory: Mathematical Foundations. Academic Press, New York, 1975.

80. Aldrich, J.F., Happ, H.H. and Lever, J.F.; "Multi-area dispatch", IEEE, PICA-71, p. 39.

81. Long, R.W. and Juves, R.W.; "The partitioning of networks through the use of precedence conditions", IEEE, PICA-73, p. 85.

82. Undrill, J.M. and Happ, H.H.; "Automatic sectionalization of power system networks for network solutions", IEEE, PAS 90, 46, 1971.

83. Aboytes, F. and Sasson, A.M.; "A power systems decomposition algorithm", IEEE, PICA-71, p. 448.

84. Bosarge, E. and Schlaepfer; "Algorithms for interactive design of power systems", JACC, Paper 13-6, 1972.

85. Andretich, R.G., Brown, H.F., Hansen, D.H. and Happ, H.H.; "Piece wise load flow solution of very large size networks", IEEE Trans., PAS 90, 950, 1971.

86. Tinney, W.F., Powell, W.L., Peterson, N.M.; "Sparsity-oriented network reduction", IEEE, PICA-73, p. 384.

87. Steward, D.V.; "Partitioning and tearing systems of equations", SIAM J. Numer. Analysis, 2, 345, 1965.

88. Erda, "Systems engineering for power", ERDA 76-82/1.

89. Handshin, E. and Bongers, C.; "Theoretical and practical considerations in the design of state estimators for electric power systems", in Computerized Operation of Power Systems. Savulesco, S.C., Ed., p. 104, Elsevier Scientific Pub., Amsterdam, 1976.

90. Koglin, H.J.; "Optimal measuring system for state estimation", Paper 2.3/12, PSCC 1975.

91. Handshin, E., Schweppe, F.C., Kholas, J. and Fletcher, A.; "Bad data analysis for power system state estimation", IEEE Trans., PAS 94, 329, 1975.

92. Prim, R.C.; "Shortest connection networks and some generalizations", The Bell System Technical Journal, p. 1389, 1957.

93. Galvão, R.D.; "The optimal location of facilities on a network", Ph.D. Thesis, Imperial College of Science and Technology, Univ. of London, 1977.

94. Kevin, V. and Whitney, M.; "Algorithm 422-minimal spanning tree", Com. of ACM, p. 273, 1972.

95. Salkin, H.M.; Integer Programming. Addison-Wesley, USA, 1975.

96. Galvão, R.D.; "A direct tree search algorithm for the solution of the p-median problem programmed in Fortran IV", unpublished report, Dept. of Management Science, Imperial College of Science and Technology, Univ. of London, 1976.

97. Garfinkel, R.S. and Nemhauser, G.L.; Integer Programming. John Wiley, New York, 1972.

98. Eldelmann, H.; "A universal assessment of the superior quality of distribution of measuring points for the state estimation of high voltage networks", Proc. PSCC, Paper 2.3/7, 1975.

99. DeVille, T. and Schweppe, F.C.; "On-line identification of interconnected network equivalents from operating data", IEEE Summer Power Meeting, Paper C72 464-6, 1972.

100. Schwartz, M.W., Park, G.L. and Schlueter, R.A.; "Model identification using tie line power and frequency measurements", IEEE, Winter Power Meeting, Paper C74 128-5, 1974.

101. Quentin, J.F., Testud, J.L. and Richalet, J.; "Identification of thermal power plants", IFAC Symp. on System Identification and Estimation, p. 407, 1973.

102. Lindhal, S. and Ljung, L.; "Estimation of power generator dynamics from normal operating data", Ibid, p. 367.

103. Price, W.U., Schweppe, F.C., Gulanchenski, E.M. and Silva, R.F.; "Dynamic equivalents from on-line measurements", IEEE Trans. PAS, 94, 1349, 1975.

104. Ibrahim, M.A.H. and El-Abiad, A.H.; "On-line estimation of dynamic equivalents of external systems", Int. Conf. on On-line Operation and Optimization of Transmission and Distribution Systems, p. 28, London, 1976.

105. Phua, K. and Dillon, T.S.; "Optimal choice of measurements for state estimation", IEEE, PICA-77, p. 431.

106. Rao, A.; "The multiple set covering problem: a side stepping algorithm", Operations Research and Statistics Center Research Paper No. 37-71-P6, Rensselaer Polytechnic Institute, 1971.

107. Debs, A.S.; "Estimation of external network equivalents from internal system data", paper T74 339-8, IEEE Summer Power Meeting, 1974.

108. Lee, C.C. and Owen, T.T.; "A weighted-least-squares parameter estimator for synchronous machines", IEEE Trans. PAS-96, 97, 1977.

109. Handschin, E. and Galiana, F.D.; "Hierarchical state estimation for real-time monitoring of electric power systems", IEEE PICA, p. 304, 1973.

110. Happ, H.H.; "Multicomputer configurations and diakoptics: dispatch of real power in power pools", IEEE Trans. PAS-88, 1969.

111. Dy Liacco, T.E.; "Control of power systems via the multi-level concept", Syst. Res. Center, Cleveland, Ohio, Rep. SRC-68-19, 1968.